Final report to AOARD/AFOSR

Secondary Electron Emission Measurements on Materials under Stress

October 2004

Shinichi Kobayashi[1] and Yoshio Saito[2]

[1] Department of Electrical and Electronic Systems
Saitama University
255 Shimo-Okubo, Sakura-ku, Saitama-shi, Saitama, 338-8570, Japan
s.kobayashi@ees.saitama-u.ac.jp

[2]Accelerator Laboratory
High Energy Accelerator Research Organization
1-1 Oho, Tsukuba-shi, Ibaraki, 305-0801, Japan
yoshio.saito@kek.jp

REPORT DOCUMENTATION PAGE

Form Approved

OMB No. 0704-0188

PLEASE DO NOT RETURN YOUR FORM TO THE ABOVE ADDRESS.

1. REPORT DATE *(DD-MM-YYYY)*	2. REPORT TYPE	3. DATES COVERED *(From - To)*
19-11-2004	Final	18-Sep-03 - 23-Jun-05

4. TITLE AND SUBTITLE

Increasing the Power Capacity in RF Delivery Devices: Secondary Electron Emission Measurements on Materials under Stress

5a. CONTRACT NUMBER

F6256203P0543

5b. GRANT NUMBER

5c. PROGRAM ELEMENT NUMBER

6. AUTHOR(S)

Dr. Shinichi Kobayashi

5d. PROJECT NUMBER

5e. TASK NUMBER

5f. WORK UNIT NUMBER

7. PERFORMING ORGANIZATION NAME(S) AND ADDRESS(ES)

Saitama University, Dept. of Electrical and Electronic Systems
255 Shimo-Okubo
Saitama-shi 338-8570
Japan

8. PERFORMING ORGANIZATION REPORT NUMBER

N/A

9. SPONSORING/MONITORING AGENCY NAME(S) AND ADDRESS(ES)

AOARD
UNIT 45002
APO AP 96337-5002

10. SPONSOR/MONITOR'S ACRONYM(S)

AOARD

11. SPONSOR/MONITOR'S REPORT NUMBER(S)

AOARD-034029

12. DISTRIBUTION/AVAILABILITY STATEMENT

Approved for Public Release. Distribution unlimited.

13. SUPPLEMENTARY NOTES

14. ABSTRACT

The breakdown of rf windows used in high-power klystron is one of the most serious problems in the development of klystrons. The dielectric breakdown strength of an alumina ceramic surface depends on the secondary electron emission which is influenced by the electronics states of the oxygen vacancy existing adjacent to the ceramic surface. In this report, the durability of several dielectric materials used for rf windows is discussed in terms of secondary of electron emission (SEE), cathode luminescence, and dielectric loss. High-power tests of these materials with TiN coating, thus having low SEE, were also carried out using a traveling wave resonant ring. The samples were compared under the conditions of annealing and X-ray irradiation. The influences of annealing and X-ray irradiation on the SEE coefficients and CL spectra were investigated. Energy distributions of secondary electrons under high temperature were analyzed as well. The results show that alumina ceramics are superior to sapphire and aluminum nitride. The original of breakdown was investigated and the requirement for rf window materials presented.

15. SUBJECT TERMS

High Power Microwaves

16. SECURITY CLASSIFICATION OF:			17. LIMITATION OF ABSTRACT	18. NUMBER OF PAGES	19a. NAME OF RESPONSIBLE PERSON
a. REPORT	b. ABSTRACT	c. THIS PAGE			Misoon Y. Mah, Ph.D

U	U	U	UU	54	**19b. TELEPHONE NUMBER** *(Include area code)* +81-3-5410-4409

Contents

First interim report

- Review and preliminary work -

Interim report to AOARD/AFOSR

Secondary Electron Emission Measurements on Materials under Stress

Shinichi Kobayashi[1] and Yoshio Saito[2]

[1]Saitama University
255 Shimo-Okubo, Saitama, Saitama, 338-8570, Japan

[2]High Energy Accelerator Research Organization (KEK)
1-1 Oho, Tsukuba, Ibaraki, 305-0801, Japan

Abstract

The breakdown of rf windows used in high-power klystrons is one of the most serious problems in the development of klystrons. The dielectric breakdown strength of an alumina ceramic surface depends on the secondary electron emission which is influenced by the electronic states of the oxygen vacancy existing adjacent to the ceramic surface. In this report, the durability of several dielectric materials used for rf windows is discussed in terms of secondary electron emission (SEE), cathodoluminescence, and dielectric loss. High-power tests of these materials with TiN coatings, thus having low SEE, were also carried out using a traveling wave resonant ring. The samples were compared under the conditions of annealing and X-ray irradiation. The influences of annealing and X-ray irradiation on the SEE coefficients and CL spectra were investigated. Energy distributions of secondary electrons under high temperature were analyzed as well. The results show that alumina ceramics are superior to sapphire and aluminum nitride. The original of breakdown was investigated and the requirements for rf window materials presented.

1. Introduction

In rf accelerator systems, ceramic rf windows are generally used to separate the high vacuum of such devices from atmospheric pressure. There are some basic requirements regarding the properties of an rf window; (1) low rf dissipation, (2) low rf reflection, and (3) a vacuum-tight seal.

Pillbox rf windows are used for the output of S-band(2856MHz) pulsed klystrons(3.5 μs, 30MW peak)in the KEK linac. The window comprises a high-purity alumina ceramic disk (3.5mm thick, 92mm in diameter)and a pillbox housing. Breakdown of the alumina ceramics sometimes takes place, thus creating punctures. It results in breaks of the vacuum seal or reflection of the rf power. Several window materials (such as alumina and beryllia) were investigated at the Stanford Linear Accelerator Center [2-4]. It was concluded that alumina ceramics are superior to all of the other materials examined.

Breakdown of alumina ceramic windows has also been studied at KEK [1,5-7]. The results are summarized below.

(1) An optical emission (glow) from the window was observed during rf operation. It comprises a luminescence caused by electron bombardment, since the glow has a similar spectrum to alumina cathodoluminescence (CL) excited by electron beam irradiation.

(2) An observation of an electron multipactor effect (resonant multiplication of secondary emitted electrons in the rf field) occurred on alumina surfaces with high SEE yields, which was confirmed by noticeably decreased luminescence intensities when the window is coated with thin films of low SEE yields (such as TiN).

(3) Bright spots of luminescence with a band at 410nm(due to F-center defects of oxygen vacancies) were sometimes observed due to the multipactor effect, in which surface melting or puncturing is found to occur. It is considered that the generation of F-center defects induced surface melting.

(4) Two colored areas were often observed on the alumina ceramic disks after rf operation. These colorings probably result from the electron multipactor effect. The degree of these colorings and the surface melting depends on the material.

In order to prevent breakdown, it is necessary to select durable materials, as well as to suppress the multipactor effect by coating TiN [8]. However, there are a wide variety of possible alumina ceramics, depending on the manufacturing process. It is thus important to investigate the dielectric properties of materials for practical use in more detail.

In this study, three kinds of alumina ceramics were examined. Sapphire and aluminum nitride (AIN) were also studied for material comparison. These materials were investigated from the standpoints of (1) electron multipactor evaluated by SEE yields, (2) F-center defects which can be evaluated by cathodoluminescence(CL), (3) rf power dissipation estimated by dielectric loss tangent ($\tan\delta$) and bulk resistivities. High power tests (maximum220MW) were carried out using the resonant ring. In these tests the effects of TiN film coatings (2.5nm thick) on multipactor suppression were also examined. From these results, the essential requirements for dielectric materials to be used as rf windows, were presented. Effects of X-ray irradiation on optical absorption coefficients and energy distributions of secondary electrons were also investigated.

2. Experimental

2.1 Dielectric material examined

The alumina ceramics studied were 99%(UHA-99), 99.7%(HA-997), and 99.9%(XKP-999) pure alumina. The published values of their physical properties are listed in Table 1; they depend on the grain structures and sintering processes as well as the content purity of alumina. UHA-99 comprises small grains with diameters of ~1 μm and have a highly dense structure [1] (compared to the other ceramics which show spray-dried powders of 50 μm in diameter). HA-997 is specially sintered for crystallizing additives of SiO_2 and MgO in order to reduce rf losses. XKP-999, though sintered without additives, has a rather high porosity and the density is much lower than that of sapphire. Sapphire (single crystal of alumina) includes neither grain boundaries nor additives. Aluminum nitride(AIN) has a high thermal conductivity.

2.2 Secondary electron emission (SEE)

The SEE coefficients were measured using a single pulsed electron beam (1 ms, 100pA) with a scanning electron microscope (SEM)[5] in order to avoid any surface charging. Primary electrons and secondary emitted electrons were collected by a biased (+40V) Faraday cup. The ratio of secondary to primary current gives the SEE coefficient.

The SEE coefficient γ measured for alumina ceramic(HA-997),sapphire and AIN disks are shown in Fig. 1 as a function of the primary electron energy. The other alumina ceramics had similar γ values to that of HA-997, which were more than unity in the energy region to 20keV;this indicates that multipactor is liable to occur at an rf transmission power of~30MW, when the incident energy of multipactor electrons is~10keV[9,10]. The γ of the sapphire was 4 at a primary energy of 20keV, which was higher than those of any other material. The SEE coefficient γ of the AIN, on the contrary, was much smaller and <1.0 when the primary electron energy was> 5keV. Multipactor would be liable to occur on all of the materials examined, except AIN.

2.3 Cathodoluminescence (CL)

The spectra of CL were observed using a SEM with a 5 and 10keV electron beam (20nA)[8]. The

CL spectrum of alumina ceramic (HA-997), sapphire and AIN are shown in Fig. 2. The spectrum of HA-997 comprises broad bands at~300nm, which are attributed to the F-center of oxygen vacancies [11]. The peak at 694nm is caused by impurity levels of Cr^{3+} (ruby) [5] . The CL spectra obtained for the other alumina ceramics were similar to that of HA-997. The sapphire exhibited a luminescence band not only at 300nm, but also at 410nm, which is due to the F-defect sites of oxygen[11],as described before. A major emission band near 360nm in CL spectrum of AIN (Figure 2(c)) should be due to the F-center nitrogen defects, which are suggested from UV absorption of the F center in AIN [12]. From these results one can anticipate that alumina ceramics containing no F defects would be durable for high power operation, which will be described later.

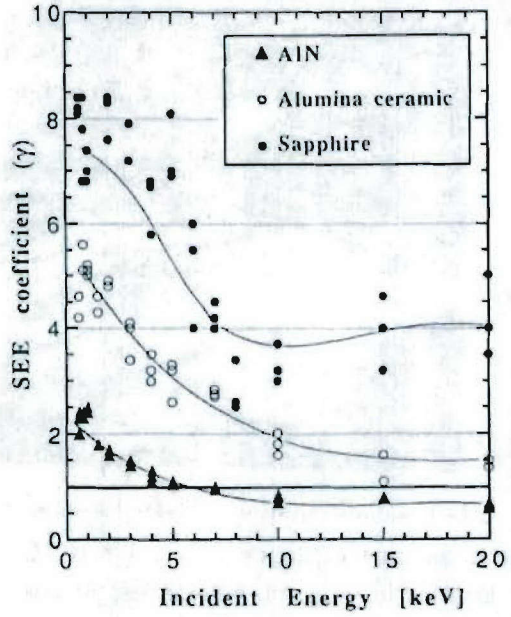

Figure 1.

SEE coefficients γ of alumina ceramic (HA-997), sapphire, and AIN. The lines are averages of the experimental points, and only for guiding the eye.

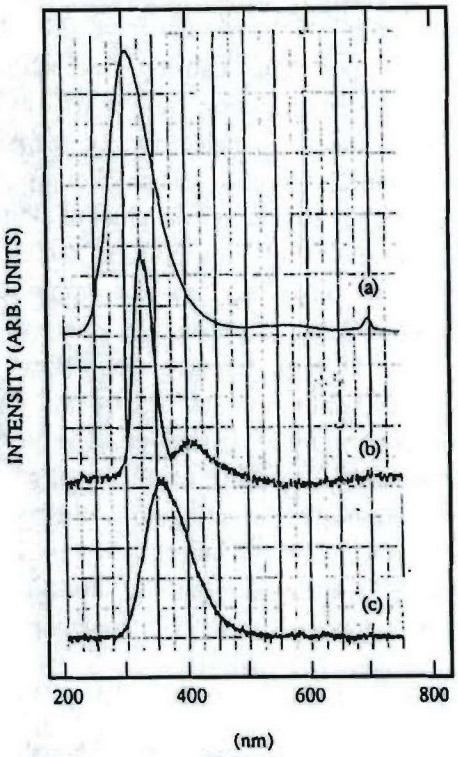

Figure 2.

CL spectra of HA-997 (a), sapphire (b) and AIN (c).

2.4 X-ray irradiation

Alumina samples were exposed to temperatures up 1500 ℃ in air for annealing, and set on a beam collector of a klystron being operated with a beam voltage of 300 kV as X-ray irradiation.

2.5 Analysis of secondary electron energy distribution under high temperature

Energy distributions of secondary electrons emitted from an alumina sample under high temperature were analyzed by using an Auger electron spectrometer. The primary electron energy was 1500 eV, and the temperature was at about 400 ℃

3. Dielectric loss and bulk resistivity

Dielectric loss causes excess heating, thus causing thermal stress in rf windows. Small tan δ values are therefore desirable. The permittivity ε and tan δ values were measured using a specially devised rf cavity[13]. A photograph of the equipment is shown in Fig.3. The dimensions of the cavity were designed so that the resonant frequency would be~3GHz when a dielectric disk was inserted. The ε is calculated from the measured resonant frequency of the TE_{011} mode. The tan δ value is obtained from the Q-value of the TE_{011} mode, compared to that of a cavity without dielectric disk.

The measured values of ε and tan δ of the materials are given in Table 1. The tan δ values for

these alumina ceramics were low(of the order of 10^{-4}),which could be explained by the small amounts of impurities or sintering additives in the grain boundaries[14]. This would result in a dissipation power of 0.6W at an rf power of 8 kW average(2856MHz, 200MW, 2 μs, 20pps).

Sapphire has a very low tan δ value, which is due to being a single crystal[14]. The relatively high tan δ value of XKP-999 is probably caused by its porosity[15], since the pores weaken the binding of crystalline phase and will facilitate mechanical vibration under an applied rf electric field[16]. Under an rf operation at a peak power of 200MW, the electric field of~8kV/mm is applied at the center of the rf window disk. The ceramics with high porosity have a lower dielectric strength due to local field enhancement effect around pores [14] and it is considered that such ceramics easily induce an electric avalanche.

The tan δ of AlN was larger by 40$\times$than that of other materials, thus causing dissipation power of 24W at a transmission power of 8kW average. Because of this large dielectric loss, the AlN will have much thermal stress, even though its thermal conductivity is 10$\times$larger than that of alumina.

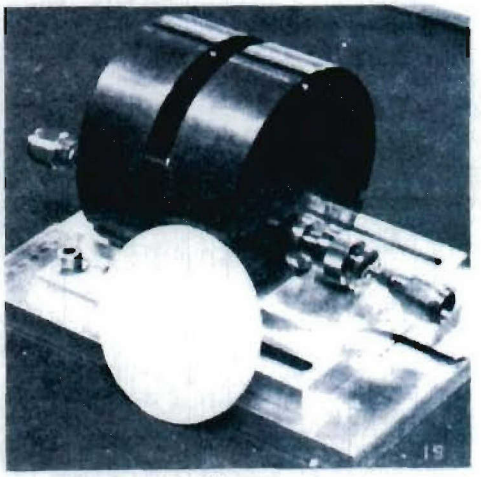

Figure 3.
Photograph of the apparatus for ε and tanδ measurements

The dielectric bulk resistivities, which are mainly affected by ions, electrons or impurities in grain boundaries [14] decrease by several orders of magnitude at high temperatures. They seem to be important because a surface can be heated by multipactor or by rf dissipation. The very large bulk resistivities(>10^{14} Ωcm) were measured using guard ring electrodes[8] which guards the main electrode from surface leakage current. The bulk resistivities of alumina ceramics were >$1\times10^{15}\,\Omega$cm. Especially, the larger resistivity observed for ions or electrons in the grain boundaries. AlN which has rather low bulk resistivity together with high tan δ value, does not seem to be good for high-power rf window material.

Table 1. Physical and dielectric properties of test materials.

materials		Manufacturer	purity (%)	specific gravity	ε	tan δ (10^{-3})	resistivity ($10^{13}\Omega$cm)	sintering additives
alumina ceramics	UHA-99	NTK	99.0	3.90	9.81	9.4	>1000	SiO_2,MgO,CaO
	HA-997	NTK	99.7	3.95	9.95	4.2	6.7	SiO_2,MgO
	XKP-999	NTK	99.9	3.91	9.67	13.3	3.3	---
sapphire		ASGAL	100	3.98	10.16	2.3	>1000	---
AlN		Sumitomo Denko	99.5	3.26	8.35	420	0.56	Y_2O_3
cathodoluminescence spectra			F^+, Cr^{3+} (in alumina ceramics)					
			F^+, F (in sapphire)					
			F (in AlN)					

3.1 High-power tests by resonant ring

High-power tests of rf window disks whose surface were coated with 2.5nm thick TiN over 75% of their area, were performed using the resonant ring [5,6]. It is expected that multipactor effect on the dielectric surface can be observed by comparing luminescence intensities. The dielectric disk was fixed in the pillbox housing by an aluminum helicoflex (shrunk in periphery without brazing), which is used in the KEK linac waveguide system [1]. With such vacuum seal, even materials which are rather difficult to metalize due to their high purity, could be examined. In the resonant ring, the rf output power from a pulsed klystron (30MW, 2856MHz, 2 μs, 20pps or 50pps) was transmitted through an input directional coupler and resonated in the ring[17]. An rf window could

be examined at a maximum power of 220MW in this experiment. The base pressure was~10^{-8}Pa after a bakeout, and the pressure was kept <10^{-6}Pa during rf operation.

The results are summarized in Table 2. Alumina ceramics of UHA-99 and HA-997 were superior to sapphire and AIN. Cracks were produced on the alumina ceramic with high tan δ (XKP-999).

Table 2. Results of high power tests.

materials		characteristics	transmittable power	remarks	luminescence *
alumina ceramics	UHA-99	dense structure, high resistivity	>220 MW	melting, coloring	F, (F^+, Cr^{3+}) **
	HA-997	crystallized additives, low tanδ	>220 MW	melting	(F^+, Cr^{3+}) ***
	XKP-999	micro-porosities, high tanδ	144 MW	crack, puncture, coloring	F, (F^+, Cr^{3+})
sapphire		F-center, low tanδ	75 MW	melting	(F^+, F)
AIN		F-center, high tanδ	35 MW	Al-groove	(F)

* ( ); pre-existing
** No F-centers were created on the TiN coated surfaces where the multipactor was suppressed.
*** No F-centers were created even where the multipactor took place.

3.2 Alumina ceramic

The luminescence pattern from the alumina ceramic window during rf operation is shown in Fig. 4. It has been confirmed that the multipactor took place at locations where the ceramic was uncoated with TiN(upper left).

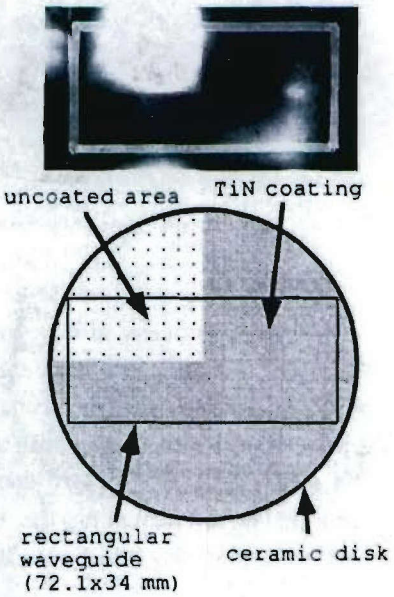

Figure 4.
Luminescence caused by multipactor on the alumina ceramic (XKP-999). The line in the photograph is a rectangular waveguide.

3.2.1 XKP-999

The luminescence spectra shown in Fig. 5(a) and (b) were measured during rf operation at a power of 1.5MW before and after high power operation above 100MW, respectively. F-center defects of oxygen vacancies, showing a luminescence band at 410nm, were found to be generated. Colorings, as described before, were also observed at the uncoated area. Those probably result from excess heating due to its high tan δ value, which will be discussed later. The cracks and punctures on the center of the disk, where the electric field was maximal, were generated during rf operation at 144MW(Fig. 6). This may be related to the high porosity of the ceramic as described before.

3.2.2 UHA-99

After operation above 100MW, that band at 410nm appeared in the luminescence spectrum. Colorings were also observed on the uncoated area.

3.2.3 HA-997

Although the multipactor took place on the uncoated area, no defects contributing to the luminescence band at 410nm appeared during rf operation, and no colorings were observed.

3.3 Sapphire

Bright spots appeared on the uncoated surface when operated at 50MW. The microscopic observation after high power tests showed surface melting of these spots [18] and thermal etching on the uncoated area[18], which indicate that excess heating took place, probably due to a multipactor on the surface having high SEE yields.

3.4 AlN

The multipactor also occurred on AlN to ~10MW corresponding to ~3keV of incident energy of the multipactor electrons [9.10]. Under 35 MW operation, an Al segregated groove parallel to the rf electric field appeared at the center of the disk. After that, the AlN disk could not transmit an rf power higher than 30kW. Excess heating due to the low bulk resistivity and the high tan δ value seemed to result in a breakdown at lower power, such as 35MW.

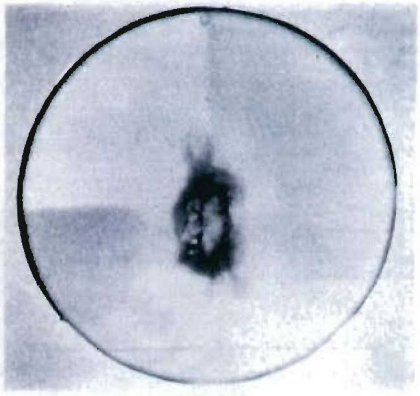

Figure 6.
Photograph of the XKP-999 after breakdown.

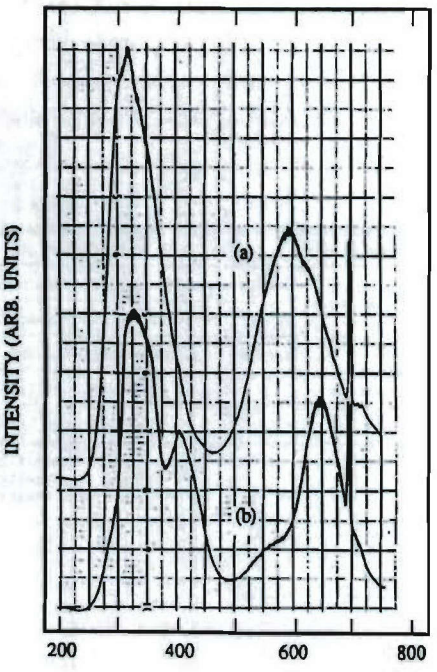

Figure 5.
Luminescence spectra observed for the alumina ceramic (XKP-999) surface during rf operation at 1.4 MW before (a) and after (b) > 100 MW operation.

4. Annealing effects

The annealing process affects the alumina ceramic properties concerning the trapped or stored charges in the vacancies. It is interesting to know the annealing effects on the SEE coefficients and CL, since the secondary electrons generated by primary injected electrons may be trapped or scattered at such defects as vacancies before they escape to a vacuum.The micro structures of an alumina ceramic surface before and after annealing up to 1500℃ in air are shown in Fig. 7. It is observed that after annealing the boundaries of an alumina grains appear clearly, caused by the evaporation of sintering additives [20].

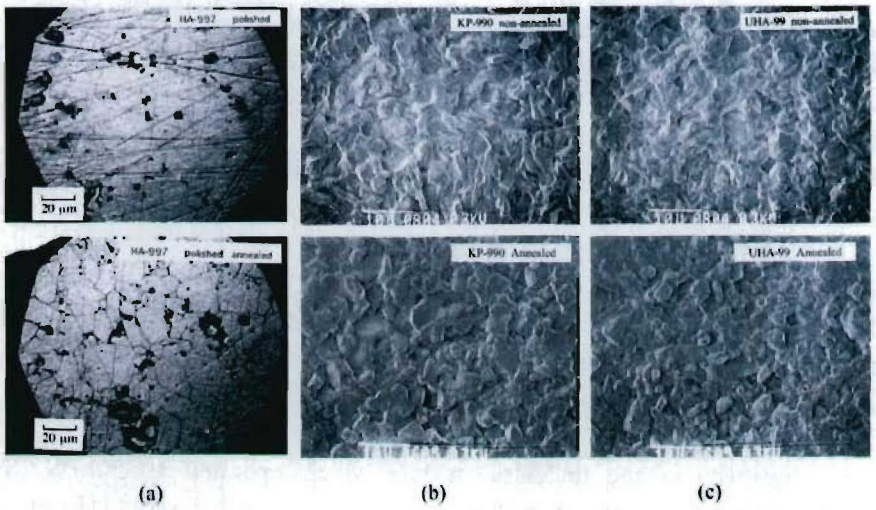

(a) (b) (c)

Fig. 7 Grain structures of alumina ceramics. As-received (above) and annealed (below) samples are shown. (a) HA-997 polished, (b) KP-990, and (c) UHA-99.

The SEE coefficients measured before and after annealing are listed in Table 3. Before annealing it is found that the SEE coefficients depend on the alumina content ; the higher the content, the higher the coefficients. Although HA-997 has higher values of the SEE coefficients, it shows a higher breakdown strength [19]. The breakdown phenomena, especially in the thermal process, is therefore strongly related to the oxygen vacancy rather then the SEE coefficients. After annealing, an increase in the SEE coefficients is observed, especially for ceramics having a lower alumina content. The ceramics with high alumina contents, such as KP-990, HA-997, XFA-40 and sapphire, originally having high SEE coefficients, do not show any substantial increase upon annealing.

Table 3 SEE values with incident energy (Ep=1keV) of alumina samples with as-received and annealed.

	HA-92	HA-95	HA-997	KP-95	KP-990	UHA-99	XFA-40	Sapphire
As-received	6.7	6.4	9.9	7.5	10.2	7.3	9.6	10.0
Annealed	7.7	8.6	9.7	9.5	10.1	10.4	10.2	9.8

Some possible mechanisms for the increase in the SEE coefficients by annealing can be considered: (1) in-air annealing recovers the oxygen vacancies or relaxes the surface residual stress, thus reducing trapping sites; (2) annealing causes a charge transfer, then neutralizes the localized potential at point defects of F^+-centers, as well as at other defects, such as dislocations; and (3) sintering additives, such as SiO_2 and MgO, which should absorb secondary electrons, have been evaporated by annealing. Mechanism (3) seems to be the most possible, since evaporation of the additives was observed on the ceramic surface, as described above. A ceramic having a lower content has sufficient additives for supplying to the surface; thus, the SEE coefficients are considered not to reach as a value as those of high-purity ceramics.

The intensity of the F^+-, F-center and Cr^{3+} peak measured for samples before and after annealing are listed in Table 4. Only sapphire has F^+- and F-centers originally. Most of the ceramics show a decrease in the CL intensity contributing to the F^+-center after annealing, while the intensity contributing to Cr^{3+} does not decrease for all of the ceramic samples.The former indicates a recovery of the oxygen vacancy, or otherwise the conversion of F^+-to F-centers as a change transfer [21], though no peaks contributing to the F-center were observed under this irradiation condition.

The ceramics of UHA-99 and KP-990, comprising smaller alumina grains and having a high flexural strength, did not show a decrease, suggesting that the annealing is not sufficient for such dense ceramics to relax the electronic state in the trapping site. Also, for sapphire it is confirmed that annealing the intensity contributing to the F^+-center decreases and the F-center peak disappears [22].

Table 4 Intensity of F^+(F) center and Cr^{3+} peaks in CL spectra; in [arbitrary units] and absorption ratio (400 nm):in [%] of alumina ceramics with as -received , annealed and X-ray irradiated.

		HA-92	HA-95	HA-997	KP-95	KP-990	UHA-99	XFA-40	Sapphire	
F^+ [arbitrary units]	As-received	2.8	4.3	13	0.6	1.8	2.8	7.0	2.4	6.5[a]
	Annealed	2.2	4.0	10	1.0	1.8	3.5	3.6	1.4	0[a]
	X-ray irradiated	1.6	2.5	6.4	0.6	1.1	1.8	7.7	1.0	1.5[a]
Cr^{3+} [arbitrary units]	As-received	1.0	0.7	0.5	0.5	0.7	0.8	0.5		
	Annealed	1.4	1.0	0.5	0.9	0.7	0.9	0.5		
	X-ray irradiated	0.8	0.7	0.5	0.5	0.6	0.7	0.5		
absorption (400 nm) [%]	As-received	3	1	22	10	12	17	3		
	X-ray irradiated	58	60	60	71	73	74	40		
	Annealed[b]	9	8	23	14	19	22	12		

[a]Intensity of F-center peak.
[b]Annealed after X-ray irradiated.

5. X-ray irradiation effects

The X-ray irradiation of dielectric material leads to the formation of color centers. This induces a

modification of electronic states in the vacancies. Upon performing X-ray irradiation on ceramic samples, a brown coloring was observed. Fig. 8 shows the optical-absorption coefficients measured for UHA-99 and HA-997 before and after irradiation, together with that of an irradiated sample followed by annealing. The increase in the coefficients of HA-997 is smaller than that of UHA-99, indicating fewer defects. It was also found that the degree of coloring does not depend on the alumina purity, but does depend on the manufacturing process (such as HA, KP and XFA), as listed in Table 4. The coloring by X-ray irradiation vanished upon annealing. The electronic states having been excited are, therefore, relaxed by thermal activation.

The CL measurement shows neither an additional peak as an F-center nor a new band for all of the ceramics. The X-ray irradiation does not create a new defect which contributes to alumina luminescence. The intensity of the F^+-center and Cr^{3+} peak measured for samples before and after X-ray irradiation are listed in Table 4. A decrease in the intensity contributing to the F^+-center is observed for most of the ceramics. However, it is difficult to estimate the changes in the F^+-center densities, since the luminescence should be absorbed by coloring.

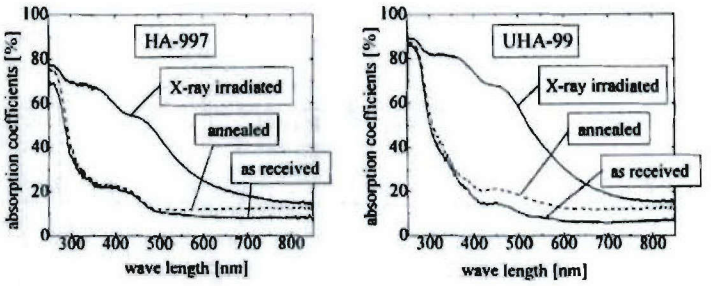

Fig. 8 Optical absorption coeeficients. The samples were annealed after X-ray irradiated.

No change in the SEE coefficients before and after X-ray irradiation was observed as far as the X-ray source used here is concerned.

6. Energy distributions of secondary electrons under high temperature

Secondary electron energy distribution provides information to discuss secondary electron emission mechanism and hence difference of SEE coefficient with samples. Energies of secondary electrons of an alumina sample excited by 1500 eV primary electrons were analyzed by a double pass Cylindrical Mirror Analyzer (CMA, PHI 15-255G ; its resolution $\Delta E/E = 0.007$, thus $\Delta E = 0.175$ eV for the pass energy E=25 eV). The alumina sample used was HA-997, and the samples was heated up to about 400 ℃ in vacuum by electron back bombardment. Distributions of SEE under room temperature and 400 ℃ were compared.

Figure 9 shows energy spectra of secondary electrons measured under room temperature and 406 ℃. The pressure in the chamber during heating the samples and analyzing electron energies was in $5X10^{-6}$ Pa. The comparison reveals that at higher temperature the peak of the spectrum in creases and shifts to the higher energy. According to the mechanism of secondary electron yield in insulators based on the interaction with lattice vibrations the yield and the average energy loss suffered by the secondary per collision decrease with raising temperature [23]. The result shown in Fig. 9 seems to be consistent with the theory in the peak position, while the temperature dependence of intensity exhibits reverse relationship. The surface condition of the sample is one of causes to dominate secondary electron yield. The sample surface was covered with hydro-carbon contaminants layer as shown in Fig. 10. It should, therefore, be noticed that to discuss the secondary electron yield preparation of clean surface is required.

Figure 9 also shows that the value of full width at half maximum (FWHM) may be estimated as about 5 eV. For metal, silver for example, the value is about 20 eV [24]. The value of FWHM obtained from Fig. 9 may reflect the secondary electron emission characteristic of insulators [25].

Energy spectra of elastic reflected electrons are shown in Fig. 11. Two peaks are precisely coincide with each other, and the peaks locate at the energy position equal to the incident electron energy

(1500 eV). These spectra illustrate that charging effect due to electron bombardment is almost same under the present heating condition.

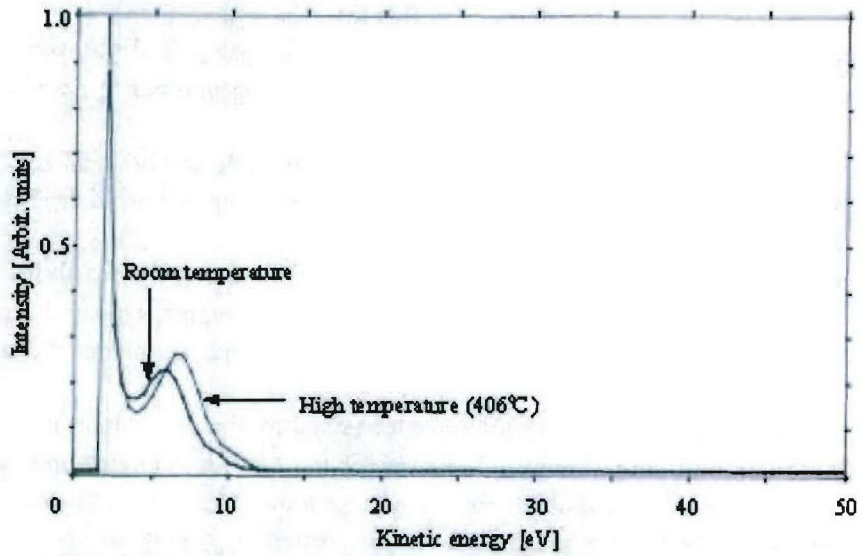

Fig. 9 Secondary electron energy distributions demonstrating temperature dependence.

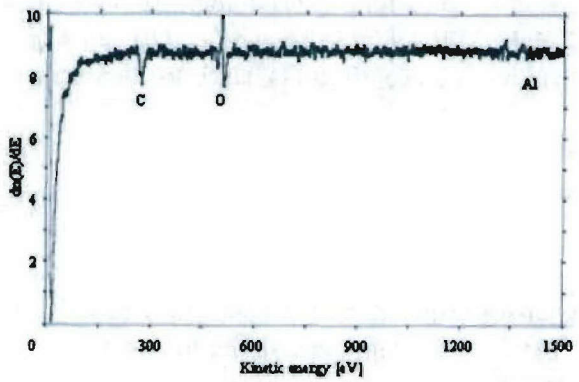

Fig 10 Auger spectra of in vacuum heated alumina.

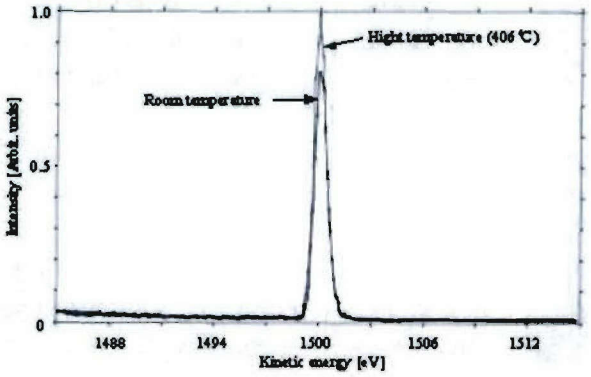

Fig. 11 Elastic peak of reflected electrons.

7. Conclusion and discussion

From the CL spectra after high-power tests, it was confirmed that F-center defects (pre-existing or generated during rf operation) lead to surface melting. The susceptibility to F-center generation depends on the materials and the operation condition. The defects seem to be produced on materials with high porosity (XKP-999),or around which multipactor took place(uncoated area of UHA-99). On the contrary, no F-center defects were generated on alumina ceramics with low tan δ (HA-997), which is probably due to the suppression of excess heating.

It was reported that F-center defects are introduced by heating under a reducing atmosphere [26]. It is thus considered that excess heating due to the multipactor or localized rf dissipation results in the production of the F-center defects. Defect generation of the F center should be prevented as well as selecting the materials without pre-existing F-center defects. It can be accomplished by using materials having low tan δ (low porosity) in order to avoid any localized heating and by thin-film coating in order to suppress the multipactor.

Lee et al. indicated that excited electrons in F centers are able to contribute to electric conduction [27]. If electrons trapped in F-center defects are excited by electron irradiation (such as multipactor bombardment), it would be expected that localized ohmic losses due to excited electrons take place

under an rf electric field, which would enhance F center generation. Such a 'runaway' phenomenon probably causes surface melting or dielectric breakdown.

8. Summary of this interim report

The SEE yields, CL spectra, tan δ and bulk resistivities of dielectric disks were measured. High-power tests were performed using a traveling wave resonant ring in order to examine the breakdown of the disks.

It was found that excess heating due to multipactor bombardment or localized rf dissipation at pores, probably causes F center generation. This might enhance localized heating and results in surface melting or a dielectric breakdown.

It is concluded that alumina ceramics with a low tan δ have a good feasibility for high-power operation, though they must be coated with TiN films in order to suppress the multipactor.

The SEE coefficients are found to depend on the alumina content: the higher the content, the larger the coefficients.

An in-air annealing treatment up to 1500℃ is ascertained to dissolve colouring. In the CL spectra, the intensity contributing to the F^+-center decreases for most of the ceramics upon annealing. Based on these results, the annealing possibly causes a charge transfer between the oxygen vacancies. An increase in the SEE coefficients was observed for ceramics having a lower alumina content. Evaporation of the sintering additives which absorb the secondary electrons is one of the possible mechanisms of this phenomenon.

The X-ray irradiation effects in this study were found to be as follow: (1) colouring, (2) a change in the optical-absorption coefficient, (3) no change in the SEE coefficients, and (4) a decrease in the CL intensity contributing to the F^+-center. It is difficult to estimate effect (4), since the luminescence should be absorbed by effects (1) and (2).

Analysis of secondary electron energies revealed that secondary electrons emitted at higher temperature have higher energies than those at room temperature.

9. Further experiments

As an interim report previously published findings have been summarized and some experimental results have been described as well. These are the first step to obtain the measure to select insulating materials for high power use. We are, therefore, planning to pursue the following experiments.

1. Measurements of temperature dependence of secondary electron emission coeeficient.
2. Secondary electron emission measurements under highly stressed conditions.
3. Canvassing materials whose emitted electrons have low emission energy.

References

[1] Y.Saito, N.Matuda, S.Anami, H.Bara, A.Kinbara and G.Horikoshi, "Breakdown of Alumina rf Window" . , Rev. Sci. Instrum. , Vol. 60, pp. 1736-1739, 1989.

[2] J.Jasberg and J.V.Lebacqz, "High Power Microwave Windows", SLAC-PUB-49, September 1964.

[3] R.W.Bierce, W.R.Fowkes and J.H.Jasberg, "Window Materials Design And Properties For Use In High Power Klystrons", SLAC-PUB-92, March 1965.

[4] J.Jasberg and J.V.Lebacqz, "Problems Related to Very High Power Windows at Microwave Frequencies", in Advan. Vacuum Sci. Technol., Proc. First. Int. Congr. Vacuum Techniques, Macmillan (Pergamon) Newyork, Vol.II, pp.667-671, 1960.

[5] Y.Saito, N.Matuda, S.Anami, A.Kinbara, G.Horikoshi and J.Tanaka, "Breakdown of Alumina RF Windows", IEEE Trans. on Electr. Insul. ,Vol.24, pp.1029-1032, 1989.

[6] Y.Saito, S.Yamaguchi, S.Anami, S.Michizono, A.Kinbara and N.Matuda, "Breakdown of Alumina RF Window", Proceedings of XIVth International Symposium on Discharges and Electrical Insulation in Vacuum, Santa Fe. New Mexico, USA, September, pp.372-376, 1990.

[7] Y.Saito, N.Matuda, S.Anami, A.Kinbara and G.Horikoshi, "High Power Test of Microwave Window Using Resonant Ring (II)", J. Vac. Soc. Japan, Vol. 32, pp.270-273, 1989 (in Japanese).

[8] S.Michizono, A. Kinbara, Y.Saito, S.Yamaguchi, S.Anami and N.Matuda, "Tin Film Coatings on Alumina Redui Frequency Windows", J. Vac. Sci. Technol. Vol.A10, pp.1180-1184, 1992.

[9] S.Yamaguchi, Y.Saito, S.Anami, and S.Michizono, "Trajectory Simulation of Multipactoring Electrons in an S-band Pillbox RF Window", IEEE Trans. on Nucl. Sci., Vol.39, pp.278-282, 1992.

[10] Research on Microwave Window Multipactor and its inhibition, Eitel-Mccullough, Inc., 1964.

[11] A.Al Ghamdi and P.D.Townsend, "Ion Beam Excited Luminescence OF Sapphire", Nucl. Instr. and Meth. Vol.B46, pp.133-136, 1990.

[12] K.Atobe, M.Honda, N.Fukuoka, M.Okada and M.Nakagawa, "F-type Centers in Neutron-irradiated AlN", Japanese J. Appl. Phys., Vol. 29, pp.150-152, 1990.

[13] Y.Kobayashi and J.Sato, "Complex Permittivity Measurement of Dielectric Plates by Cavity Resonance Method", IEICE Technical Report (Japan), MW-88-40 (Nov.1988).

[14] W.D.Kingery, H.K.Bowen and D.R.Uhlmann, Introduction to Ceramics Second Edition, chap.18, pp.913-974, John & Sons, Inc., New York, 1976.

[15] S.Sakka and M.Tashiro, "Studies on the Dielectric Loss of Polycrystalline Material Produced from the Glass of the System Li_2-MgO-Al_2O_3-SiO", J. Ceram. Assoc. Japan, Vol.69, pp.393-400, 1961.

[16] M.M.Bunag and J.H.Koenig, "Ultra Low Loss Ceramic Dielectrics", J. Am. Ceram. Soc., Vol.42, pp.442-447, 1959.

[17] L.J.Milosevic and R.Vautey, "Traveling-wave Resonators", Inst. Radio Engrs. Trans., Vol.MTT-6, pp.136-143, 1958.

[18] Y.Saito, S.Michizono, S.Anami and S.Kobayashi, "Surface Flashovewr On Alumina rf Windows for High Power Use", Proceedings of XVth International Symposium on Discharges and Electrical Insulation in Vacuum, Darmstadt, Germany, September, pp.227-231, 1992.

[19] S.Michizono, Y.Saito, S.Yamaguchi, S.Anami, N.Matuda, A.Kinbara, "Dielectric Materials for Use as Output Window in High-power Klystrons", IEEE Trans. Electr. Insul., Vol.28, pp.692-699, 1993.

[20] H.Kawai, H.Matsuura, S.Michizono, Y.Saito, A.Inagaki, J. Vac. Soc. Jpn. 36 pp.257-259, 1987, (in Japanese).

[21] C.Jardin, L.Martinez, M.Ghamnia, P.Durupt, "Electron Trapping Phenomena at TiN/α-Al_2O_3 Interfaces", CEIDP'97, Minneapolis, Oct. 1997.

[22] K.H.Lee, J.H.Crawford Jr., "Luminescence of F-centers in sapphire", Phys. Rev. B 19, pp.3217-3221, 1979.

[23] A. J. Dekker, Solid State Physics, p.442, Prentice Hall, 1957.

[24] A. J. Dekker, Solid State Physics, p.419, Prentice Hall, 1957.

[25] K. Ariyam et al. ed., Boundary Phenomena and Lattice Defects, p.68, Kyoritu Shuppan, 1961 (in Japanese).

[26] K.H.Lee, J.H.Grawford and Jr., "Additive Coloration of Sapphire", Appl. Phys. Lett., Vol.33, pp.273-275, 1978.

[27] K.H.Lee, J.H.Grawford and Jr., "Luminescence of F-center in Sapphire", Phys. Rev., Vol.B19, pp.3217-3221, 1979.

Second interim report

- Preliminary measurements of SEE under high temperature condition -

May 23, 2003

Report to AOARD/AFOSR

Secondary Electron Emission (SEE) Measurements on Materials under Stress (Preliminary measurements of SEE under high temperature condition)

Shinichi Kobayashi[1] and Yoshio Saito[2]

[1] Department of Electrical and Electronic Systems
Saitama University
255 Shimo-Okubo, Sakura-ku, Saitama-shi, Saitama, 338-8570, Japan
Tel : +81-48-858-3469
Fax : +81-48-855-7832
E mail : s.kobayashi@ees.saitama-u.ac.jp

[2] Accelerator Laboratory
High Energy Accelerator Research Organization (KEK)
1-1 Oho, Tsukuba, Ibaraki, 305-0801, Japan

Summary

Secondary electron emission (SEE) coefficient of sapphire and Si and energy distributions of secondary electrons from aluminas were measured under high temperature at about 400 ℃. These measurements intended to establish measurement systems of SEE coefficient and energy analysis of secondary electrons under high temperature conditions. Sample stages of scanning electron microscope (SEM) and X-ray photoelectron spectroscope (XPS) were modified to enable a sample to heat upto a temperature. SEE coefficients were measured by the modified SEM with pulsed electron beam. The modified XPS system was used to analyze energies of secondary electrons.

Results can be summarized as follows;

1. The SEE coefficients of silicon and sapphire could be measured under room and high temperature.
2. In relative high temperature (200 ℃), an appreciable reduction in the SEE coefficient was confirmed for both silicon and sapphire.
3. Position dependence (not only temperature dependence) of the SEE coefficient was observed in sapphire.
4. The peak of energy distribution for secondary electrons was in about 8 eV, and the width spreaded over about 3.4 eV. The temperature rise caused decrease of energy about 0.7 eV, and did not affect the spread.
5. The peak height of the distribution decreased with temperature.

1. Introduction

Klystrons, the high power microwave generator, are used for particle acceleration energy sources in the high energy accelerator. In the klystron, there is a rf window which made of an insulator. Surface flashover along the surface of rf window insulator is a present problem in the klystron applications for high power use. Therefore, it is necessary to understand the surface flashover phenomena and thus improve transmission capability of high power microwave [1,2].

The important points in the breakdown mechanism along the rf window insulator are multiplication of secondary electrons emitted from the insulator surface and the temperature rise caused by microwaves which pass through the insulator. In the previous interim report, SEE, CL, effect of X-ray irradiation, and tentative results of SEE energy distribution were reported [3]. These results, however, were measured under room temperature condition except the last one. An rf-window of a klystron under operation may be heated by loss caused by the microwave transmission. Therefore, study of temperature effect on secondary electron emission (SEE) characteristic is required to understand the breakdown process in the rf window.

Some theories have proposed to explain the SEE characteristic under high temperature conditions [4,5,6,7]. However, there are still only few data of the SEE under high temperature conditions, especially for technical material. This study aims to measure the SEE coefficient under high temperature conditions of technical materials insulators, such as alumina. At present, the samples measured were silicon and sapphire. The measurement of silicon was carried out because of two reasons; (a) the electronic state of silicon looks like that of insulator, (b) there is no charge up on this sample surface when an electron beam is injected. Therefore, the silicon is a good sample to practice measurement skill at beginning of this study. The SEE coefficient of alumina will be measured in the next experiments.

This time our experimental systems have been modified to enable measurements under high temperature conditions. In this interim report, firstly experimental systems prepared for the SEE coefficient measurements and secondary electron energy distribution analysis system under high temperature conditions have been described, then temperature dependence of the SEE coefficient and secondary electron energy distributions have been reported and discussed, and finally results have been summarized.

2. Experimental

2-1 SEE measurement system and sample heating unit

In this study, the secondary electron emission coefficients (δ) were measured under room and high temperature conditions by using Scanning Electron Microscope (SEM). A heater circuit was used to observe SEE coefficients (δ) under high temperature conditions. Measurements of SEE coefficients could be carried out by two methods: (i) measuring the absorption currents, or (ii) measuring the secondary electron currents.

Schematic diagram of the absorption current measurement method is shown in Fig. 1. The absorption currents were measured by applying a negative bias voltage to insure that the secondary electron emissions were not absorbed into the sample. In order to measure primary currents, a

faraday cup was installed on the sample holder. A sapphire insulator (0.3 mm thickness) was used to prevent currents flowing to ground. Fig. 2 shows photograph of sample holder used in this experiment.

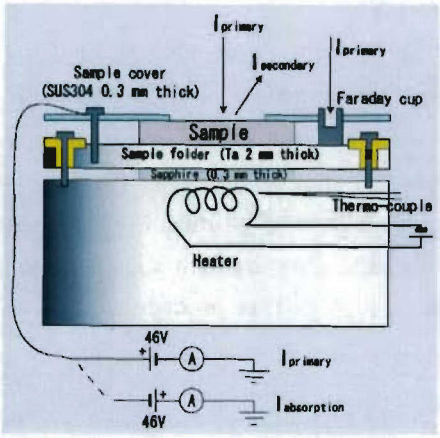

Fig. 1 Schematic diagram of absorption current measurements

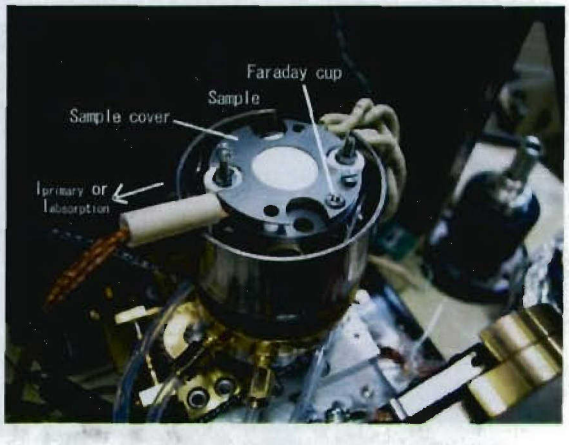

Fig. 2 Picture of sample holder used in this experiment.

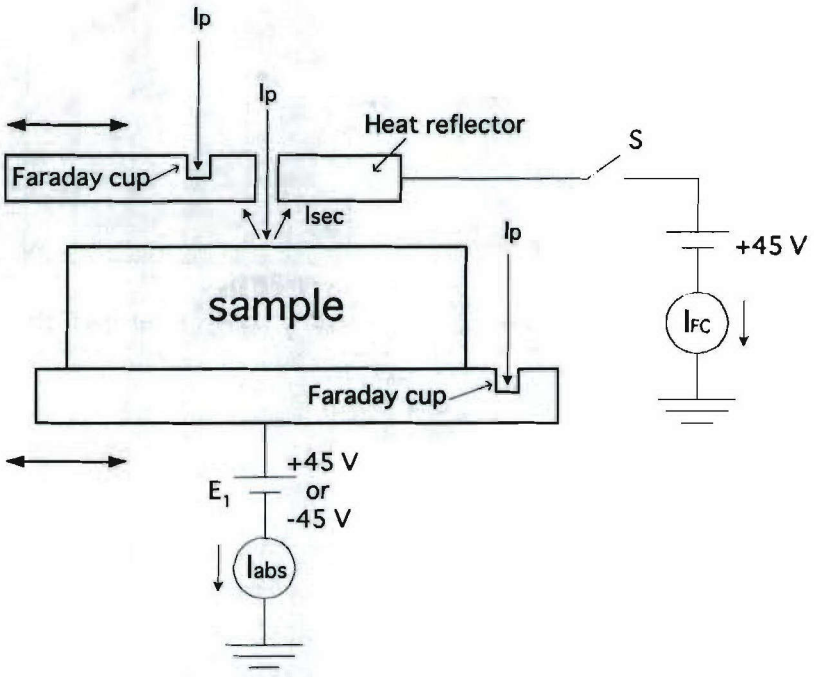

Fig. 3 A new configuration of SEE coefficient measurements.

Schematic diagram of the secondary electron current measurement method is shown in Fig. 3. The secondary electron currents were measured using faraday cup installed above the sample. A positive bias voltage was applied to the faraday cup to ensure all of the secondary electrons were measured (switch S was ON). A negative bias voltage was applied to the sample holder to insure that the secondary electron emissions were not absorbed into the sample.

2-2 Sample and procedure

Samples used in this experiment were silicon (semiconductor), sapphire and alumina KP990 (insulator). For silicon sample, the primary current was one shot pulsed electron beam with 400 pA amplitude for 1 ms duration. There is no charge up on the silicon sample, so the measurements of SEE coefficient (δ)can be carried out at the same site of the sample.

The insulator samples were annealed at 1400℃ in air for 4 hours before measurements. This annealing process affects the insulator properties concerning the trapped or stored charges in the vacancies [2].

The primary current used for the insulator samples was one shot pulsed electron beam with 100 pA amplitude for 1 ms duration. For insulator, only once measurement at one site of the sample was carried out. Then, the insulator sample was traveled to the next measurement site by moving 2 mm for x direction and or 1 mm for y direction, as shown in Fig. 4. This procedure reduces the influence of surface charging on the measurements.

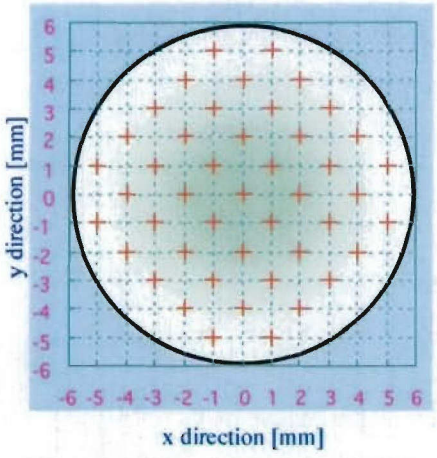

Fig. 4 Positions of measurement sites for sapphire.

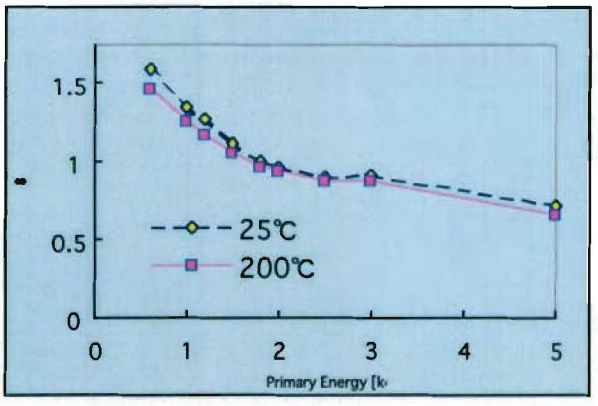

Fig. 5 SEE coefficient (δ) of silicon.

2-3 Energy distribution measurement system

Energy distributions of secondary electrons from samples were analyzed by an XPS/AES system. Schematic diagram of electron energy measurement with sample heating circuit is shown in Fig. 6. A cylindrical mirror analyzes (CMA; PHI 15-255G, energy resolution ΔE=0.15 eV) with a coaxial electron gun is used. Primary electrons (Acceleration voltage:1500 V, current:2 μA) from the coaxial gun excite sample surface to emit secondary electrons. Then energies of emitted secondary electrons are analyzed by CMA operated under the XPS mode. The picture of the total system is shown in Fig. 7.

A W-Re heater mounted behind the sample holder heated the sample. Electron bombardment heating using thermionic emission from the heater is possible as well. The maximum temperature achieved was about 400 ℃, and the pressure of the vacuum chamber was in 10^{-5} Pa orders. A picture of the sample holder is shown in Fig. 8. The detail of the sample holder part is shown in Fig. 9. In this system primary electrons impinge on the sample surface continuously, then it is inevitable to suffer some influences on the energy distribution from surface charging. Even so, some valuable

information may be obtained, since auger electron spectroscopy is useful to analyze insulator surface.

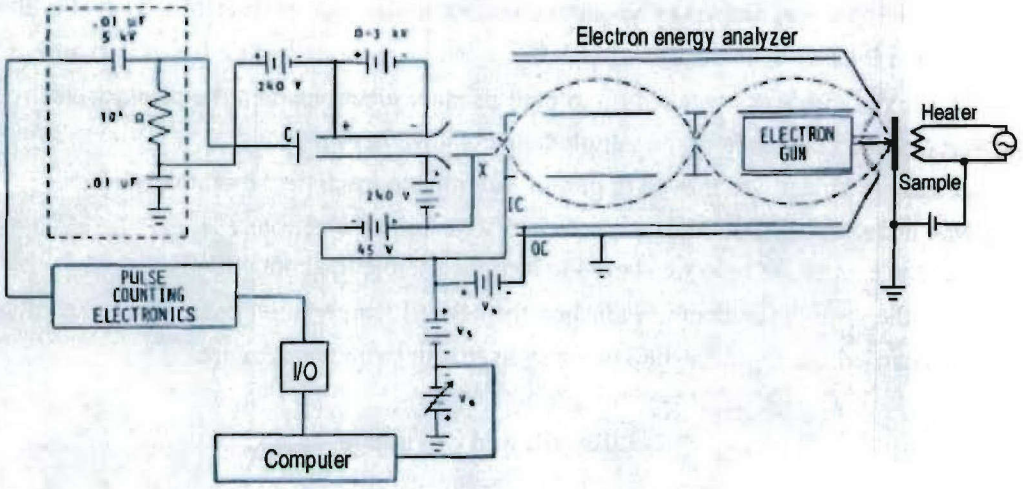

Fig. 6 Electron energy analyzer with sample heating circuit.

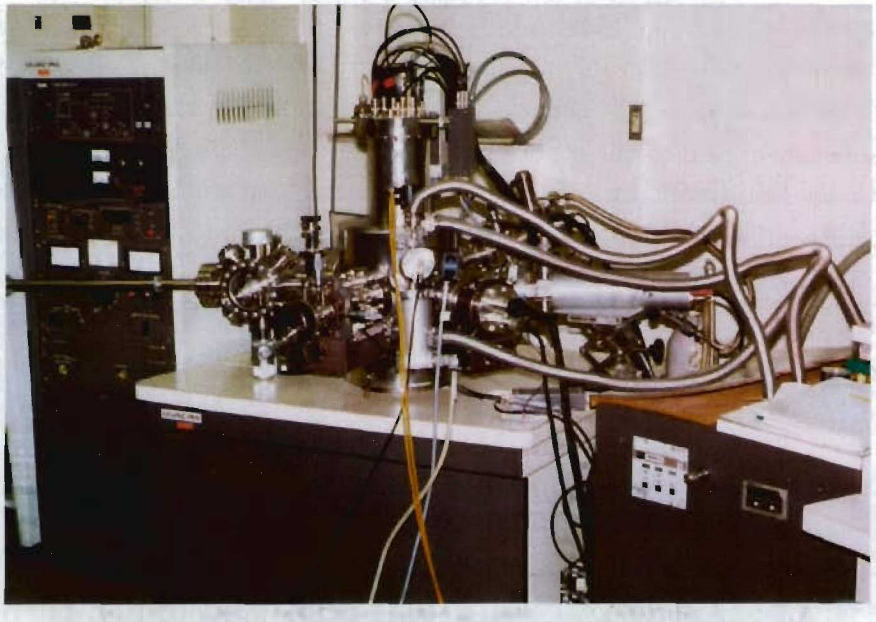

Fig. 7 A picture of electron energy analysis system having cylindrical energy analyzer.

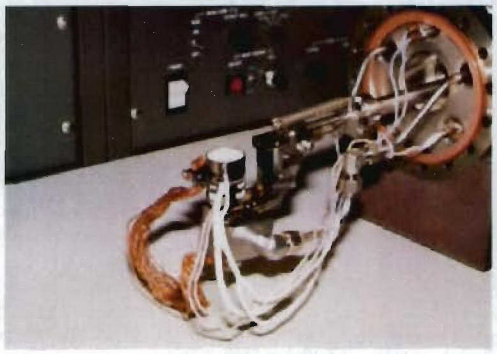

Fig. 8 Picture of sample stage.

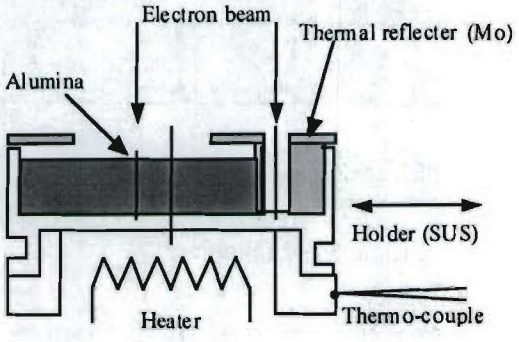

Fig. 9 Detail of the sample stage

2-4 Measurement procedure

Measurements were carried out under the following procedure

1. A test sample was set in the vacuum chamber under the pressure of $2X10^{-7}$ Pa, then it was tilted to 30° and located at the analyzing point.

2. The coaxial gun was switched on to emit primary electrons, and the primary electron current was measured at the hole made in the sample holder shown in Fig. 9.

3. The sample holder was moved to permit electrons to irradiate the sample surface.

4. CMA under the XPS-mode analyzed energy of emitted electrons.

5. After the energy analysis we started to heat the sample to about 400 ℃.

6. When the sample temperature reached the desired temperature, energy analysis of secondary electrons was carried out again by the same way as that in room temperature.

3. Results and discussion

3.1 SEE coefficients of silicon

Measurements of SEE coefficients (δ) of silicon sample were carried out by using the absorption current method under room and relative high temperature (200℃). Results of the measurements are shown in Fig. 5. The peak of the SEE coefficient curve could not be measured, because measurement of SEE coefficient using the SEM at low primary energy was very difficult.

At 200℃, the SEE coefficients of silicon are lower than that room temperature condition. The decrease of SEE coefficient of silicon at higher temperature is caused by the increased interaction between the internal secondary electron and the augmented density of free electrons in the conduction band [6].

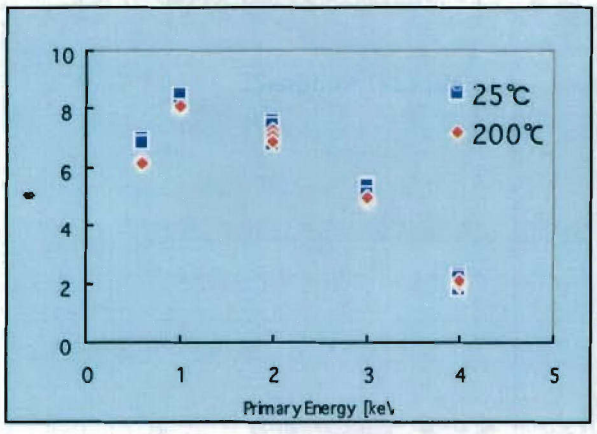

Fig.10 SEE coefficient of sapphire (sample A).

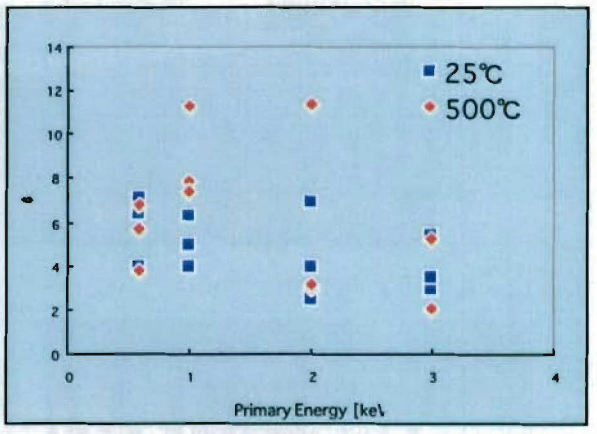

Fig.11 SEE coefficient of sapphire (sample B).

3-2 SEE coefficients of sapphire

The SEE coefficients of sapphire (sample A) under room temperature and 200℃ are shown in Fig. 10. At 200℃, the SEE coefficients of sapphire are lower than that obtained under room temperature condition. Fig. 11 shows SEE coefficients of another sapphire sample (sample B) under

room temperature and 500℃. For the sample B of sapphire, the SEE coefficient data have high standard deviation. It shows position dependence possibility of the SEE coefficient.

At present, there are still only few theories of the SEE under high temperature conditions, especially for insulator material. However according to empirical data and references, it is considered that the decrease of SEE coefficients of sapphire when temperature increases may be caused by phonons and electrons scattering in the bulk before escaping from the surface. Therefore, under high temperature conditions, the secondary electron emitted to the surface is less than that of in room temperature.

The SEE coefficients of sapphire in Fig. 10 and Fig. 11 are larger than those of silicon shown in Fig. 5. This difference may be ascribed primarily to two sources; those are (a) the energy required for a free electron to escape from the solid, (b) the rate of energy loss of internal secondaries as they approach the surface [6]. These two factors do not act independently, for, if the rate of energy loss is high for all energies of the internal secondaries which lie between their initial energy and that required for escape, the coefficient should be low. This represents the situation in semiconductor where there are more electrons with which the secondaries can make allowable collisions involving either large or small transfers of energy.

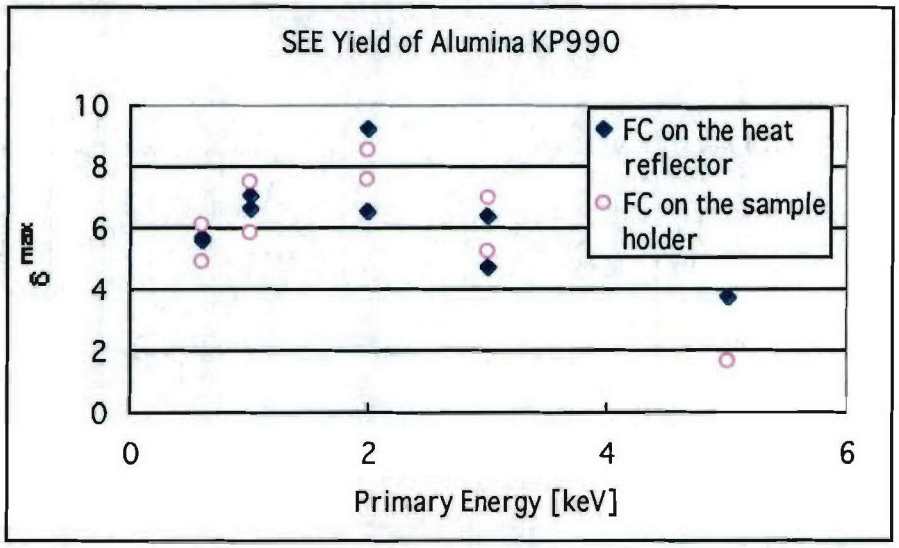

Fig. 12 SEE coefficients of alumina KP990

- Faraday cup (FC) on the heat reflector:

Ip : E_I=+45V, S=ON

Isec: E_I= –45V, S=ON

- Faraday cup (FC) on the sample holder:

Ip : E_I=+45V, S=OFF

Isec: E_I= –45V, S=OFF

3-3 SEE coefficients of alumina

The SEE coefficients of alumina KP990 (Alumina purity : 99.5 %) under room temperature measured by absorption and secondary current method is shown in Fig. 12. SEE coefficients of the sample measured by both of the methods were almost same. The SEE coefficients of the sample under high temperature conditions will be measured in the next experiments.

3-4 Energy distribution

3-4-1 SEE energy distribution

Energy distributions of secondary electrons measured at room temperature (22 ℃) and high temperature (429 ℃) for alumina HA95 (Alumina purity : 95 %) are shown in Fig.13. At room temperature energy at peak position locates at about 7.6 eV, and its full width at half maximum is about 3.4 eV.

The peak height decreases with temperature. In addition the peak of the spectrum shifts towads lower energy side with temperature. In this case its shift is can be estimated as 0.7 eV. The decrease of peak height with temperature is reasonable [4]. The rate of decrease, however, seems fairly large, since secondary electron yield δ at 700 ℃ and 1.0 keV primary electron energy decreases to 90 % of the value at 25 ℃ for Mg single crystal [8].

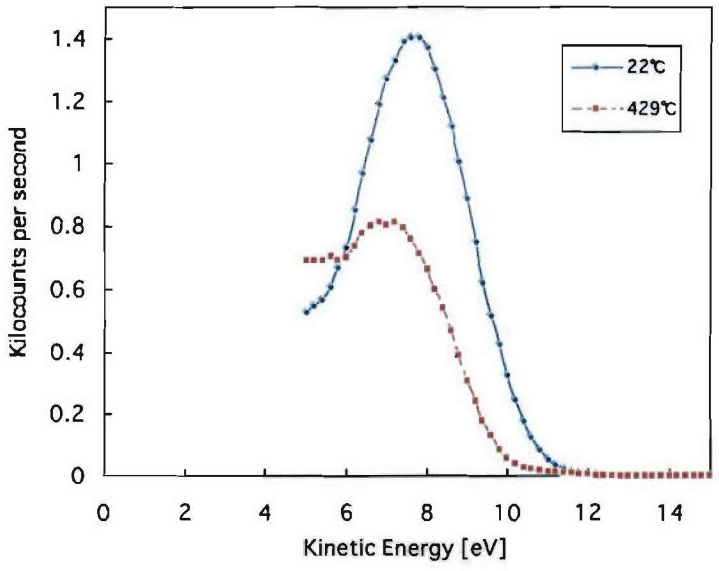

Fig. 13 Secondary electron energy distributions at room temperature and 429 ℃
(Sample:Alumina HA95)

Further measurements were carried out for another type of aluminas ; named KP95 (Alumina purity : 95 %), and KP990. Results are shown in Fig.14 for KP95 and Fig. 15 for KP990.

Both Fig.s show decrease of secondary electrons with temperature. Shift of spectrum to lower energy side is significant for alumina KP990, while it is not obvious for alumina KP95. At room temperature the peak of the energy distribution locates at the energy of 8.5 eV. This value is 0.9 eV higher than that of HA95. This difference may come from not only intrinsic characteristics of material but also many factors surface charging, surface contamination, etc.. The full width at half maximum of the spectrum for KP990 at room temperature can be estimated as 3.3 eV. This value almost coincides with that for HA95. Peak shift of the spectrum at high temperature for KP990 is about 0.93 eV.

For KP95 the full width at half maximum could not be estimated, since the slope of lower side of energy spectra were eliminated. This is because the lower limit of energy that the energy analyzer

is capable to analyze energy is 5 eV. When the sample surface is positively charged, emitted electrons decelerated to less than 5 eV can not be analyzed. To eliminate this defect in analyzer behavior, it is effective to bias sample negatively. In the future experiment program we will prepare a power supply to apply bias voltage.

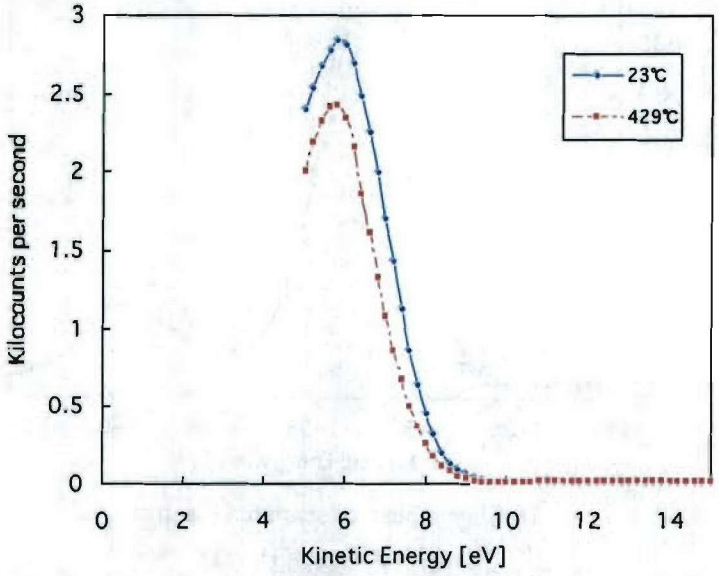

Fig. 14 Electron energy distributions at room temperature and high temperature.
(Sample: Alumina KP95)

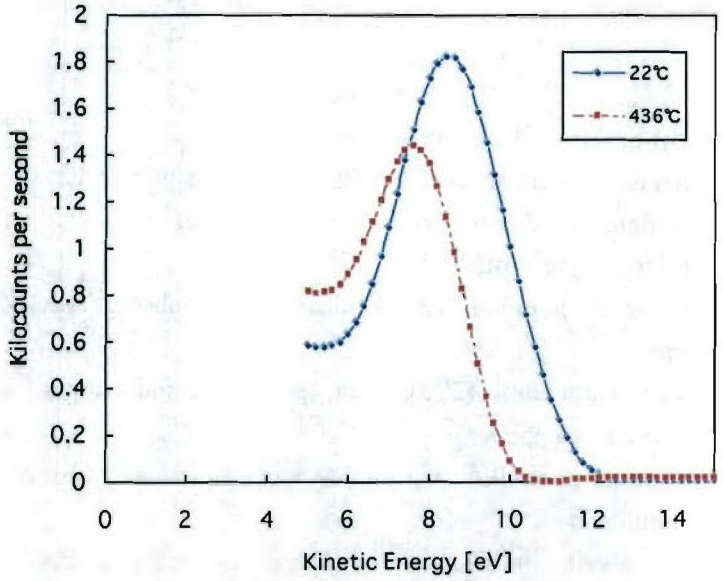

Fig. 15 Electron energy distributions at room temperature and high temperature.
(Sample: Alumina KP990)

3-4-2 Elastic peak

Elastic peak was analyzed as well, since the energy of the elastically scattered electrons is independent of surface charging. Example of elastic peak is shown in Fig. 16. This figure. compares elastic peaks obtained for alumina HA95 at room temperature with that at high temperature. While

shift of the peak is not found, intensity decreases at high temperature.

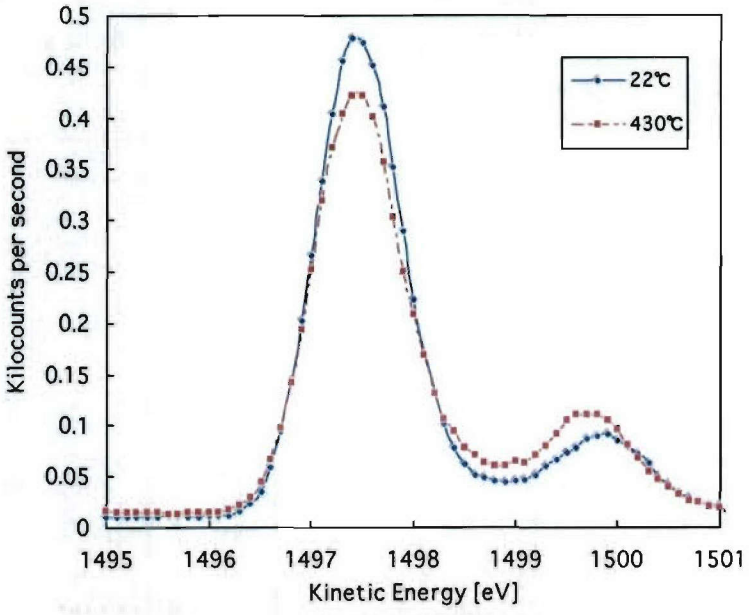

Fig. 16 Elastic peak of scattered electrons.
(Sample: Alumina HA95)

Electron emission is very sensitive to surface conditions. Electron energy spectra shown in Fig. 13 to 16 are influenced surface conditions of samples. To canvass electron energy distribution, it is to analyze surface condition of samples.

4. Conclusion

According to results of this study, it can be conclude that:

a. SEE coefficients of silicon and sapphire could be measured under room and high temperature. SEE coefficients of alumina also were measured under room temperature by absorption and secondary current method.

b. SEE coefficients of alumina KP990 measured by absorption and secondary current method were almost same.

c. In relative high temperature (200℃), an appreciable reduction of SEE coefficient was confirmed for both silicon and sapphire.

d. Position dependence possibility (not only temperature dependence) of SEE coefficient was observed in sapphire (sample B).

e. Electron energy distribution showed that energies of emitted electrons are in about 8 eV at room temperature and its full width at half maximum is in about 3.4 eV at room temprature. These values are independent of samples measured.

f. At high temperature (about 430 ℃) energies of emitted electrons decreases about 0.7 eV, and the number of electrons decreased.

g. To canvass electron emission characteristics described above, it is necessary to analyze surface condition, since sample surface conditions strongly influence on electron emission characteristics.

5. Further experiments planned

In the future, this study will be continued to:

a. Improve the sample holder in order to carry out more high temperature measurement.

b. Investigate the position dependence possibility of secondary electron emission (SEE) coefficient of the insulators.

c. Carry out SEE coefficient measurements under room and high temperature conditions for technical materials, such as alumina.

d. Analyze sample surface condition by for example XPS or AES, in conjunction with electron energy distribution measurements.

e. Process sample surface in vacuum.

References

[1]. Y. Saito, N. Matuda, S. Anami, A. Kinbara, G. Horikoshi, J. Tanaka, "Breakdown of alumina rf windows", IEEE Transaction on Electrical Insulation, Vol. 24, pp. 1029-1036, 1989.

[2]. T. Sato, S. Kobayashi, S. Michizono, Y. Saito, "Measurements of secondary electron emission coefficients and cathodoluminescence spectra for annealed alumina ceramics", Appl. Surface Science 144-145, pp.324-328, 1999.

[3] S. Kobayashi and Y. Saito, "Secondary Electron Emission Measurements on Materials under Stress", Interim report to AOARD/AFOSR, December, 2001.

[4]. A.J. Dekker, "Solid State Physics", pp. 440-442, Prentice-Hall, New York, Maruzen Asian Edition, 1968.

[5]. J.B. Johnson and K.G. McKay, "Secondary electron emission from germanium", Phys Rev, Vol. 91, pp. 582-587, 1953.

[6]. J.B. Johnson and K.G. McKay, "Secondary electron emission of crystalline MgO", Phys Rev, Vol. 93, pp. 668-672, 1954.

[7]. H. Seiler, "Secondary electron emission in the scanning electron microscope", J. Appl Phys, Vol. 54, No. 11, pp. R1-R18, 1983.

[8] A. J. Dekker, "Solid State Physics", p. 421, Prentice-Hall, New York, Maruzen Asian Edition, 1968.

Third interim report

- Measurements under high temperature and multi-pulse technique -

Interim Report to AFOSR/AOARD

Secondary Electron Emission (SEE) Measurements of Materials under Stress

Shinichi Kobayashi[1)] and Yoshio Saito[2)]

[1)]Department of Electrical and Electronic Systems
Saitama University
255 Shimo-Okubo, Sakura-ku, Saitama-shi, 338-8570, Japan
Tel : +81-48-858-3469
Fax : +81-48-855-7832
E mail : s.kobayashi@ees.saitama-u.ac.jp

[2)]Accelerator Laboratory
High Energy Accelerator Research Organization (KEK)
1-1 Oho, Tsukuba, Ibaraki, 305-0801, Japan

Summary

Surface flashover along the rf window insulator of high-power klystrons is a present problem in the their applications. In the mechanism of the surface flashover, multiplication of secondary electrons emitted from the insulator surface and the temperature rise caused by microwave passing through the insulator often take place. Therefore, studies on secondary electron emission (SEE) characteristic under high temperature condition are required to understand the breakdown process in the rf window insulator. In this experiment the SEE coefficients of various alumina ceramics, sapphire, SiO_2 and MgO were measured under room and high temperature (up to 700℃) conditions. The measurements were carried out using a scanning electron microscope (SEM) with single pulsed electron beam of primary current (1 ms duration, 100 pA). A reduction of SEE coefficients of the samples with temperature rise was confirmed, except for sapphire. This reduction is considered due to the larger phonon and electron scattering at high temperature. To investigate the realistic SEE with surface charging, measurements of SEE with double-pulses and two patterns of multi-pulse series of primary electron current were also carried out. Then the waveforms of the SEE pulses under room and high temperature were compared.

1. Introduction

Klystrons, the high power microwave generator, are used for particle acceleration energy sources in a high-energy accelerator. In the klystron, there is an rf window which is made of an insulator. Flashover along the insulator surface is a present problem in the klystron applications for high power use. Therefore, it is necessary to understand the surface flashover phenomena in order to improve transmission capability of the high power microwave [1) 2)].

The important points in the breakdown mechanism along the rf window insulator are multiplication of secondary electrons emitted from the insulator surface and temperature rise of the insulator, since the rf window of a klystron under operation may be heated by energy loss caused by the microwave transmission. Therefore, study on secondary electron emission (SEE) characteristic under high temperature condition is required to understand the breakdown process in the rf window.

Some theories have been proposed to explain the temperature effect of SEE [3-6)]. However, there are still only few data of SEE under high temperature condition, especially for technical material. This study aims to observe secondary electrons emitted from technical insulator materials under room and high temperature.

2. Experimental Setup

2.1. SEE measurement system

The measurements of SEE coefficients were carried out using a scanning electron microscope (SEM). Sample stage of the SEM was modified to enable a sample to heat up to 750℃. Schematic diagram of the measurement system is shown in Fig. 1. Single short-pulsed electron beam (1 ms, 100 pA) was used as primary current to avoid surface charging on the insulator sample. The primary current was measured using a Faraday cup installed on the heat reflector set above the sample. The primary electron was irradiated to the sample through a hole (about 2 mm of diameter) on the heat reflector. Then

the secondary electrons emitted from the sample were captured by the heat reflector, which was coated with a diamond like carbon (DLC) film in order to minimize the SEE from the reflector surface. A positive bias voltage (+40 V) is applied to the reflector to ensure all of the secondary electrons were captured.

To reduce the influence of surface charging, measurements by one shot of primary electron beam irradiation at one site on the sample insulator surface were is carried. Then, the sample was moved to the next measurement site by about 2 mm for x direction and or about 1 mm for y direction.

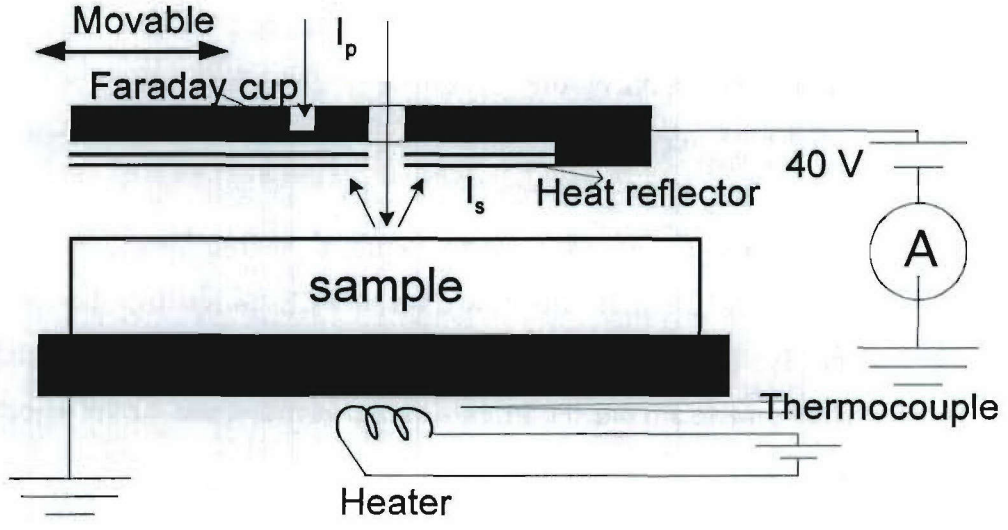

Fig. 1. Schematic diagram of the SEE coefficient measurement system.

2.2. Samples

Examined samples in this study were HA series (HA-92, HA-96, HA-997) and KP series (KP-990, KP-999) of alumina ceramics, sapphire, SiO_2 and MgO. Properties of the samples are listed in Table 1.

Table 1 Properties of examined samples.

Material name	Purity	Grain size (μ m)
Alumina HA-92	92 %	4
HA-960	96 % + HIP	4~5
HA-997	99.7 %	18
KP-990	99.5 %	2~3
KP-999	99.9 %	-
Sapphire	Single crystal	-
SiO_2	Single crystal	-
MgO	Single crystal	-

3. Results and Discussion

3.1. Secondary electron current waveform

For SEE measurement of insulator materials, even if a single short-pulsed electron beam with quite low charge density (3 μ C/m^2) was applied, build-up of surface charging took place resulting a decrease of the secondary current pulse. Fig. 2 shows the waveform of the secondary current (bottom line). In the figure the rapid decrease in the SEE current corresponds to the build-up of the surface charging. In that case, the secondary current is defined at the maximum of the pulse.

3.2. SEE coefficients of alumina ceramics and sapphire

Alumina ceramics and sapphire disk (single crystal alumina) were annealed up to 1400℃ in air for 1 hour in oder to remove the mechanical stress which affects their properties concerning the trapped or stored charges in the vacancies [2].

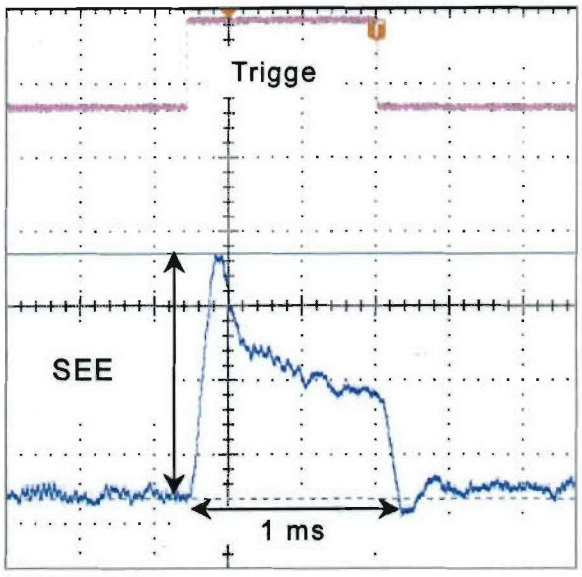

Fig. 2. Waveform of secondary electron current emitted from insulator (bottom line).

The SEE coefficients (δ) of alumina ceramics were measured under room temperature and 700℃. Fig. 3 and Fig. 4 show the SEE coefficients of HA series aluminas (HA-92, HA-960, HA-997) and KP series aluminas (KP-990, KP-999), respectively. Although there is scattering of data, it is found that the SEE coefficients of the samples under 700℃ are lower than those obtained under room temperature condition. At present, there are still only few theories of the SEE under high temperature conditions, especially for insulator materials. However there is a consideration that the decrease of SEE coefficient of insulators at high temperature may be caused by the shorter mean free path of the secondary electrons due to the larger phonon and electron scattering in the bulk [3) 6)]. Therefore, under high temperature condition the number of secondary electrons approaching the surface are less than those at room temperature.

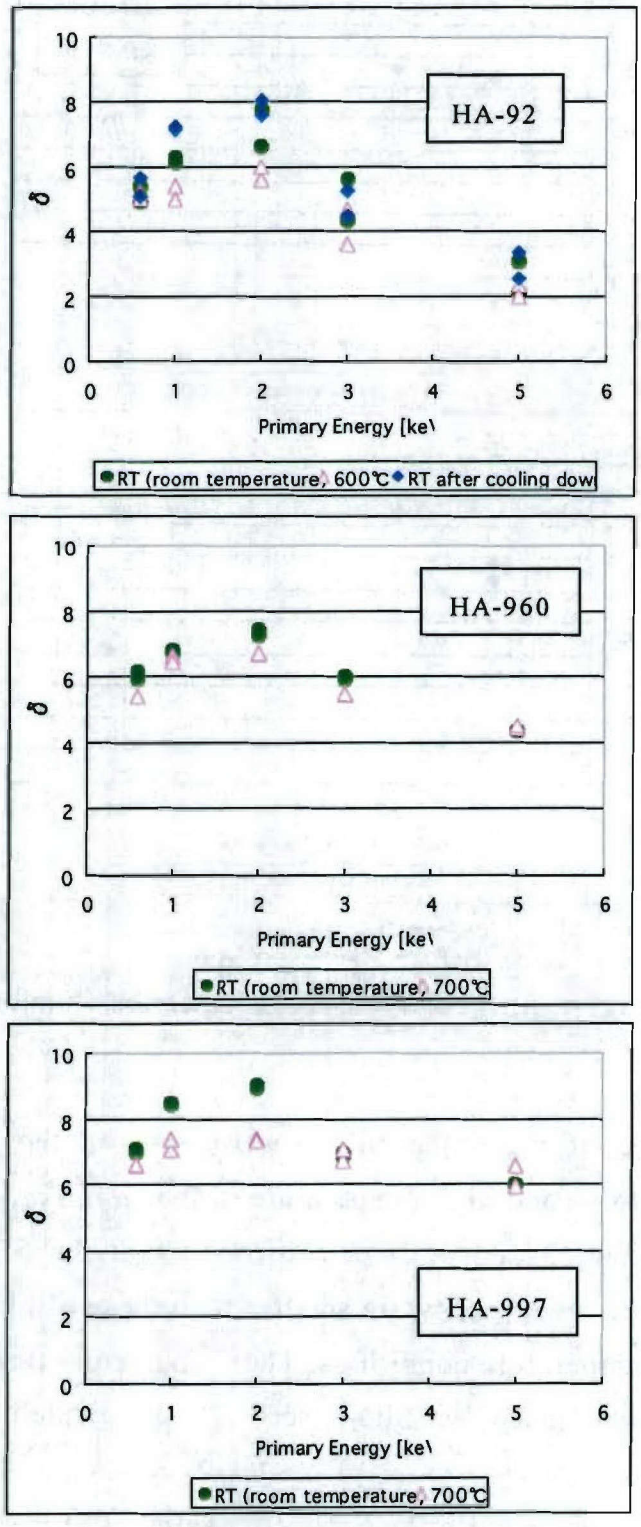

Fig. 3. SEE coefficients of HA series aluminas.

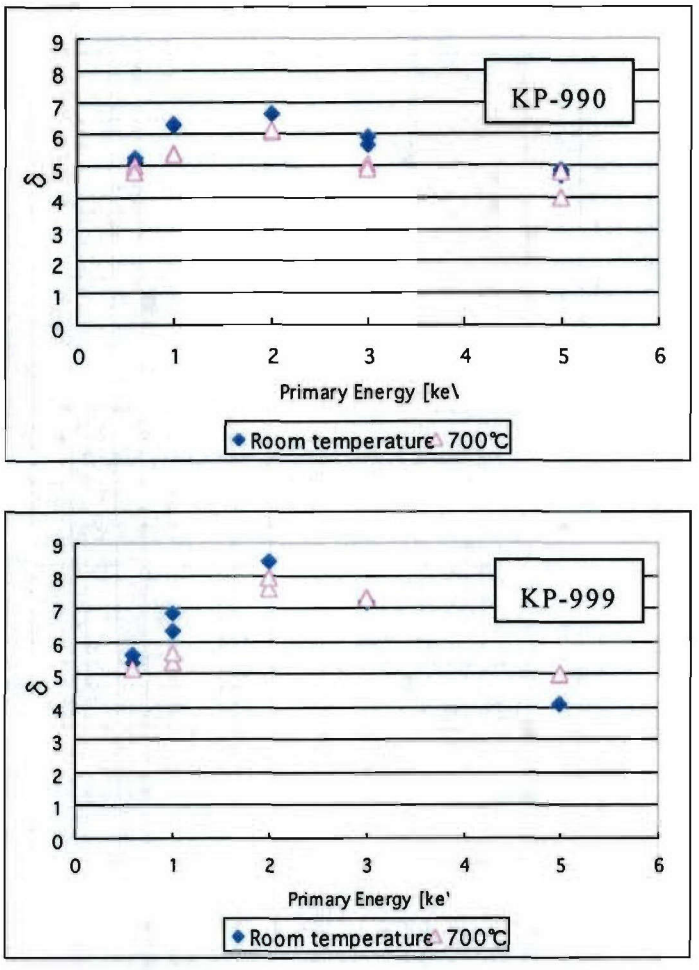

Fig. 4. SEE coefficients of KP series aluminas.

Dependence of maximum SEE coefficients on the purity of various aluminas under room and high temperature is shown in Fig. 5. These data were compiled from Fig. 3 and 4. It is confirmed that the SEE coefficients of alumina contained lower purity are smaller than those of higher purity at both room and high temperature conditions. These characteristics may be caused by sintering additives, such as SiO_2 (see Fig. 8), which have small SEE coefficients.

Fig. 6 shows the correlation between maximum SEE coefficients and the grain size of alumina ceramics under room and high temperature. It is found a trend that the SEE coefficients increase with the grain size of aluminas.

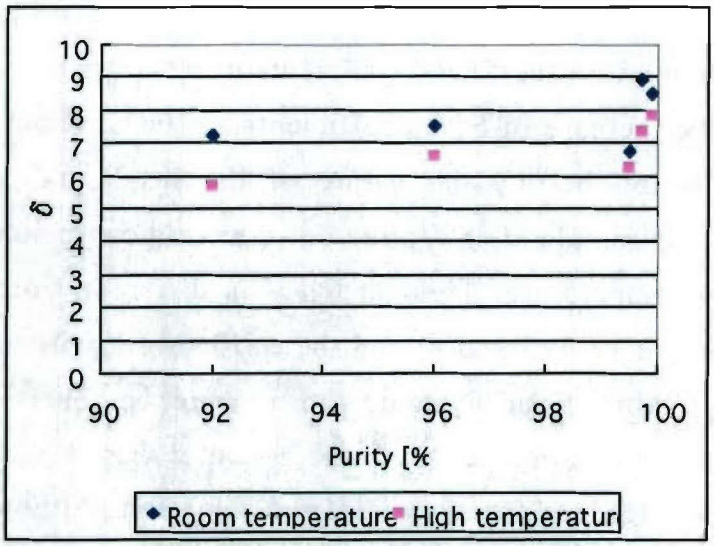

Fig. 5. Correlation between SEE coefficients and purity of aluminas.

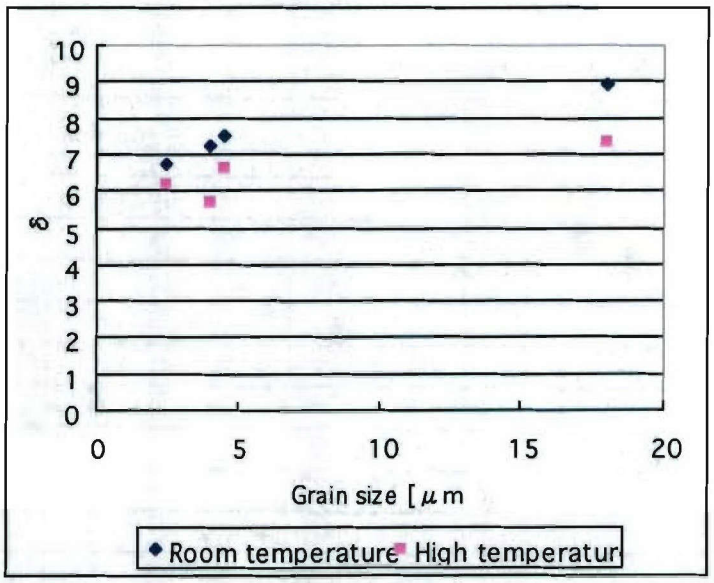

Fig. 6. Correlation between SEE coefficients and grain size of aluminas.

The SEE coefficients of sapphire disk were measured at room temperature and 700℃. The measurement result is shown in Fig. 7. It is found that at high temperature the SEE coefficients were larger than those at room temperature. The increase of SEE coefficients at 700℃ is not caused by the surface modification but by the nature of the insulators, since the SEE coefficients of this sample after cooling down are almost same as the previous values at room temperature. This tendency is different from measurement results for aluminas (Fig. 3 and 4) and the earlier work obtained for MgO [4]. The defect transition from F^+-center to F-center probably enhanced the secondary electron creation because the F-center has a state near to the conduction band, leading the easy electron emission. Although the escape depth of secondary electrons decrease at high temperature due to an increase of the phonon scattering, it is considered that the increase of the secondary electron creation rate at high temperature is dominated in the SEE of the sapphire disk. The excess surface heating due to multipactor would result in higher SEE yields, and advance the multipactor.

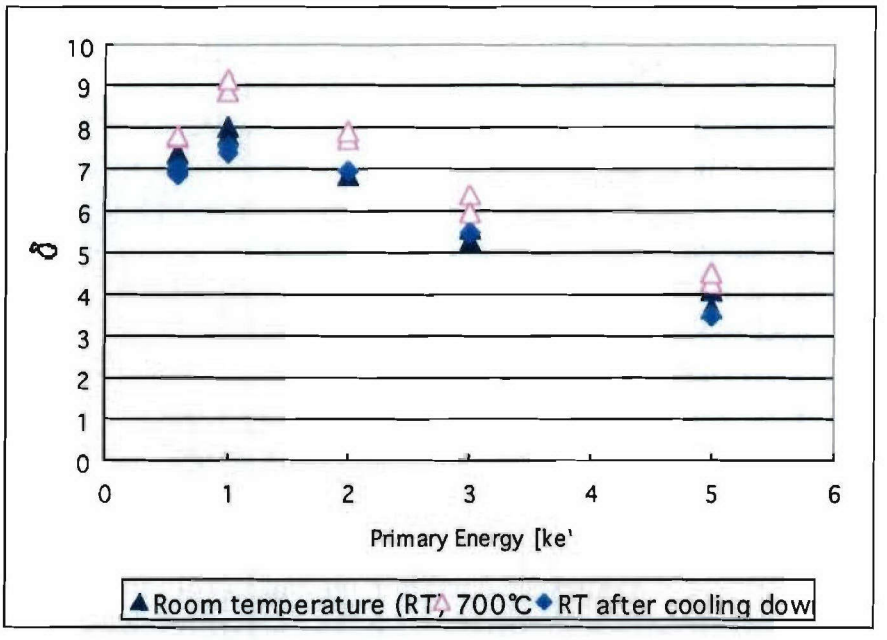

Fig. 7. SEE coefficients of sapphire.

3.3. SEE coefficients of SiO_2 and MgO

SiO_2 and MgO are usually used as sintering additives for alumina ceramics [2]. Therefore it is necessary to measure the SEE coefficients of those materials under high temperature condition. SiO_2 sample used in this study was a disk with diameter of 19 mm and thickness of 1 mm. To remove mechanical defects and surface charging, the SiO_2 sample was also annealed in air up to 700℃ for 1 hour before measurement. The SEE coefficients of SiO_2 were measured at both room temperature and 400℃. Results are shown in Fig. 8. From this figure, it is confirmed that the SEE coefficients of SiO_2 decrease with temperature rise, which can be interpreted by the smaller escape depth due to phonon scattering at high temperature.

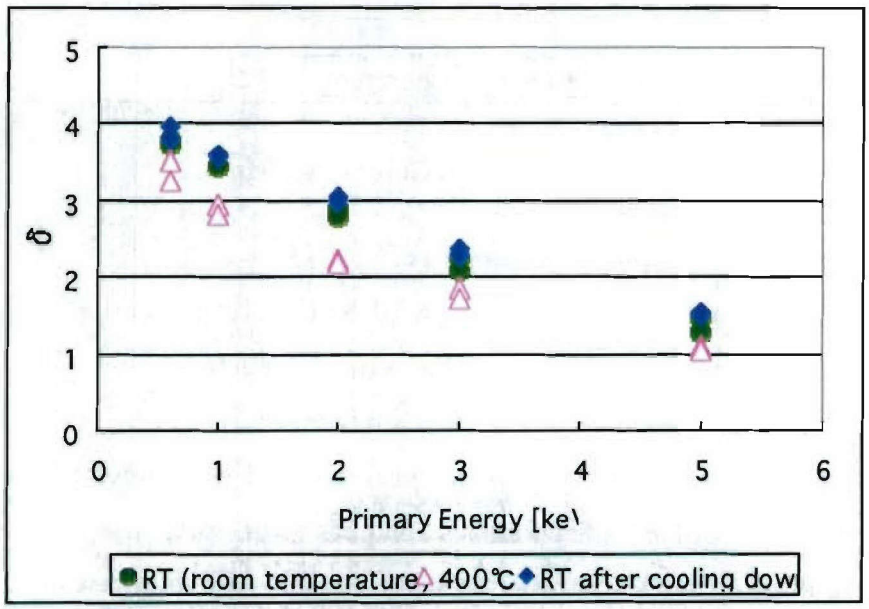

Fig. 8. SEE coefficients of SiO_2.

Measurements of SEE coefficient of MgO disk (19 mm in diameter, 1 mm in thickness) were carried out at room temperature and 700℃. Before measurements the MgO sample was annealed up to 1400℃ in air for 1 hour, as well as for the alumina and SiO_2 samples. The measurement result is shown in Fig. 9. At 700℃, the SEE coefficients of the MgO are lower than those at

room temperature condition. This result agrees with the earlier work [4]. The decrease of the SEE coefficient is caused by the same reason as those for alumina and SiO_2 samples.

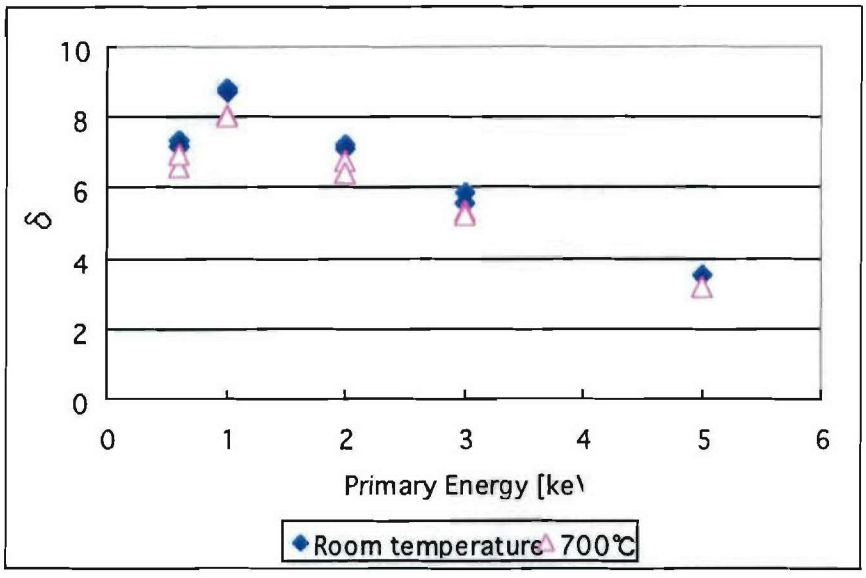

Fig. 9. SEE coefficients of MgO.

3.4. SEE with multi-pulse measurements

According to Fig. 2, the waveform of SEE current decrease caused by a build-up of surface charging on the sample surface was observed. To investigate the SEE characteristics with surface charging, SEE measurements with double-pulses of primary current were carried out under room and high temperature. Two pulses of primary currents (100 pA, 1 ms) with 1 keV energy were applied with various rest time. Fig. 10 shows the waveform of the first and second SEEs of alumina HA-997 for rest time duration 0.5, 3, and 10 ms, respectively. Relation between δ_2/δ_1 and rest time duration at room temperature and 700℃ is shown in Fig. 11, where δ_1 denotes the SEE coefficient of the first pulse and δ_2 denotes the SEE coefficient of the second pulse. At room temperature peaks of the SEE current excited by second pulses becomes higher with longer rest. However, at 700℃ the peaks of the second pulses are almost same as the first one. It indicates that there is surface charging modification on the insulator when temperature becomes high.

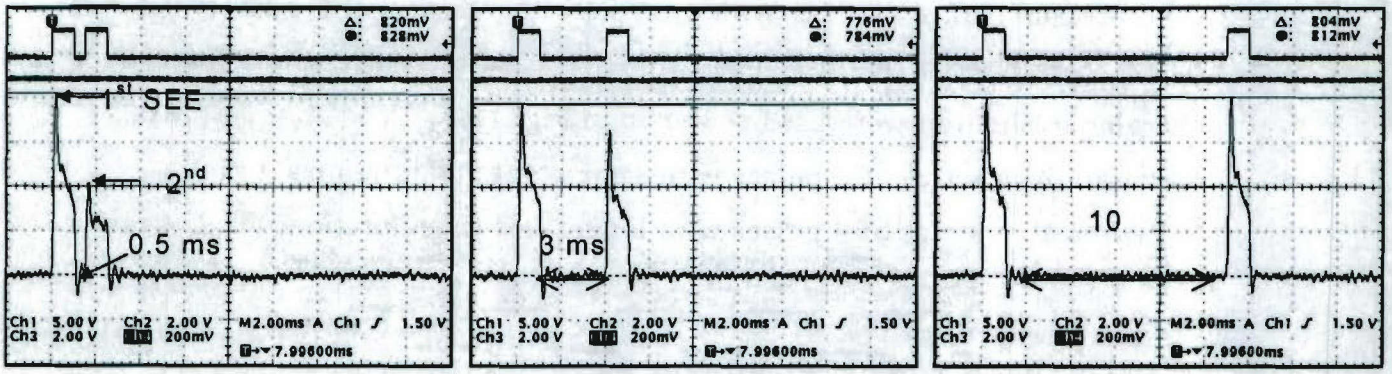

(a) Room temperature

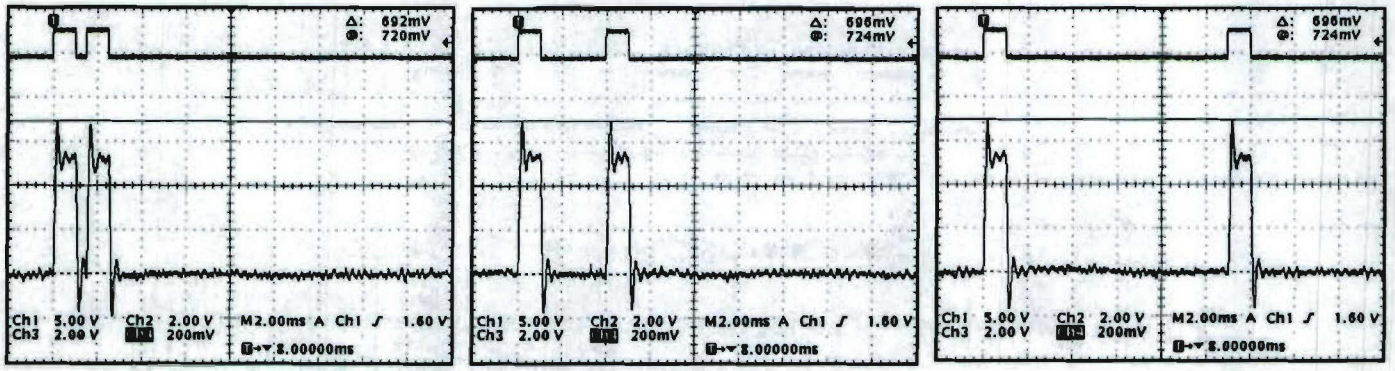

(a) High temperature (700℃)

Fig. 10. Waveforms of the first and second SEEs for the rest time duration of 0.5, 3, and 10 ms. Sample was alumina HA-997.

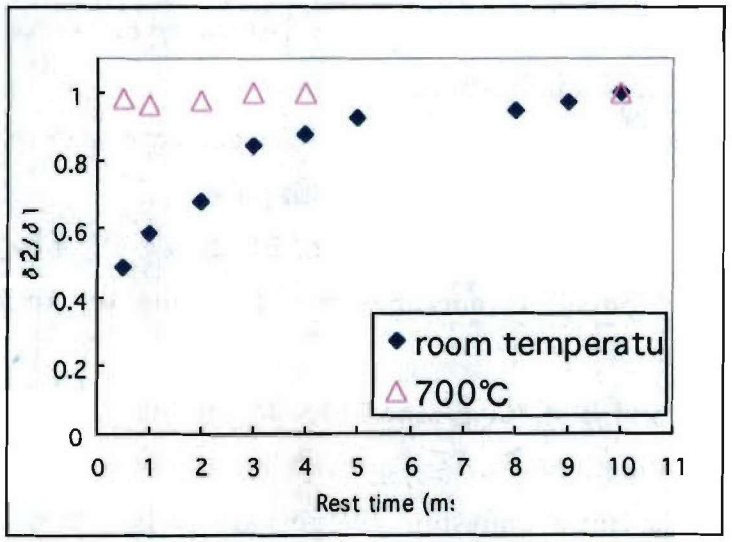

Fig. 11. Relation between δ_2/δ_1 and rest time duration at room temperature and 700℃. δ_1:SEEs at the 1st pulse, and δ_2:SEEs at the 2nd pulse.

Measurements of SEE with two patterns of series of primary current pulses were also carried out. The two patterns of the pulse series for surface charging evaluation were used as shown in Fig. 12.

1. Pattern A, a series of 5 pulses with same rest time durations (1 ms).
2. Pattern B, a series of 4 pulses with longer rest time durations (1, 2, 4 ms).

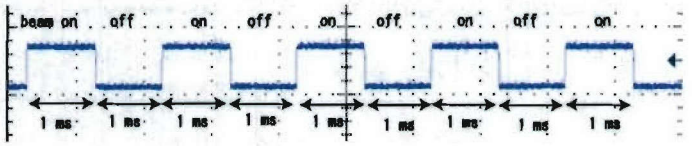

(a) Pattern A

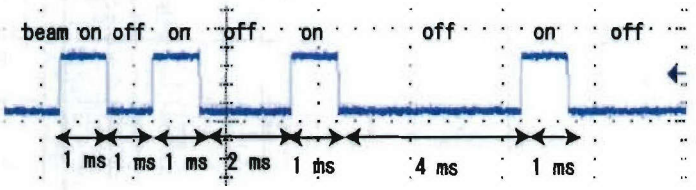

(b) Pattern B

Fig. 12. Two patterns of series of primary current pulses used for multi-pulses measurements.

SEEs of alumina KP-999 with multi-pulses primary current were measured. Fig. 13 shows the waveform of the SEE at room temperature and 700℃ for pattern A and pattern B. Fig. 14 and 15 show SEE coefficients and total emission charge calculated from each SEE pulse (1ms) for both patterns, respectively. The results indicate that:

1. For pattern A at room temperature the SEE decrease with pulse series, and total emission charges also decrease with pulse.
2. For pattern B at room temperature the SEE at the 4^{th} pulse is larger than that at the 3^{rd} pulse. It may be caused by the reluxation of surface charging.
3. For patterns A and B at 700℃ the SEEs do not change with pulse series. It may be due to the higher surface electric conductivity at high temperature. In addition, the total emission charges are larger than those at room temperature, though the SEE coefficient is smaller. In the insulator application this emission charge enhances field stress on its surface, and in

turn, leads to a breakdown.

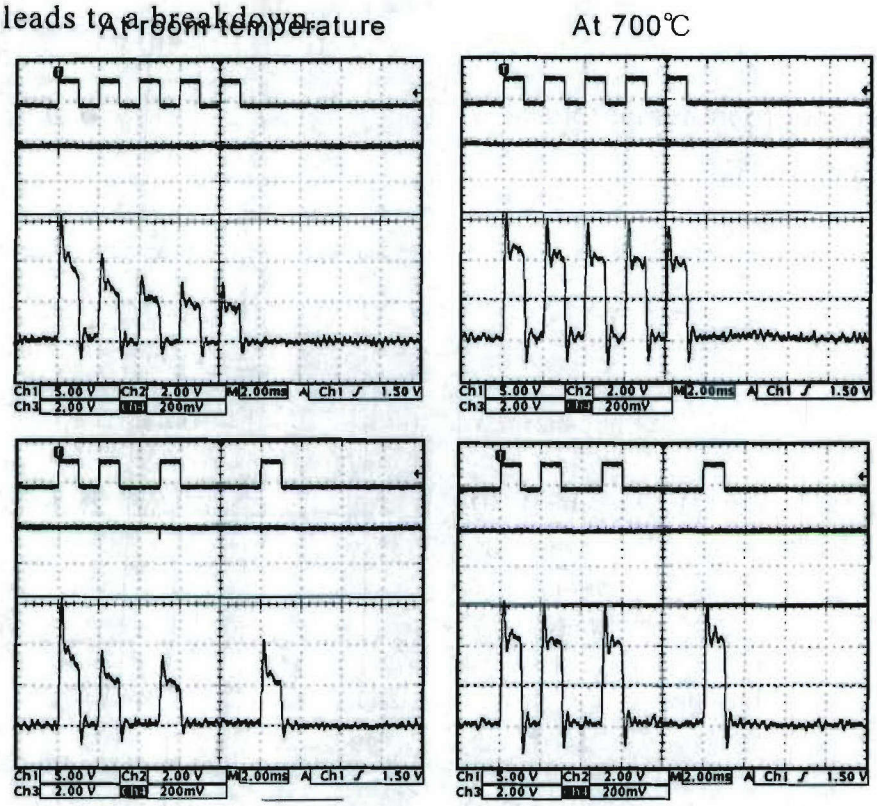

(a) sample: alumina KP-990

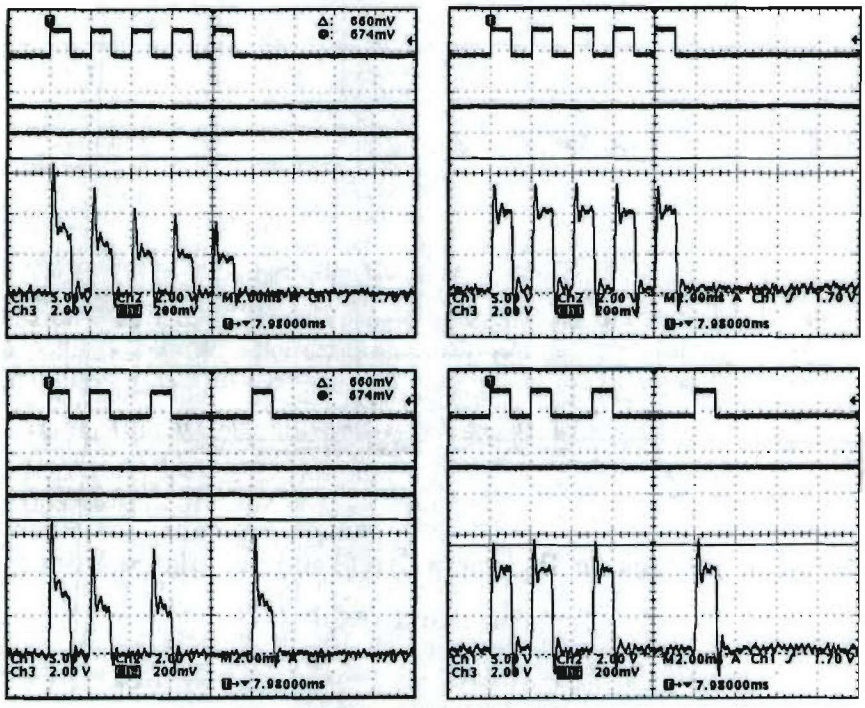

(b) sample: MgO

Fig. 13. SEE current waveform of alumina KP-990 and MgO obtained by

multi-pulse measurements.

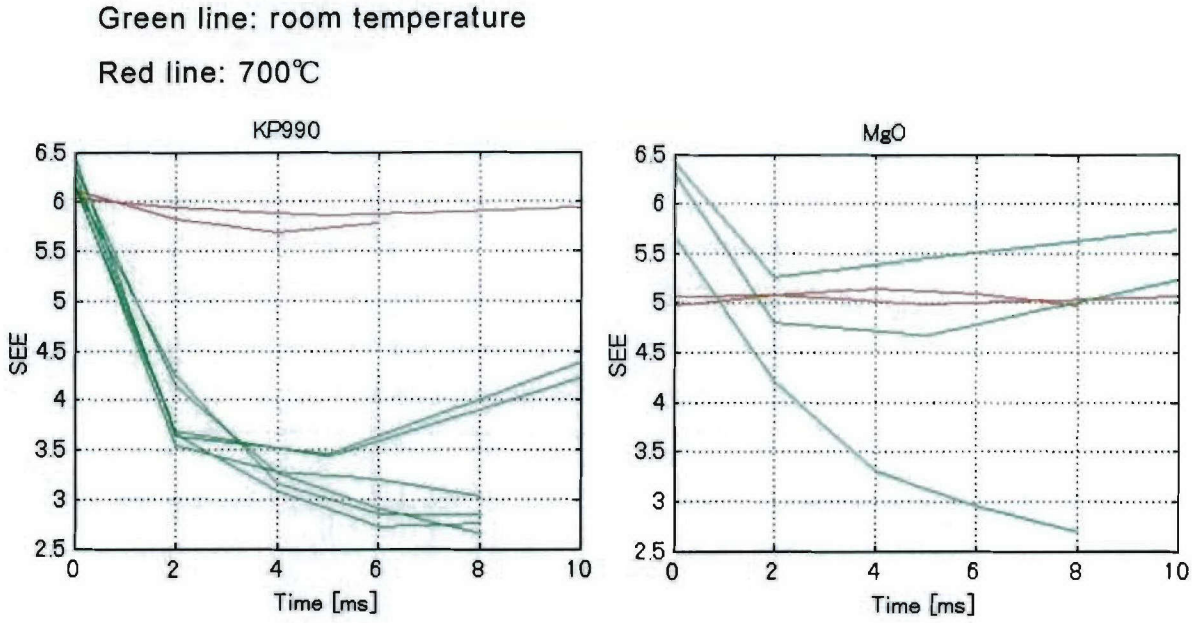

Fig. 14. SEE coefficients obtained by multi-pulse measurements.

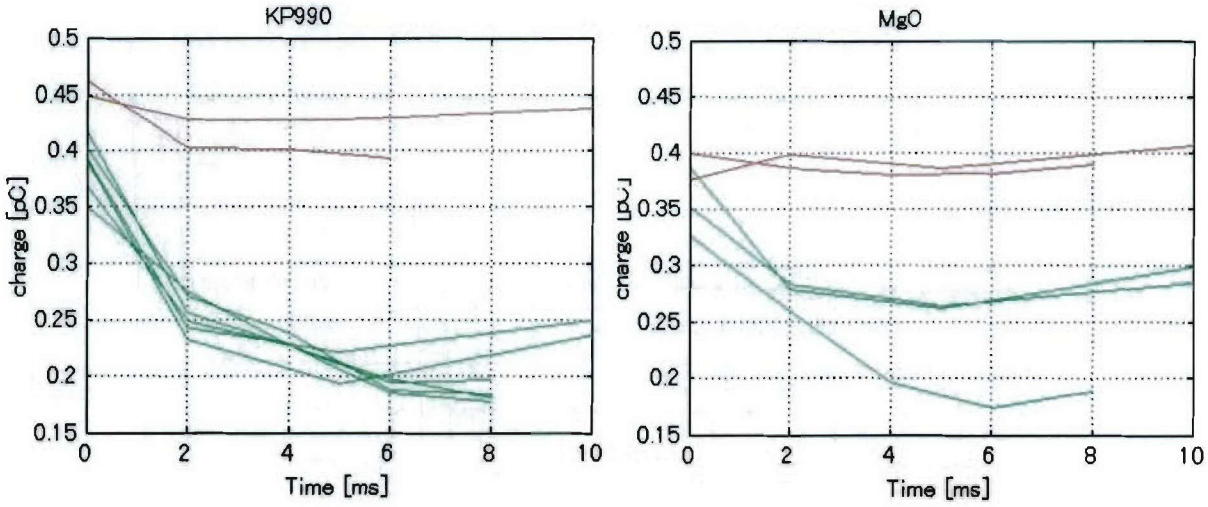

Fig. 15. Emission charges during one pulse (1ms) calculated from multi-pulse measurement results.

4. Conclusion

a. SEE coefficients of various kinds of alumina ceramics, sapphire, SiO_2, and MgO could be measured under room temperature and up to 700℃.
b. A reduction of SEE coefficient of the samples under high temperature condition was confirmed, except for sapphire. This reduction may be caused by the shorter mean free path of the secondary electrons due to the larger phonon and electron scattering at high temperature.
c. An increase of SEE coefficients at high temperature was observed for sapphire sample. This may be due to the higher secondary electron creation caused by the transition of the oxides defects from F^+-center to F-center.
d. The SEE coefficients tend to increase with purity and grain size. This tendency was found at both room and high temperature conditions.
e. At high temperature (700℃) the SEE waveform did not change with pulse series. It may be due to the higher surface electric conductivity at high temperature. In addition, the total emission charges were larger than those of room temperature, though the SEE coefficient was smaller.

5. Future Work

Based on the results described above high power microwave transmission test using the resonant ring is going to be conducted. The test aims at comparing breakdown strength of kinds of alumina ceramics to correlate secondary electron emission characteristics. In addition the effect of insulator surface coating by thin films having lower secondary electron emission coefficient, such as TiN will be also investigated.

References

1) Y. Saito, N. Matuda, S. Anami, A. Kinbara, G. Horikoshi and J. Tanaka: "Breakdown of alumina rf windows", IEEE Transaction on Electrical Insulation, 24, 1989, pp. 1029-1036.
2) T. Sato, S. Kobayashi, S. Michizono and Y. Saito: "Measurements of secondary electron-emission coefficients and cathodoluminescence spectra for annealed alumina ceramics", Applied Surface Science 144-145, 1999, pp. 324-328.
3) A.J. Dekker: "Solid State Physics", Maruzen Asian Edition, 1968, pp. 440-442.
4) J.B. Johnson and K.G. McKay: "Secondary electron emission of crystalline MgO", Physical Review, 91, 1953, pp. 582-587.
5) J.B. Johnson and K.G. McKay: : "Secondary electron emission from germanium", Physical Review, 93, 1954, pp. 668-672.
6) J. Cazaux: "About the secondary electron emission yield, δ, from e^--rradiated insulators", Mikrochimica Acta, 132, 2000, pp. 173-177.

Fourth interim report

- Multi-pulse measurements and high power test -

Secondary Electron Emission (SEE) Measurements of Materials under Stress

Shinichi Kobayashi[1)] and Yoshio Saito[2)]

[1)]Department of Electrical and Electronic Systems
Saitama University
255 Shimo-Okubo, Sakura-ku, Saitama, 338-8570, Japan
Tel : +81-48-858-3469
Fax : +81-48-855-7832
E mail : s.kobayashi@ees.saitama-u.ac.jp
[2)] Accelerator Laboratory
High Energy Accelerator Research Organization (KEK)
1-1 Oho, Tsukuba, Ibaraki, 305-0801, Japan

1. Introduction

Alumina ceramics are widely used as electrical insulators in many applications of vacuum devices, such as klystron, because they have excellent characteristics as high mechanical strength, high resistivity at high temperature, small microwave losses, and few gas emissions. The klystrons are used as microwave sources to accelerate charged particles in a high-energy accelerator. The alumina ceramics are used as an rf window between the acceleration tube and the klystron to pass the microwave and to seal the vacuum.

Requirement of high-power klystron currently increases because of demand of the acceleration energy rise. One of the most serious problems for developing the high-power klystron is surface flashover along the alumina rf window [1]–[3]. The surface flashovers also often occur in other high voltage vacuum devices. It is well recognized that the flashover voltages on insulator surfaces are fairly lower than those of vacuum gaps under the same length between two conductors, because the dielectric strength of an insulator surface in vacuum is inferior to that of the insulator itself, and depends upon many parameters [4]–[6]. Therefore, the ability of an insulator to sustain high voltage in vacuum is limited by the surface flashover, and improvement of the hold-off voltage of the insulator surface is required to minimize the size of electrical equipment.

Many theories have been proposed to explain the surface flashover mechanism along insulators [4]–[7]. The most generally accepted mechanism is "secondary electron emission avalanche (SEEA)" model [6]. According to the model, the flashover may be initiated by primary electrons emitted from the triple junction. Then these primary electrons are accelerated and multiplied due to the high secondary electron emission coefficient of insulators. Unfortunately, this multiplication of the secondary electrons (multipactor) induces the excess surface heating, leading to the localized surface melting. Therefore, studies on SEE coefficient of insulators under high temperature condition are required to understand the surface flashover process.

Extensive studies on the secondary electron emission (SEE) have been carried out since the 1902 by Austin and Starke [8], and are thoroughly studied by many researchers until now. Many theories based on the studies have been proposed to explain the SEE phenomena [8]–0. However, there are still few experimental data of SEE under high temperature condition, especially for technical materials such as alumina ceramics, etc. Therefore, more empirical data are needed to support theories

and clarify the phenomena.

Objective of this study is to investigate secondary electrons emitted from several kinds of commercial alumina ceramics for electrical insulation use in vacuum and other ceramic materials such as sapphire (single crystal alumina), SiO_2, and MgO. The secondary electron emissions (SEE) were observed under room and high temperature conditions. To suppress multipactor, TiN film having low SEE is sometimes coated on the rf window. Influence of TiN film coatings on SEE coefficients of alumina ceramics under room and high temperature conditions were also investigated. To evaluate the durability, observations of the luminescence of some alumina rf window were carried out by high power tests using a resonant ring.

It is also revealed that the SEE decreases with electron irradiation due to the surface charging. The charging on the surface decreases with time. The time constant should decrease at high temperature due to the higher electric conductivity of the dielectric material. Thus, the excess heating results in the decrease on surface charging leading to the effective increase in the total SEE, so that the evaluation of the surface charging is important for understanding the electrical discharge. In order to understand the surface charging, a multi-beam irradiation method is adopted and surface charging of the commercial alumina ceramics is also summarized.

2. Experimental setup

2.1 SEE measurement system

SEE measurements were carried out using a scanning electron microscope (SEM) under room and high temperatures. Sample stage of the SEM was modified to enable a sample to be heated up to 750°C [15].The vacuum pressure during the measurement is around 10^{-4} Pa. Schematic diagram of the measurement system is shown in Fig. 1. Since the long pulse irradiation (>10 ms) and/or large number of irradiation (>10) can induce the serious charging on the surface, the primary beam of 100 pA, 1 ms with quite low current density (3 $\mu C/m^2$) is adopted. The primary current is measured at the biased (+40 V) Faraday cup made of graphite. The secondary current is captured by the biased heat-reflector coated with DLC (diamond-like-carbon) film having low SEE yield.

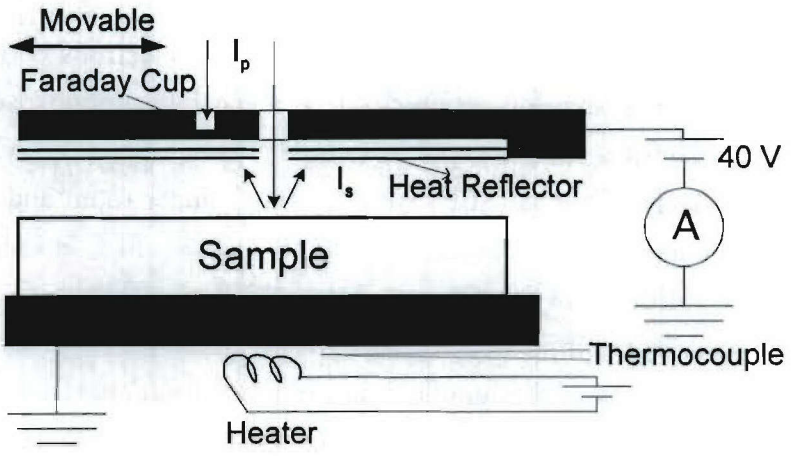

Figure 1: Schematic diagram of SEE measurement system.

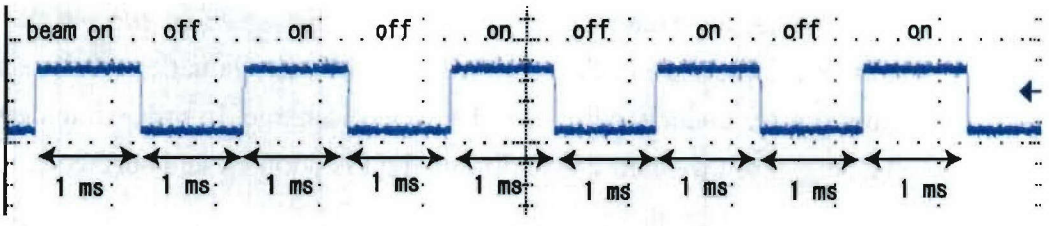

(a) Pattern A

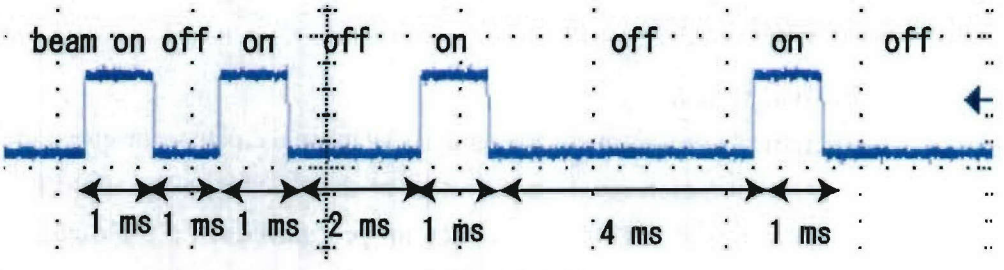

(b) Pattern B

Figure2: Two patterns of the successive pulses were (100 pA, 1 ms, 1 keV) employed in multi-pulse measurements.

SEE measurements were carried using:

a. Single-pulse measurement to observe the SEE coefficient of the sample,
b. Multi-pulse measurement to observe surface charging characteristic.

For multi-pulse measurements, two patterns are examined as shown Fig. 2. Both

patterns irradiate 4 or 5 pulses to a same point. Although the total irradiation charges become 4 or 5 times larger than the standard pulsed-beam method, both SEE and surface charging can be estimated. Pattern A is an irradiation with same intervals of 1 ms (Fig.2 (a)). The SEE at pattern A enables to evaluate the secondary electron supply. If the larger decrease is observed with the consecutive pulses, the material has smaller secondary electron supply. Pattern B is an irradiation with increasing intervals (Fig.2 (b)). The results are useful for the evaluation of the recovery time constant of the surface charging. If the SEE at 4^{th} pulse is larger than the SEE at 3^{rd} pulse, it means that the SEE recovers by the 4 ms interval corresponding to the typical recovery time of 4 ms. A DAC board installed in PC triggers the primary injection of both patterns. Since the multipactor takes place at less than 5 keV injection [5], the incident energy of 1 keV is utilized for the pattern A and B.

2.2 Examined samples

Samples are several kinds of commercial alumina ceramic disks (19 mm in diameter) used as the electrical insulation in vacuum. Properties of the samples are listed in Table 1. Single crystal alumina (sapphire) and single crystal MgO (the common additives in the commercial alumina ceramics) are also measured. HA-997 are used for high-power rf window material and UHA-99 was used before. Both ceramics are durable for the rf transmission [17]. On the other hand, the sapphire disk showed a poor performance for the rf window application [17]. Alumina HA-960 is specially sintered to make the boundary additives crystallized [16], which contributes to reduction in the dielectric loss tangent to be as small as that of sapphire.

It is well known that ceramic materials may have trapped charges in their vacancies. The trapped charges are not desired because they influence the secondary electron emitted from the ceramic. Sato et. al. reported that the annealing treatment in atmosphere at 1500°C for 1 hour is effective to remove the mechanical stress of insulators which affects their properties concerning reduction of the trapped or stored charges in the vacancies of alumina ceramics, especially for relative low purity alumina (about 90%) [18]. Therefore, all of ceramic materials examined in this study were annealed in atmosphere for 1 hour before measurements. Annealing temperature were 600°C for SiO_2 and 1400°C for other samples.

Table 1. Mechanical and electrical properties of examined samples [16]

Sample	Purity [%]	Specific gravity [g·cm^{-3}]	Flexural strength [Mpa]	Remarks
Alumina HA-92	92	3.6	350	
HA-960	96	4.0	500	Crystallized grain boundaries
HA-997	99.7	3.9	300	
KP-990	99.5	3.9	500	
KP-999	99.9	3.9	320	
UHA-99	99	3.9	520	Dense structure
SSA-S1	99.6	3.9	330	
Sapphire	100	4	420[c]	Single crystal
MgO	100	3.6		Single crystal

	Grain size [μ m]	Dielectric constant (10 GHz)	Loss tangent (10 GHz)	Volume resistivity [Ω m]
Alumina HA-92	4	8.6	8E-4	>10^{12}(25℃)
HA-960	3	10.0	4E-5	>10^{12}(25℃)
HA-997	10	9.95[a]	1E-4	>10^{12}(25℃)
KP-990	4	9.7	3E-4	>10^{12}(25℃)
KP-999	15	9.9[b]	9E-4[b]	>10^{13}(25℃)
UHA-99	4		1E-4	
SSA-S1	15		3E-4	
Sapphire	-	10.16[a]	3E-5	-
MgO				

[a]At 3.4 GHz.

[b]At 8~9 GHz.

[c]*C* plane.

2.3 TiN coating on alumina ceramics

Thin TiN films having low SEE coefficients are coated on alumina ceramic disk to suppress multipactor. Depositions of TiN films on the disks were carried out at room temperature in an ultrahigh vacuum (UHV) system whose chamber pressure was maintained in 10^{-8} Pa orders. The films were formed by reactive direct current magnetron sputtering in a mixture of N_2 and Ar [19]. The sputtering was directed to a target of 20 cm diameter high-purity Ti disk (>99.9%) without bias voltage application on the alumina disk. Thickness of TiN film was observed using a crystal thickness monitor which was calibrated by an interferometer. The deposition rate was about 0.5 nm per minute.

3. Results and Discussion

3.1 Incident energy dependence of SEE coefficient

The SEE coefficients of TiN-coated and non-coated alumina ceramics were measured under room and high temperatures. The SEE coefficients were obtained from ratio of the number of secondary to primary electrons. The measurement results for 2.5 nm TiN-coated and non-coated alumina KP-990 samples are shown in Fig. 3. The figure shows relationship between the SEE coefficient and the energy of the incident primary electrons under room and high temperatures.

The results confirmed that the SEE coefficient increases with primary energy for low energies, then goes through a maximum value, and finally decreases for high primary energies [8],[10]. At about 25°C the maximum value of SEE coefficient is about 6.5 for the non-coated alumina KP-990, and becomes about 1.8 for the TiN-coated one. The values of SEE coefficient of the TiN-coated alumina decrease up to less then unity when the primary energy reaches 5 keV. Therefore, the TiN film coating having low SEE coefficients on the alumina ceramics is expected to suppress multipactor. Optimum thickness of TiN film coatings will be discussed in the next sub-section.

At 650°C SEE coefficients of the TiN-coated and non-coated alumina ceramics are lower than those obtained at room temperature. These results agree with the earlier works for MgO [11] and TiN which was coated on [20]. The tendency was also found for SiO_2 and other commercial alumina ceramics [21],[22]. At present, there are still only few theories of the SEE under high temperature condition. However it is considered that the decrease of SEE coefficient of insulators at high temperature may be

caused by the shorter mean free path of the secondary electrons due to the larger phonon and electron scattering in the bulk, affecting the shorter escape depth [9]-[12]. Therefore, under high temperature condition the secondary electrons approaching the surface are less than those at room temperature.

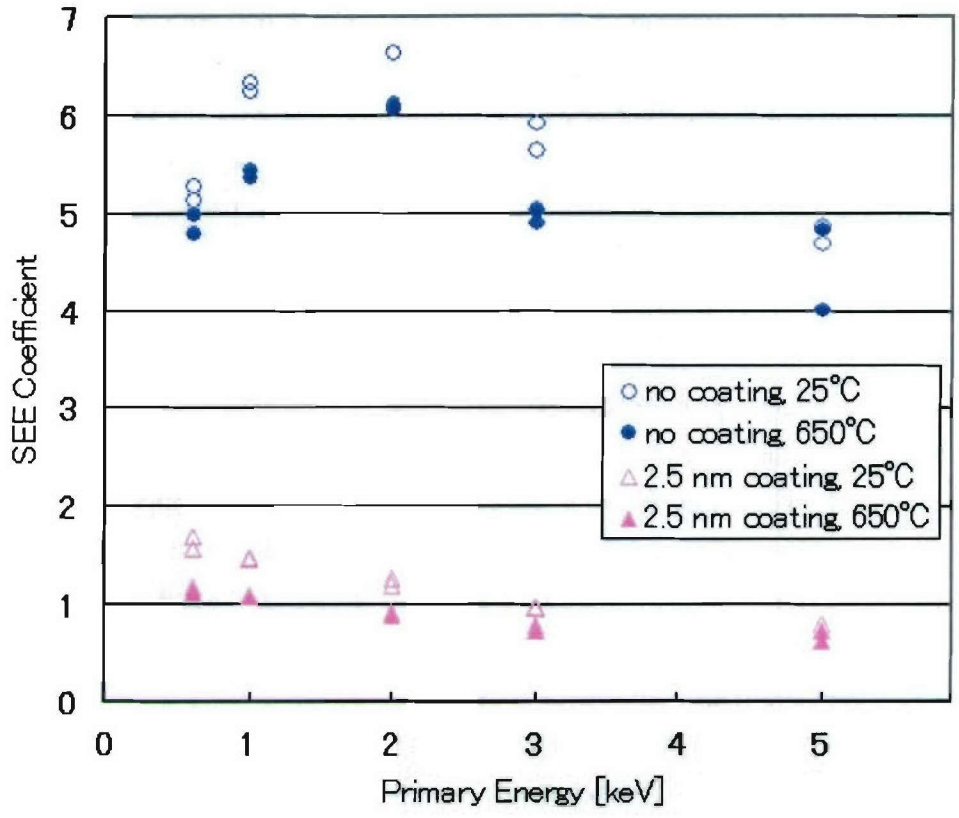

Figure 3: SEE coefficients of 2.5 nm TiN-coated alumina KP-990 at room temperature and 650℃.

3.2 Dependence of SEE coefficient on TiN film thickness

Dependence of SEE coefficients on thickness of the TiN film which are coated on alumina HA-960 (96%), KP-990 (99.5%), KP-999 (99.9%), and sapphire (single crystal alumina) were observed at 25°C and 650°C. Thickness of the TiN film coatings were 0, 0.5 nm, 1 nm, and 2.5 nm. Figure 4 and 5 summarize the relationship between the SEE coefficient and the TiN film thickness obtained by the observation. The primary energies were 1 keV.

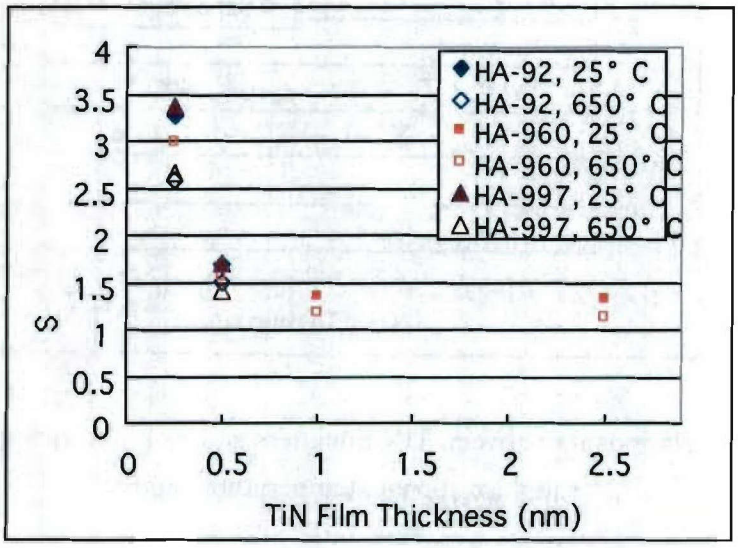

(a) HA series alumia

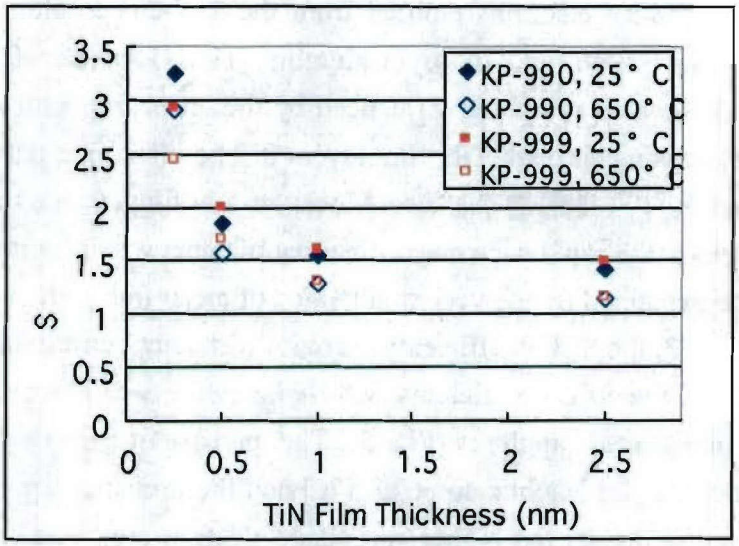

(b) KP series alumina

Figure 4: Relationship between TiN thickness and SEE coefficients of TiN-coated alumina at room temperature and 650℃.

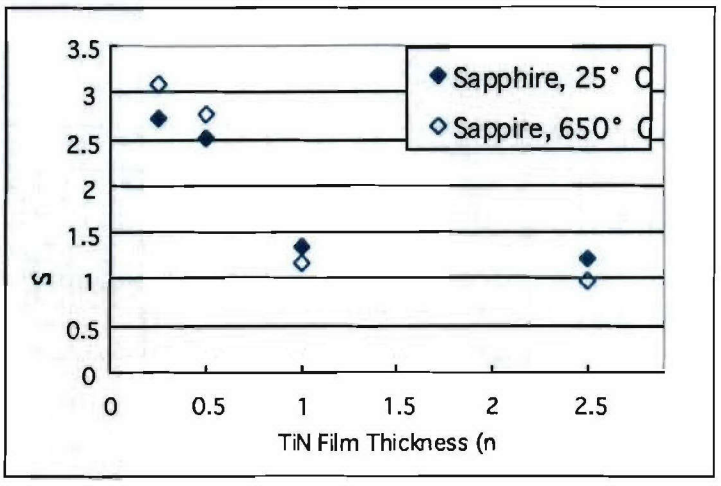

Figure 5: Relationship between TiN thickness and SEE coefficients of TiN-coated sapphire at room temperature and 650℃.

According to the Fig. 4, SEE coefficients of the samples at 25°C decrease with TiN thickness. Secondary electrons emitted from the TiN-coated alumina comprise those generated in TiN films and those in alumina [19]. Decrease of secondary electron number in TiN-coated sample is influenced by the mean free path when the secondary electrons are passing through TiN film layers 0. The mean free path is about 0.4-1 nm for metal and 50-100 nm for insulator. Since the TiN films formed on the alumina disk were conductive, the rapid decrease of SEE coefficients with film thickness as shown in Fig. 4 can be explained by the very small value of mean free path of the film [19]. Same as those of Fig. 3, the SEE coefficients decrease with temperature for all film thickness.

Increase of the SEE coefficients with temperature was observed for 0.5 nm TiN-coated and non-coated sapphires (Fig. 5). The increase of SEE coefficients of sapphire were reported also by Michizono et. al. [20] and the previous report of this work [21]. This is probably due to the higher secondary electron creations caused by the defect transition from F^+-center to F-center in sapphire [20], since the F-center has a state near to the conduction band, leading the easy electron emissions. Therefore, most of secondary electron emissions of sapphire having 0.5 nm film thickness are probably produced from the sapphire and the TiN layers, but dominated from the sapphire layer. This possibility may take place not only in TiN-coated sapphire, but also in the TiN-coated aluminas.

Moreover, it is found that SEE coefficient values of 1 nm and 2.5 nm film thickness

are almost same, but smaller than those of 0.5 nm or less. However the alumina having 0.5 nm TiN thickness still has low SEE coefficients comparing to those of non-coated alumina ceramics.

In practical design of insulation system, the TiN film coatings are made as thin as possible because the conductivity and loss tangent of TiN film is high (bulk conductivity is about $6x10^6$ S/m) [20]. Therefore, it is concluded that the 0.5–1 nm is the optimum thickness of TiN film for alumina rf window coatings to suppress multipactor.

3.3 Dependence of SEE coefficient on purity and grain size of aluminas

Figure 6 shows dependence of the SEE coefficients on the alumina purity (a) and grain size (b) at 25°C and 650°C for HA and KP series alumina at primary energy of 1 keV as a parameter of the TiN film thickness and temperature. Slightly increase of SEE coefficients with purity is found for KP series (0.5 nm TiN) and HA series (0.25 nm TiN). However, it is difficult to find clearly the dependence of purity (i.e. 0.25 nm TiN-coated KP series) and grain size on SEE coefficients of the TiN-coated alumina. The dependency of SEE coefficients of alumina on purity and grain size were founded for non-coated alumina [21, 22]. This is because the SEE coefficient values of TiN-coated alumina are much smaller than those of non-coated alumina and the variant of SEE coefficient of the insulators is rather large.

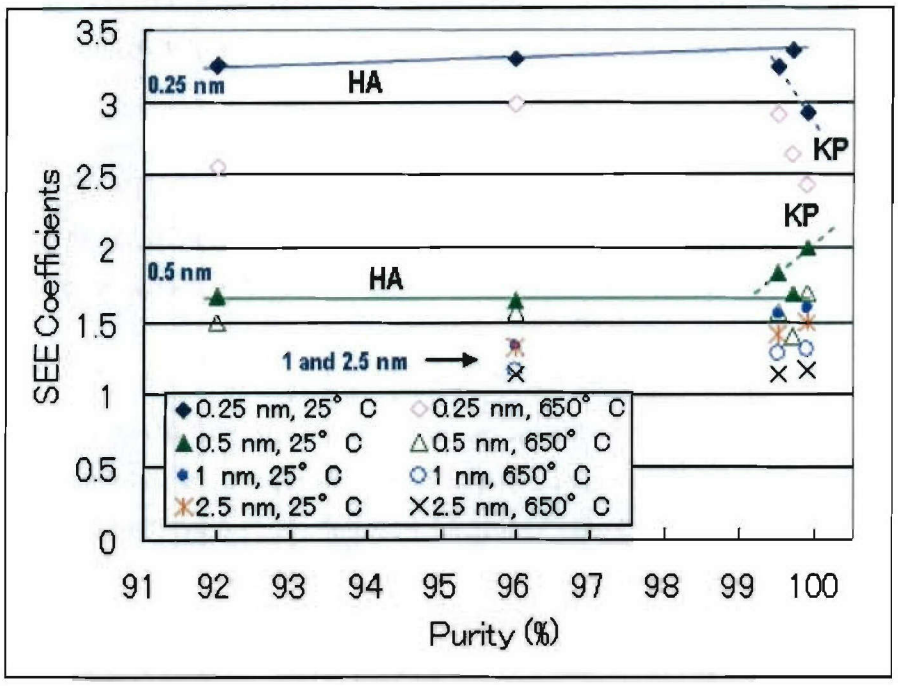

(a)

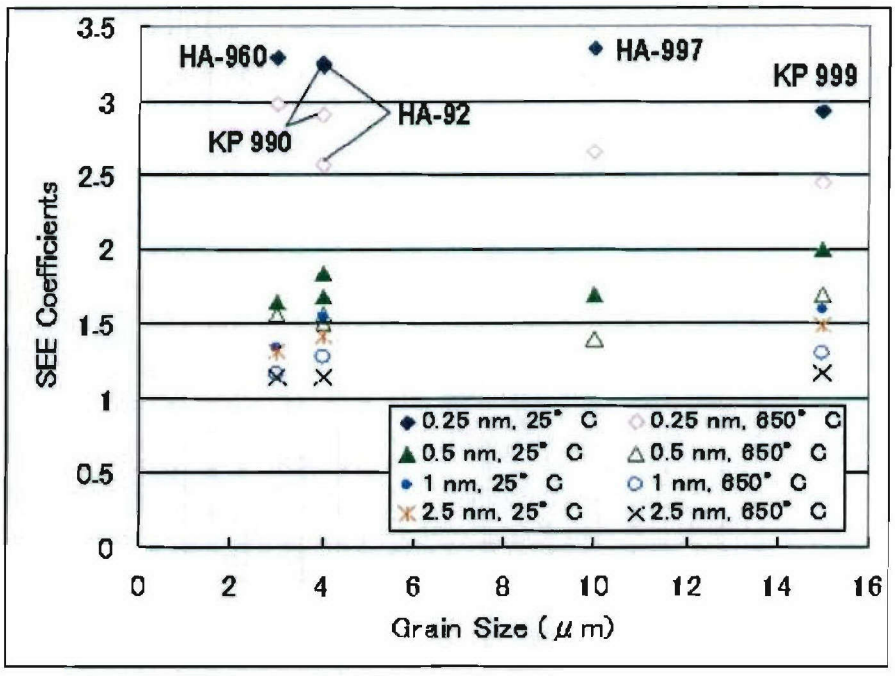

(b)

Figure 6: Relationship between SEE coefficients of TiN-coated alumina and (a) purity; (b) grain size at room temperature and 650℃.

3.4 SEE obtained by the multi-pulse injection

Figure 7 shows the obtained SEE of HA-960 at room temperature with pattern A and B. In case of pattern A, the ratio of the SEE of the 5th pulse and 1st pulse ($\rho_{5/1}$~0.35) will become the typical index for the decrease on SEE. The recovery of the SEE is observed at the 4th pulse of the pattern B. The ratio of the SEE of the 4th pulse and 3rd pulse ($\rho_{4/3}$~1.7) can be the typical index of the recovery. Here the integrated secondary currents in the pulse are used at calculation of the ratio of $\rho_{5/1}$ and $\rho_{4/3}$ so as to average SEE.

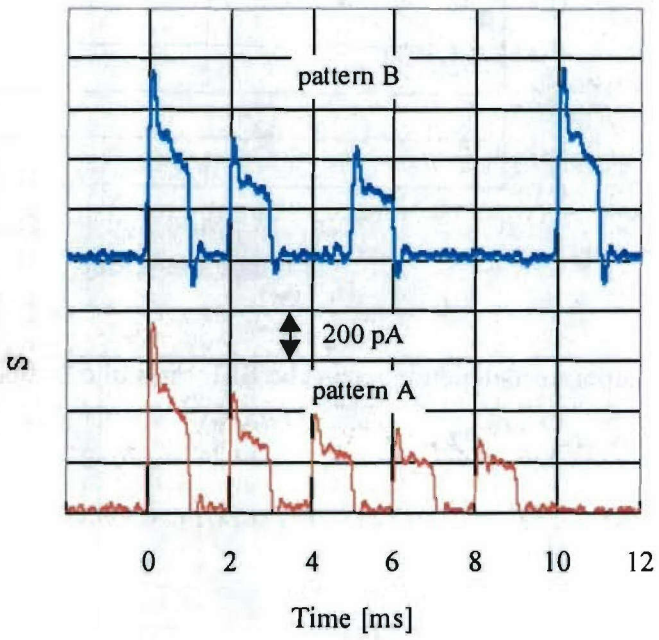

Figure 7: Multi-pulse waveforms of "pattern A" and "pattern B"at room temperature.

Figure 8 shows the temperature dependence of the ratio ($\rho_{5/1}$) at pattern A. It is found that the higher the temperature becomes, the higher the ratio ($\rho_{5/1}$), which indicates that the supply of the secondary electrons increase due to the higher mobility of the electrons at high temperature. Although the SEE becomes lower at high temperature around 10% [21]-[23], the effective SEE increases due to the lower charging at high temperature.

The ratio ($\rho_{5/1}$) at room temperature and 650°C are shown in Fig. 9. At room temperature, sapphire is the lowest compared with the other samples, meaning that the

electron supply is lowest. At 650°C, the ratios are around unity at the samples except sapphire, which can be interpreted that the surface charging becomes less at high temperature.

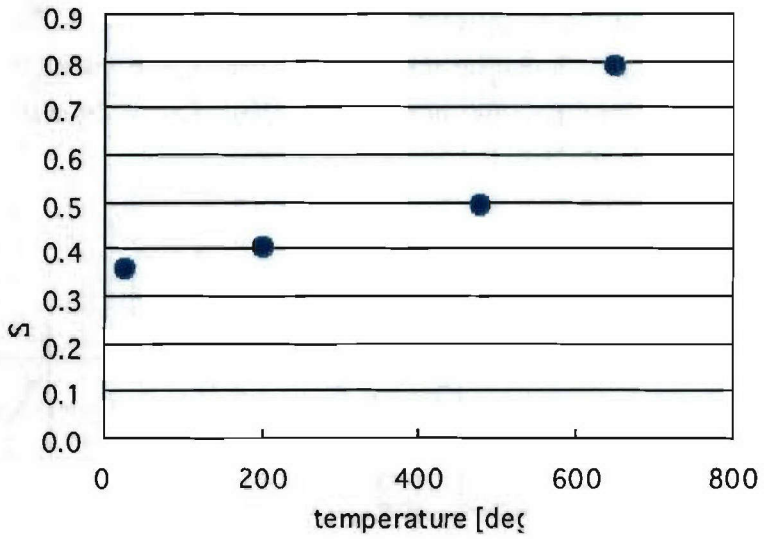

Figure 8: Temperature dependence of the SEE ratio of 5th pulse and 1st pulse ($\rho_{5/1}$) of HA-960.

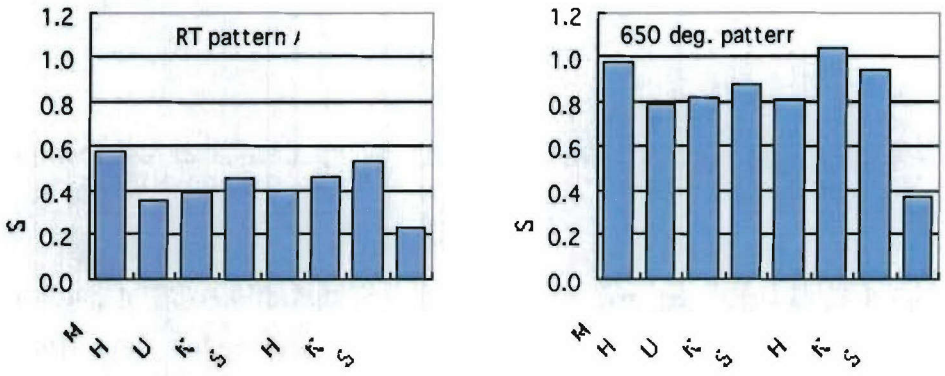

Figure 9: The SEE ratio of 5th pulse and 1st pulse ($\rho_{5/1}$) at room temperature (left) and at 650°C (right).

The ratio ($\rho_{4/3}$) of the samples are shown in Fig. 10. The recovery of the SEE at room temperature is larger at HA-960, SSA-S1 and HA-997 and the tendency is not explained by neither the purity nor the grain size. The ceramic structures and/or production process will be important for the surface charging. The $\rho_{4/3}$ of around unity of alumina ceramics at 650°C is owing to the lower surface charging, where the recovery time constant is less than 4 ms. The sapphire's rather larger ratio results from the recovery of SEE, which means that the time constant of the SEE recovery is around 4 ms at 650°C. The strict difference between the sapphire and other commercial ceramics are partly explained by the existence of the additives. MgO crystal shows the rather lower surface charging as shown in Fig. 9 (a). The additives at the grain boundary plays important role for the surface charging and its recovery. At high temperature, it is confirmed that effective SEE increase due to the increase in the secondary electron supply and the decrease in the recovery time.

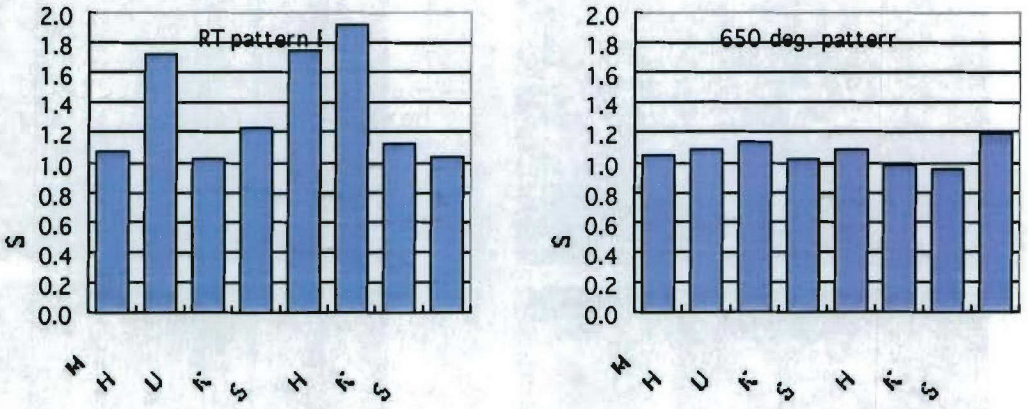

Figure 10: The SEE ratio of 4th pulse and 3rd pulse ($\rho_{4/3}$) at room temperature (left) and at 650°C (right).

It is found that the sapphire sample shows the good electrical insulation. However, such a high insulation will be harmful from the viewpoints of the pile-up of charging. It will be better to decrease the surface charging because the accumulated charges will be discharged at the threshold. The anti-multipactor coating such as TiN [24] will be useful not only for the reduction of SEE but also the less surface charging. It is considered that the material with rather higher recovery and higher secondary electron stock (or discharge threshold) will be durable due to the higher threshold.

3.5 High power tests by resonant ring

High power test of rf window disks (alumina HA-997 and HA-960) were performed using the resonant ring [1],[17]. The resonant ring can be operated up to 250 MW of peak power and 25 kW average (2 μ s, 50 pps).

Figure 11 shows photographs of the luminescence of alumina HA-997 due to multipactor bombardment during rf operation at various peak powers. The luminescence of alumina HA-997 seems normal and no F-center peak was observed in the both spectra at 5 MW before and after 200 MW operation as shown in Fig. 12. The abnormal luminescence may found for TiN-coated alumina HA-960 (Fig. 13) during rf operation at peak power of 50 MW or more. Breakdown of this alumina rf window occurred after 200 MW operation as shown in Fig. 14. Figure 15 shows that the peak of F-center was found in the spectrum of the rf window at 5 MW before 200 MW operation. The peak intensity of the F-center became larger after 200 MW operation.

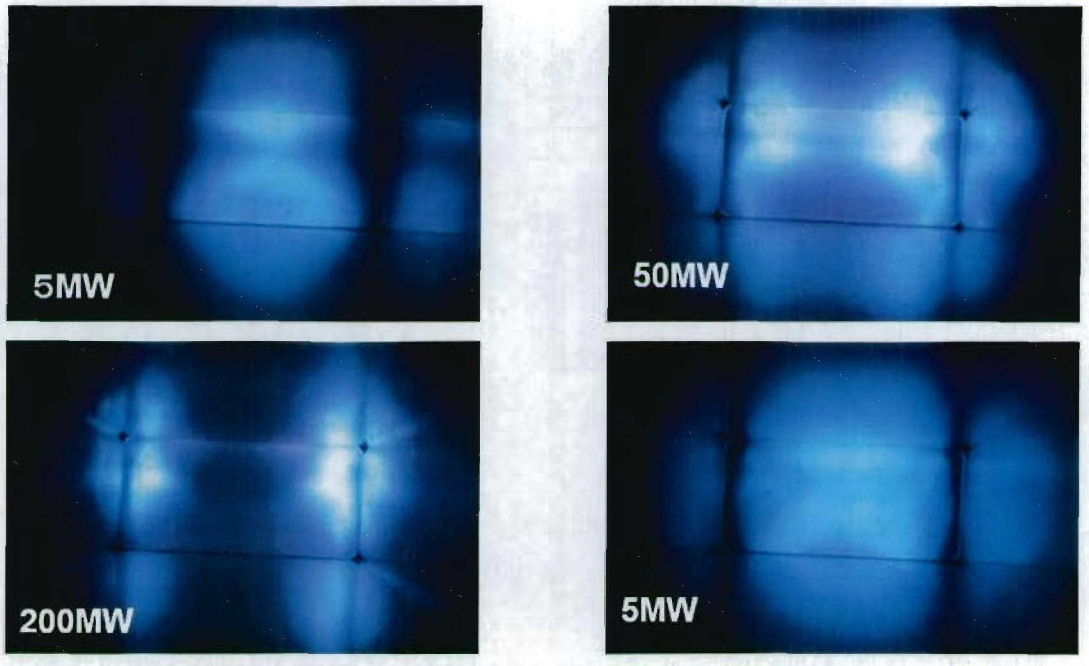

Figure 11: Photographs of alumina HA-997 rf window taken during rf operation at peak power of 5 MW, 50 MW, 200 MW, and 5MW after 200 MW operation.

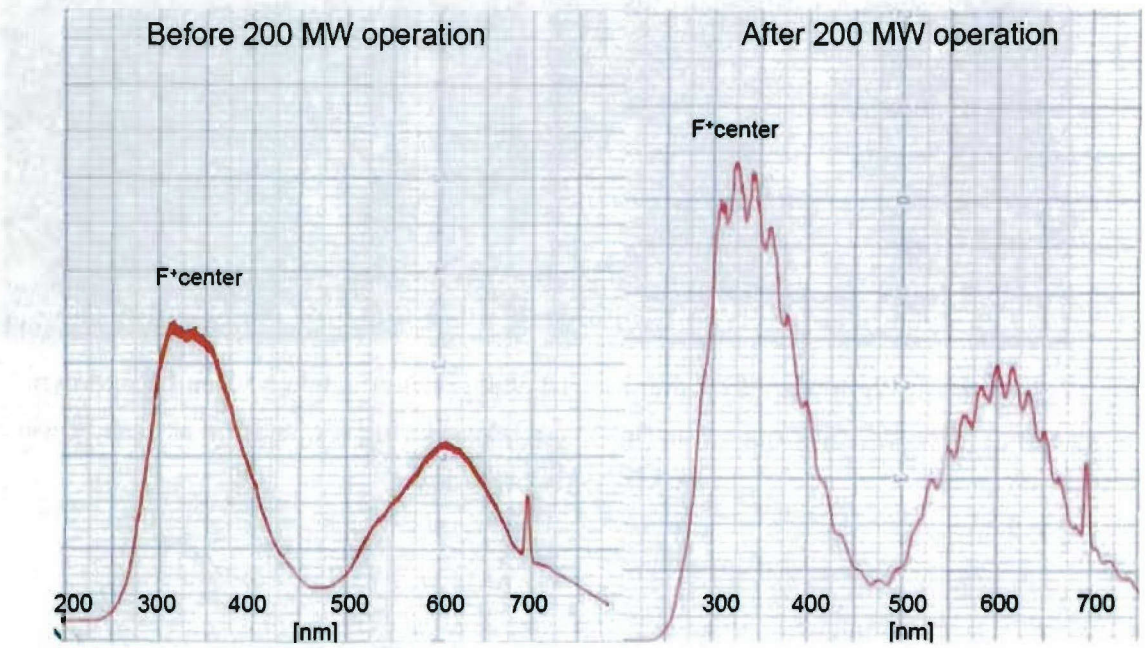

Figure 12: Luminescence spectra of alumina HA-997 rf window at 5 MW.

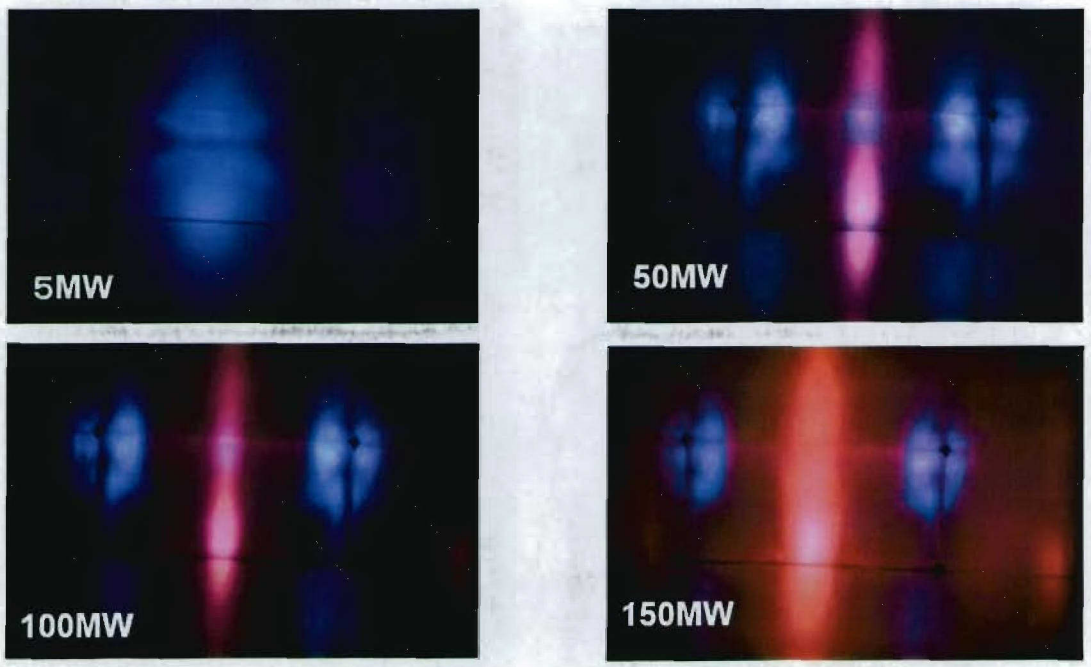

Figure 13: Photographs of alumina HA-960 rf window taken during rf operation at peak power of 5 MW, 50 MW, 100 MW, and 150 MW.

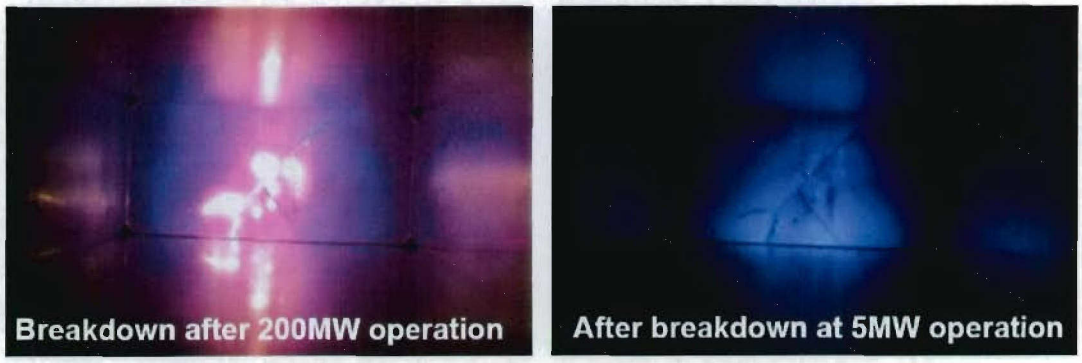

Figure 14: Photographs of alumina HA-960 rf window taken when breakdown occurred after 200 MW operation (left), and taken during rf operation at peak power of 5 MW after breakdown.

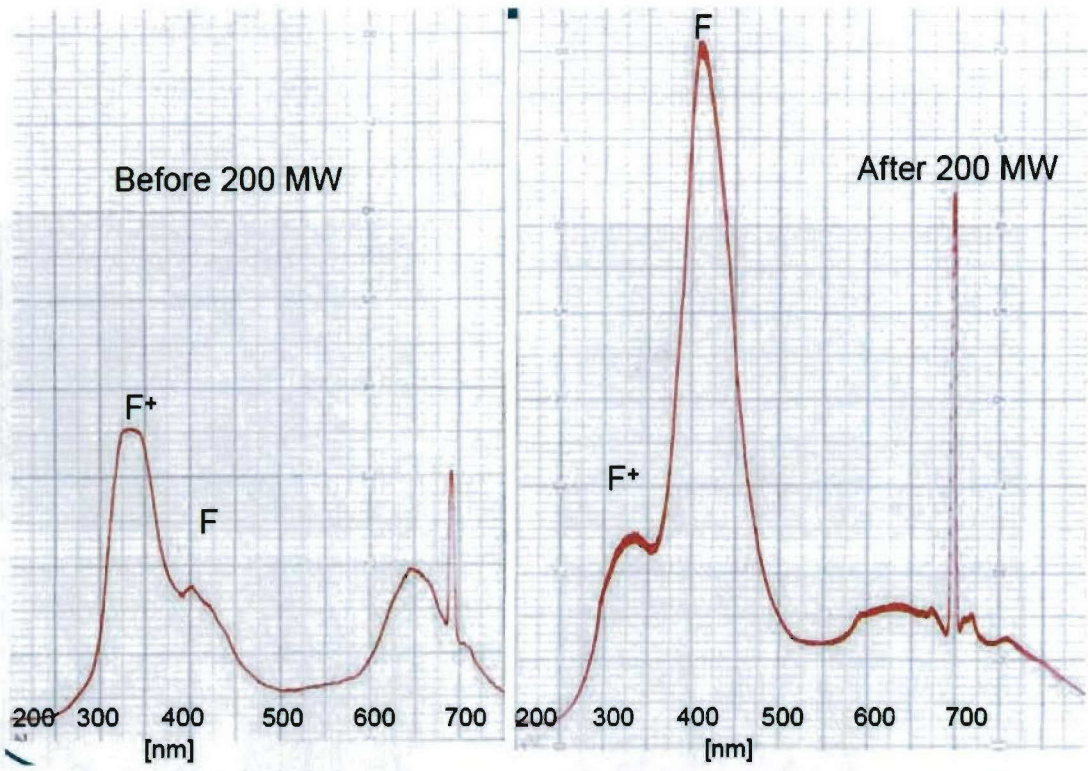

Figure 15: Luminescence spectra of alumina HA-960 rf window at 5 MW.

The results of this work are summarized in Table 2. It can be concluded that the

alumina HA-997 shows the best performance, and that the alumina HA-960 is a good candidate for new material of rf window because of the faster charging recovery and F-center free. The breakdown of alumina HA-960 rf window is probably caused by the lower purity. However, this speculation should be confirmed by examining the same HA-960 disk or an alumina HA-960 disk with HIP.

Table 2. Summarized of results

	purity [%]	Grain size [micro-m]	CL	surface charging	charging recovery	Max power [MW]
HA92	92	10	F+	---		120
HA960	96	3	F+	2	3	<200
UHA99	99	4	F+	4	6	>220
KP990	99.5	4	F+	5	4	>200
SSA-S1	99.6	15	F+	3	2	---
HA997	99.7	10	F+	7	1	>220
KP999	99.9	15	F+	6	5	---
Sapphire	100	---	F+,F	1	7	<40
MgO	100	---	---			---

4. Conclusion

a. SEE coefficients of several kinds of commercial alumina ceramics decrease with temperature, but the values of the SEE coefficients are still high. To suppress multipactor, TiN-coated aluminas were investigated. As results:
   - ✓ SEE coefficients became low (nearly unity for TiN thickness of 1 nm or more).
   - ✓ For TiN thickness of 0.5 nm or less, the alumina layer may still plays important role in generating the secondary electrons. Thus, 0.5~1 nm is the optimum TiN thickness for rf window coating to suppress multipactor.
   - ✓ The SEE coefficients decrease with temperature for all film thickness, except for sapphire.

b. Evaluation of the SEE and surface charging at high temperature by multi-pulse measurement found that the effective SEE is higher than at room temperature because the SEE supply is larger at high temperature. Moreover, the results show that the sapphire indicates the best insulation performance but the accumulation of the surface charging will induce the surface charging.

c. It is recommended that the criteria for durable material for rf window are as follows.
   - – F-center free material
   - – Low charging material (charging free at >600°C)
   - – Highly pure material (>99%?)

References

[1] Y. Saito, N. Matuda, S. Anami, A. Kinbara, G. Horikoshi and J. Tanaka: "Breakdown of alumina rf windows", *IEEE Transaction on Electrical Insulation*, **Vol. 24**, pp. 1029-1036, 1989.

[2] Y. Saito, N. Michizono, S. Anami, S. Kobayashi: "Surface Flashover on Alumina RF Windows for High-power Use", *IEEE Transaction on Electrical Insulation*, 28, pp. 566-573, 1989.

[3] S. Yamaguchi, Y. Saito, S. Anami, S. Michizono, "Trajectory Simulation of Multipactoring Electrons in S-Band Pillbox RF Window", *IEEE Transaction on Nuclear Science*, **Vol. 39**, No. 2, 1992.

[4] R. V. Latham: "High Voltage Vacuum Insulation", Academic Press, London, pp.300-303, 1995.

[5] H. Craig Miller: "Flashover of Insulators in Vacuum", *IEEE Transaction on Electrical Insulation*, **Vol. 28**, No. 4, pp. 515-527, 1993.

[6] H. Craig Miller: "Surface Flashover of Insulator", *IEEE Transaction on Electrical Insulation*, **Vol. 24**, No. 5, pp. 771-772, 1989.

[7] Tumiran et. al.: "Flashover from Surface Charge Distribution on Alumina Insulators in Vacuum", *IEEE Transaction on Electrical Insulation*, **Vol. 4**, No. 4, pp. 400-406, 1997.

[8] H. Bruining, "Physic and Application of Secondary Electron Emission", Pergamon Press Ltd., London, 1954.

[9] A.J. Dekker: "Energy and Temperature of the Secondary Emission of MgO", *Physical Review*, **94**, pp.1179, 1954.

[10] A.J. Dekker: "Solid State Physics", Maruzen Asian Edition, pp. 440-442, 1968.

[11] J.B. Johnson and K.G. McKay: "Secondary electron emission of crystalline MgO", *Physical Review*, **91**, pp. 582-587, 1953.

[12] J. Cazaux: "About the secondary electron emission yield, δ, from e^--rradiated insulators", *Mikrochimica Acta*, **132**, pp. 173-177, 2000.

[13] J.B. Johnson and K.G. McKay: "Secondary electron emission from germanium", *Physical Review*, **93**, pp. 668-672, 1954.

[14] G. F. Dionne: "Effects of secondary electron scattering on secondary emission yield curves", *Journal of Applied Physic*, **Vol. 44**, No. 12, pp.5361-5364, 1987.

[15] Suharyanto, S. Michizono, Y. Yamano, Y. Saito, S. Kobayashi, "Secondary Electron Emission Coefficient Measurements of Semiconductor and Insulator Materials in Vacuum", Proc. of 2003 J-K Joint Symp. on E.D. and H.V.E., pp. 277-280, 2003.

[16] NTK, "NTK Alumina Charakteristics", 2003.

[17] S. Kobayashi and Y. Saito, "Secondary Electron Emission Measurements on Materials under Stress", Interim report to AOARD/AFOSR, 2002.

[18] T. Sato, S. Kobayashi, S. Michizono and Y. Saito: "Measurements of secondary electron-emission coefficients and cathodoluminescence spectra for annealed alumina ceramics", *Applied Surface Science*, **144-145**, pp. 324-328, 1999.

[19] S. Michizono, A. Kinbara, Y. Saito, S. Yamaguchi, S. Anami, N. Matuda, "TiN Film Coatings on Alumina Radio Frequency Windows", J. Vac. Sci. Technol. A 10(4), 1992.

[20] S. Michizono, Y Saito, Suharyanto, Y. Yamano, S. Kobayashi, "Secondary electron emission of sapphire and anti-multipactor coatings at high temperature", Applied Surface Science 235, p. 230, 2004.

[21] S. Kobayashi and Y. Saito, "Secondary Electron Emission Measurements on Materials under Stress", Interim report to AOARD/AFOSR, January, 2004.

[22] Suharyanto, S. Michizono, Y. Yamano, Y. Saito, S. Kobayashi, "Secondary Electron Emission Coefficient of Dielectric Materials under High Temperature Condition", Proc. of XXIth Int. Symp. D. E. Insul. in Vacuum (ISDEIV), pp. 17-24, 2004.

[23] J. Cazaux, J. Electron Sepc. And Rel. Phenomena 105, p. 155, 1999.

[24] A.R.Nyaiesh, et.al., J.Vac.Sci.Tech. A4, p. 2356, 1986.

Summarized results

Summarized results

Summarized results obtained from this research are described below.

At the first step (First interim report –Review and preliminary work-), secondary electron emission from an insulator, especially alumina was reviewed. The SEE yields, CL spectra, tan δ and bulk resistivities of dielectric disks were measured. High-power tests were also performed using a traveling wave resonant ring in order to examine the breakdown of the disks as a review and a preliminary measurements.

It was found that excess heating due to multipactor bombardment or localized rf dissipation at pores, probably causes F center generation. This might enhance localized heating and results in surface melting or a dielectric breakdown. It is concluded that alumina ceramics with a low tan δ have a good feasibility for high-power operation, though they must be coated with TiN films in order to suppress the multipactor. The SEE coefficients are found to depend on the alumina content: the higher the content, the larger the coefficients.

An in-air annealing treatment up to 1500℃ is ascertained to dissolve colouring. In the CL spectra, the intensity contributing to the F^+-center decreases for most of the ceramics upon annealing. Based on these results, the annealing possibly causes a charge transfer between the oxygen vacancies. An increase in the SEE coefficients was observed for ceramics having a lower alumina content. Evaporation of the sintering additives which absorb the secondary electrons is one of the possible mechanisms of this phenomenon.

The X-ray irradiation effects in this study were found to be as follow: (1) colouring, (2) a change in the optical-absorption coefficient, (3) no change in the SEE coefficients, and (4) a decrease in the CL intensity contributing to the F^+-center. It is difficult to estimate effect (4), since the luminescence should be absorbed by effects (1) and (2).

Analysis of secondary electron energies revealed that secondary electrons emitted at higher temperature have higher energies than those at room temperature.

At the second step (Second interim report –Preliminary measurements of SEE under high temperature condition-) preliminary measurements of SEE under high temperature conditions were measured and energies of secondary electrons were analyzed. Results are summarized as follows;

a. SEE coefficients of silicon and sapphire could be measured under room and high temperature. SEE coefficients of alumina also were measured under room temperature by absorption and

secondary current method.

b. SEE coefficients of alumina KP990 measured by absorption and secondary current method were almost same.
c. In relative high temperature (200℃), an appreciable reduction of SEE coefficient was confirmed for both silicon and sapphire.
d. Position dependence possibility (not only temperature dependence) of SEE coefficient was observed in sapphire (sample B).
e. Electron energy distribution showed that energies of emitted electrons are in about 8 eV at room temperature and its full width at half maximum is in about 3.4 eV at room temprature. These values are independent of samples measured.
f. At high temperature (about 430 ℃) energies of emitted electrons decreases about 0.7 eV, and the number of electrons decreased.
g. To canvass electron emission characteristics described above, it is necessary to analyze surface condition, since sample surface conditions strongly influence on electron emission characteristics.

At the third step (Third interim report –Measurements under high temperature and multi-pulse technique-) SEE coefficients of various kinds of alumina ceramics, sapphire, SiO_2, and MgO were measured under room temperature and up to 700℃. Results are summarized as follows;

a. A reduction of SEE coefficient of the samples under high temperature condition was confirmed, except for sapphire. This reduction may be caused by the shorter mean free path of the secondary electrons due to the larger phonon and electron scattering at high temperature.
b. An increase of SEE coefficients at high temperature was observed for sapphire sample. This may be due to the higher secondary electron creation caused by the transition of the oxides defects from F^+-center to F-center.
c. The SEE coefficients tend to increase with purity and grain size. This tendency was found at both room and high temperature conditions.
d. At high temperature (700℃) the SEE waveform did not change with pulse series. It may be due to the higher surface electric conductivity at high temperature. In addition, the total emission charges were larger than those of room temperature, though the SEE coefficient was smaller.

At the fourth step (Fourth interim report –Multi-pulse measurements and high power test-) effect of TiN coating on SEE coefficient was investigated and preliminary high power test was carried out to compare microwave transmission capability with kinds of alumina materials. Results are summarized as follows;

a. SEE coefficients of several kinds of commercial alumina ceramics decrease with temperature, but the values of the SEE coefficients are still high. To suppress multipactor, TiN-coated aluminas were investigated. As results:

   1. SEE coefficients became low (nearly unity for TiN thickness of 1 nm or more).
   2. For TiN thickness of 0.5 nm or less, the alumina layer may still plays important role in generating the secondary electrons. Thus, 0.5~1 nm is the optimum TiN thickness for rf window coating to suppress multipactor.
   3. The SEE coefficients decrease with temperature for all film thickness, except for sapphire.

b. Evaluation of the SEE and surface charging at high temperature by multi-pulse measurement found that the effective SEE is higher than at room temperature because the SEE supply is larger at high temperature. Moreover, the results show that the sapphire indicates the best insulation performance but the accumulation of the surface charging will induce the surface charging.

c. It is recommended that the criteria for durable material for rf window are as follows.

   – F-center free material
   – Low charging material (charging free at >600°C)
   – Highly pure material (>99%?)

Future work

Future work

As described in the previous section (Summarized results) some criteria for durable material of rf window for high power use have been proposed by the results obtained from this research. Those criteria are F-center free material, Low charging material (charging free at > 600℃), and Highly pure material, which were derived from elemental experiments, such as SEE measurements, microwave transmission tests, etc. Among these F-center may play an important role in dominating breakdown strength. Problems are how to manufacture F-center free alumina, how to find low charging material, how to sinter high purity alumina etc.. To confirm that insulating materials selected on the basis of these criteria have really higher transmission capability of microwave it is necessary to use alumina prepared by various manufacturing processes. Therefore experiments using alumina manufactured by the following processes can be proposed as a next collaborating work;

a. aluminas made of very fine grain (nano-meter scale graines)
b. aluminas having crystallized grain boundary
c. aluminas sintered by different additives and procedures

Experiments to be planned by using those manufactured aluminas are;

a. comparing microwave transmission capability with manufacturing processes (in KEK)
b. measuring secondary electron emission coefficient under room and high temperature conditions (in KEK)
c. analyzing cathodoluminescence spectra (in KEK and Saitama Univ)
   This experiments provides information on defects, especially F-centers
d. analyzing secondary electrons energies in conjunction with XPS or AES surface analysis (in Saitama Univ)
   This analysis technique provides electronic band structure.
e. analyzing gas desorption stimulated by electron irradiation (in Saitama Univ)
   Gas desorption is one of factors to initiate breakdowns. This measurement clarifies gas emissivity at alumina surface irradiated by electrons.
f. analyzing surface condition by XPS and AES (in Saitama Univ)
g. measuring charging characteristics (in Saitama Univ and KEK)

Through these experiments it will be found that dependence of breakdown strength on alumina grain size and sintering additives, and which manufacturing process provides lower F-center creation.

Publication

Proceedings of
2003 Japan-Korea Joint Symposium on
Electrical Discharge
and
High Voltage Engineering

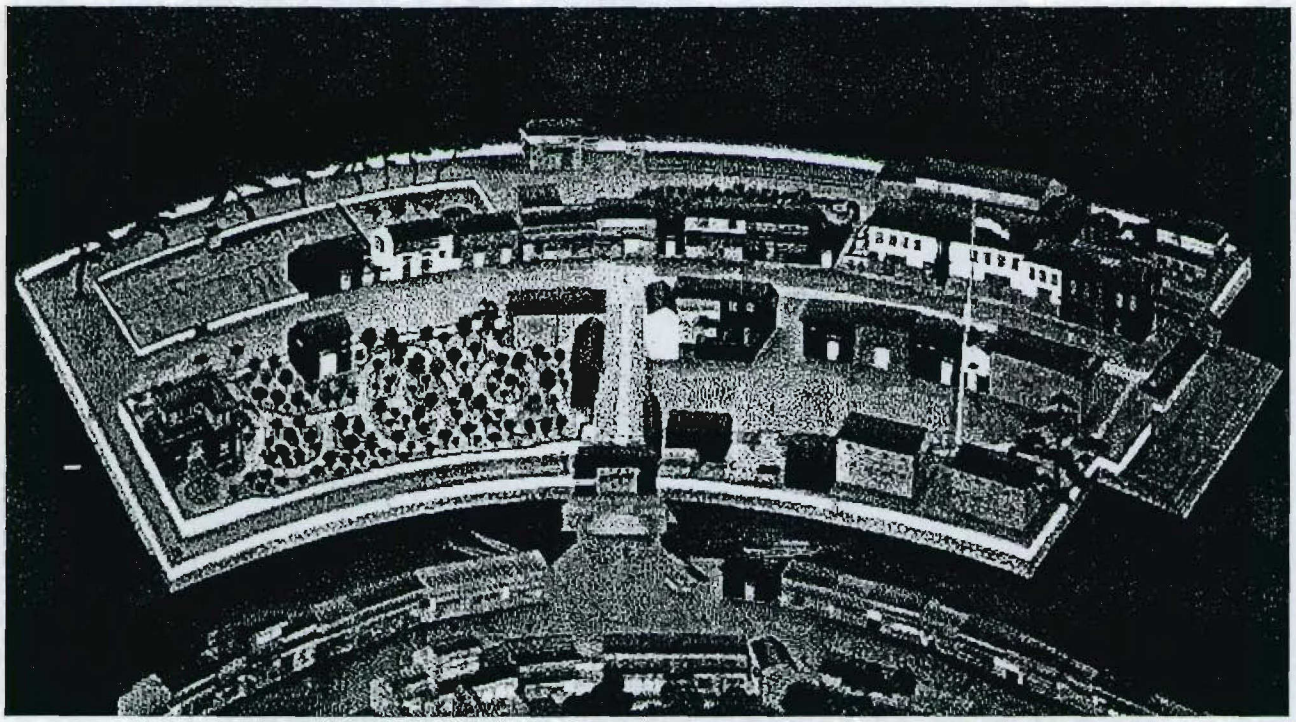

Nagasaki, Japan
November 6-7, 2003

Organized by
Technical Committee on Electrical Discharge in IEEJ
Nagasaki University

Co-organized by
Study Committee on High Voltage Engineering and Discharge Application in KIEE

In Corporation with
The Institute of Engineers on Electrical Discharges in Japan (IEEDJ)
IEEJ Kyushu Branch
IEEE Fukuoka Section

Proceedings of
2003 Japan-Korea Joint Symposium
on
Electrical Discharge and
High Voltage Engineering

6-7 November, 2003
Nagasaki, Japan

Organized by

Technical Committee on Electrical Discharge in IEEJ

Nagasaki University

Co-organized by

Study Committee on High Voltage Engineering and

Discharge Application in KIEE

In Corporation with

The Institute of Engineers on Electrical Discharges in Japan

(IEEDJ)

IEEJ Kyushu Branch

IEEE Fukuoka Section

Secondary Electron Emission Coefficient Measurements of Semiconductor and Insulator Materials in Vacuum

Suharyanto[1,2], S. Michizono[3], Y. Yamano[1], Y. Saito[3], S. Kobayashi[1]

[1]Department of Electrical and Electronic Systems, Saitama University
255 Shimo-Okubo, Sakura-ku, Saitama 338-8570, Japan

[2]Department of Electrical Engineering, Gadjah Mada University
Jl. Grafika 2, Jogjakarta 55281, Indonesia

[3]Accelerator Laboratory
High Energy Accelerator Research Organization (KEK)
1-1 Oho, Tsukuba, Ibaraki 305-0801, Japan

Abstract – Secondary electron emission (SEE) coefficients of silicon, sapphire and alumina were measured by scanning electron microscope (SEM) with short-pulsed electron beam under room and high temperature up to 600℃. An appreciable reduction in the SEE coefficients with increasing temperature was confirmed for silicon. For insulator materials, although there was rather large scattering of data, a reduction in the SEE coefficients with increasing temperature was also confirmed.

1. Introduction

Klystrons, the high power microwave generator, are used for particle acceleration energy sources in the high-energy accelerator. In the klystron, there is a rf window which made of an insulator. Surface flashover along the rf window insulator is a present problem in the klystron applications for high power use. Therefore, it is necessary to understand the surface flashover phenomena and thus improve transmission capability of the high power microwave [1,2].

The important points in the breakdown mechanism along the rf window insulator are multiplication of secondary electrons emitted from the insulator surface and temperature rise of the insulator, since a rf window of a klystron under operation may be heated by energy loss caused by the microwave transmission. Therefore, study of temperature effect on secondary electron emission (SEE) characteristic is required to understand the breakdown process in the rf window.

Some theories have been proposed to explain the temperature effect of SEE [3–6]. However, there are still only few data of SEE under high temperature condition, especially for technical material. This study aims to measure the SEE coefficients under room and high temperature condition on technical material insulators used in high power vacuum devices, such as alumina. The samples measured in this study were silicon, sapphire and alumina. The measurement of silicon was carried out because of two reasons; (a) the electronic state of silicon looks like that of insulator, (b) there is no charge up on this sample surface when an electron beam is injected. Therefore, the silicon is a good sample to practice measurement skill at beginning of this study.

2. Experimental

2-1. SEE measurement system and sample heating unit

The SEE coefficients were measured by scanning electron microscope (SEM) with pulsed electron beam. Sample stage in vacuum chamber of the SEM was modified by installing a heating unit near the sample to enable measurements of SEE coefficient under high temperature conditions.

Measurements of SEE coefficient were carried out by two methods: (i) measuring the absorption currents, or (ii) measuring the SEE currents. Schematic diagram of the absorption current measurement method is shown in Figure 1. The absorption current is measured by applying a

negative bias voltage to ensure that the secondary electron emissions were not absorbed into the sample. In order to measure primary currents, a faraday cup is installed on the sample holder. A sapphire insulator (0.3 mm thickness) is used to prevent currents flowing to ground.

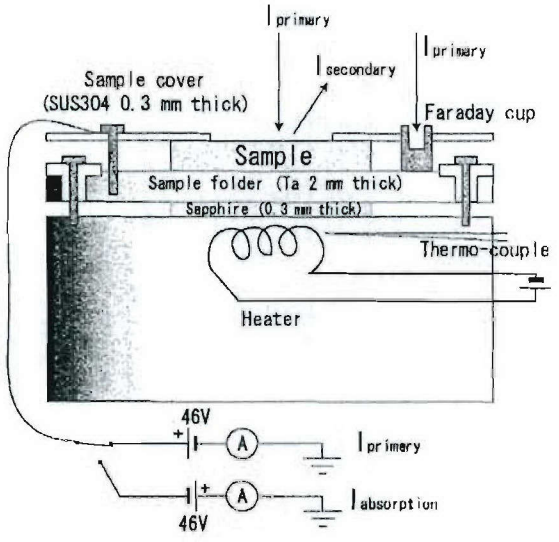

Figure 1. Schematic diagram of SEE coefficient measurements using the absorption current method.

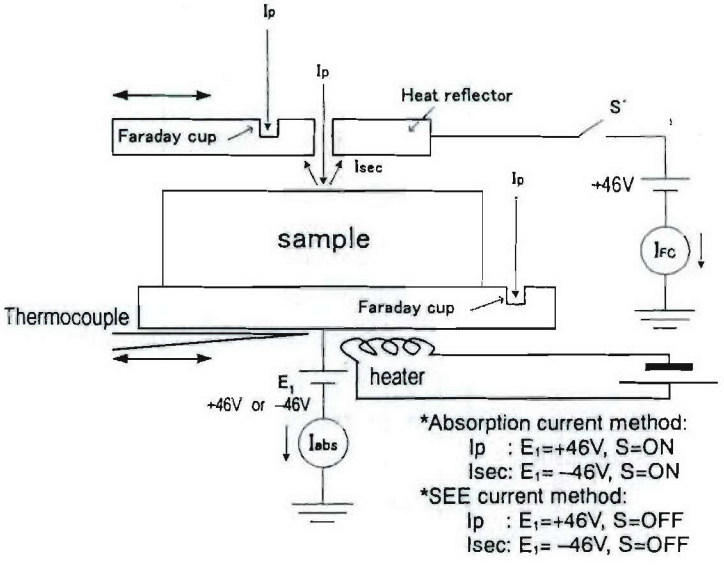

Figure 2. Schematic diagram of SEE coefficient measurements using the SEE current method.

The measurements using SEE current method are carried out by circuit modification of the absorption current method. The SEE currents are captured by a faraday cup installed on the heat reflector set above the sample as shown in Figure 2. The heat reflector was coated with a diamond like carbon (DLC) film in order to minimize the SEE from the reflector surface. A positive bias voltage is applied to the faraday cup to ensure all of the secondary electrons were measured (switch S is ON). A negative bias voltage is applied to the sample holder to ensure that the secondary electron emissions were not absorbed into the sample.

2-2. Samples and procedure

Samples used in this experiment were silicon wafer, sapphire and alumina. For silicon sample, the primary current is pulsed electron beam with 400 pA amplitude, 4 ms duration, and 50 Hz frequency. Since there is no surface charging on the silicon sample, the measurements of SEE coefficients (δ) can be carried out at the same site of the sample.

The insulator samples (sapphire and alumina) were annealed at 1400℃ in air for 1 hours before measurements. This annealing process can remove the mechanical stress of insulators and affects their properties concerning the trapped or stored charges in the vacancies [2].

The primary current used for the insulator samples is one shot pulsed electron beam with 100 pA amplitude for 1 ms duration. Only once measurement at one site of the sample is carried out on the insulator surface. Then, the sample is traveled to the next measurement site by moving 2 mm for x direction and or 1 mm for y direction, as shown in Figure 3. This procedure reduces the influence of surface charging in the measurements.

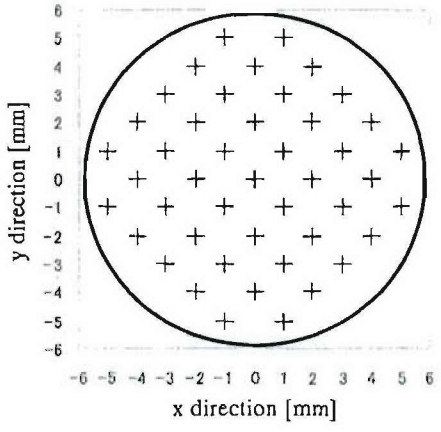

Figure 3. Position of measurement sites for insulators.

3. Results and discussion

3-1. SEE coefficients of semiconductor

Measurements of SEE coefficient (δ) of silicon (semiconductor) were carried out by the

absorption current method at room temperature and 200℃. Results of the measurements are shown in Figure 4.

At 200℃, the SEE coefficients of silicon are lower than that of room temperature condition. The decrease of SEE coefficient of silicon may be caused by the shorter mean free path of the secondary electrons at high temperature due to the larger phonon and electron scattering in the bulk before escaping from the surface. Therefore, under high temperature condition, the secondary electrons approaching the surface is less than that of in room temperature.

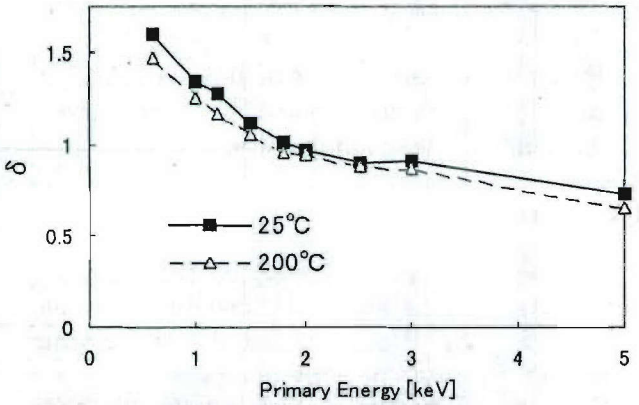

Figure 4. SEE coefficients of silicon measured by the absorption current method.

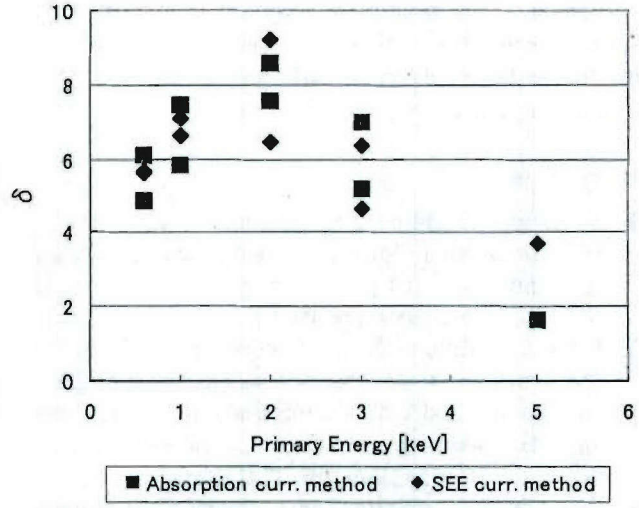

Figure 5. SEE coefficients of alumina KP-990 measured by the absorption and SEE current method at room temperature.

3-2. Comparison of SEE coefficients measured by absorption current and SEE current methods

The SEE coefficients of alumina KP-990 insulator at room temperature measured by the absorption current and SEE current method is shown in Figure 5. According to the Figure 5, SEE coefficients of the sample measured by both of the methods were almost same.

Measurements of SEE coefficient by using the absorption current method could not be carried out under the higher temperature (>>200℃) because a leakage current problem along the sapphire surface below the sample holder arose. To avoid the lakage current problem, therefore, the SEE current method is selected to measure the SEE coefficients under high temperature, such as 600℃.

3-3. SEE coefficients of insulator

Even one shot pulsed electron beams were applied, build-up of surface charging took place resulting a decrease of the secondary current pulse for insulator measurement, as shown in Figure 6. In that case, the secondary current is defined at the maximum of the pulse.

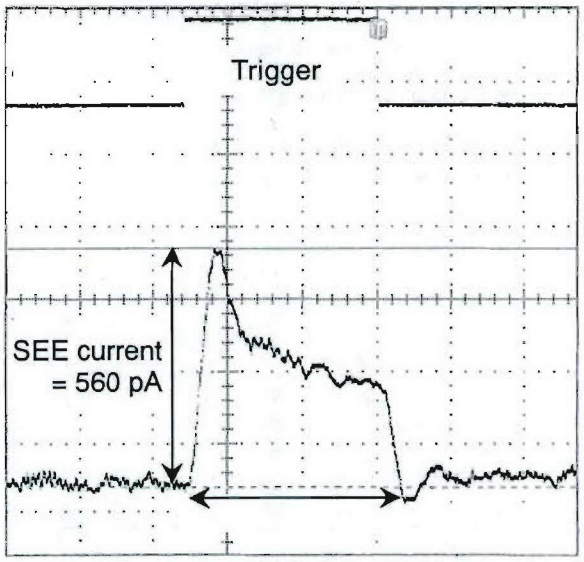

Figure 6. SEE current pulse waveform of insulator. Pulse width of 1 ms, primary electron current of about 100 pA are utilized. The rapid decrease in the SEE current corresponds to the build-up of the surface charging.

The SEE coefficients of sapphire, alumina HA-997 (99.7% purity) and HA-92 (92% purity) measured by SEE current method under room temperature and high temperature are shown in Figure 7, 8 and 9, respectively. From Figure 8 and 9, SEE coefficients of alumina HA-997 which has higher purity is higher than that of HA-92.

Although there was rather large scaterring of data, it is found that the SEE coefficients of the

samples were lower than that obtained under room temperature condition. For alumina HA-997 and HA-92, the SEE coefficients at room temperature after cooling down were measured also. Since the SEE coefficients of this sample after cooling down were almost the same as the previous values at room temperature, the decrease in the SEE coefficients at 600℃ was not caused by the surface modification, but by the nature of the insulators.

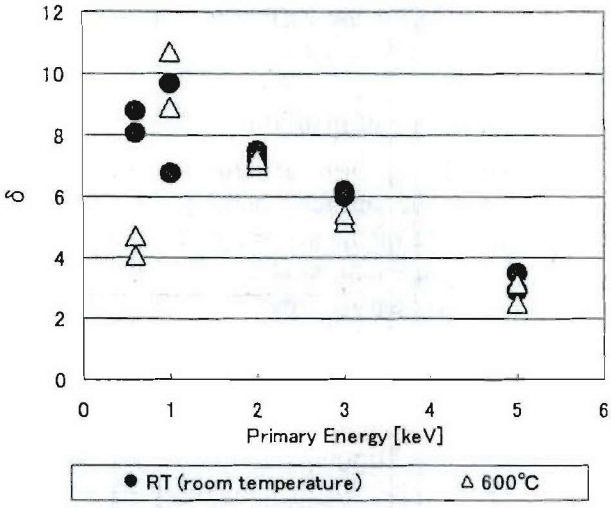

Figure 7. SEE coefficients of sapphire at room temperature and 600℃ measured by the SEE current method.

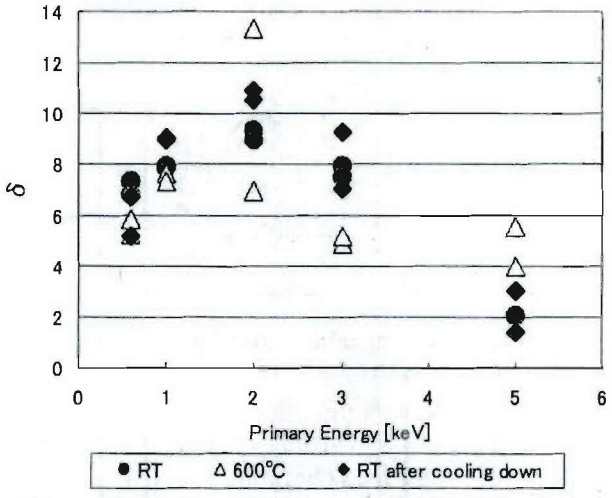

Figure 8. SEE coefficients of alumina HA-997 at room temperature, 600℃ and room temperature after cooling down.

Recently, there are still only few theories of the SEE under high temperature conditions, especially for insulator material. However according to empirical data and references, it is considered that the decrease of SEE coefficients when temperature increases may be caused by phonon and electron scattering before escaping from the surface [3,6].

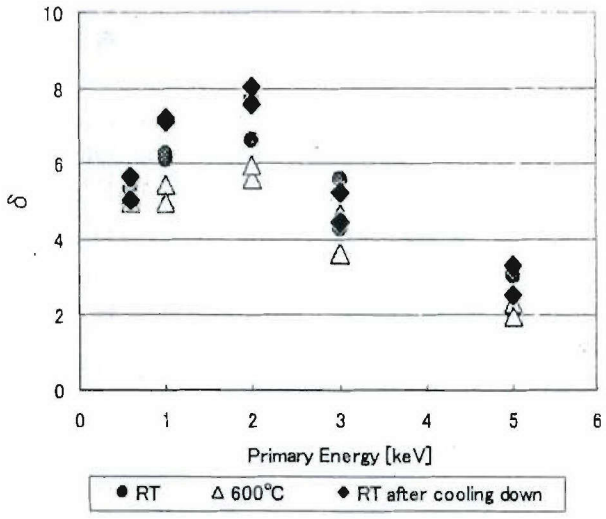

Figure 9. SEE coefficients of alumina HA-92 at room temperature, 600 ℃ and room temperature after cooling down.

4. Conclusions

The measurements of SEE coefficient using SEE current method which is adopted to avoid the leakage current problem resulted almost the same value with the absorption current method.

The measurements of SEE coefficient were carried out for silicon, sapphire and alumina (HA-997, HA-92). A reduction of SEE coefficient of the samples under high temperature was confirmed. This reduction may be caused by the shorter mean free path of the secondary electrons due to the larger phonon and electron scattering at high temperature.

References

[1] Y. Saito, N. Matuda, S. Anami, A. Kinbara, G. Horikoshi and J. Tanaka: "Breakdown of alumina rf windows", IEEE Transaction on Electrical Insulation, 24, 1989, pp. 1029-1036.

[2] T. Sato, S. Kobayashi, S. Michizono and Y. Saito: "Measurements of secondary electron-emission coefficients and cathodoluminescence spectra for annealed alumina ceramics", Applied Surface Science 144-145, 1999, pp. 324-328.

[3] A.J. Dekker: "Solid State Physics", Maruzen Asian Edition, 1968, pp. 440-442.

[4] J.B. Johnson and K.G. McKay: "Secondary electron emission of crystalline MgO", Physical Review, 91, 1953, pp. 582-587.

[5] J.B. Johnson and K.G. McKay: : "Secondary electron emission from germanium", Physical Review, 93, 1954, pp. 668-672.

[6] J. Cazaux: "About the secondary electron emission yield, δ , from e^--rradiated insulators", Mikrochimica Acta, 132, 2000, pp. 173-177.

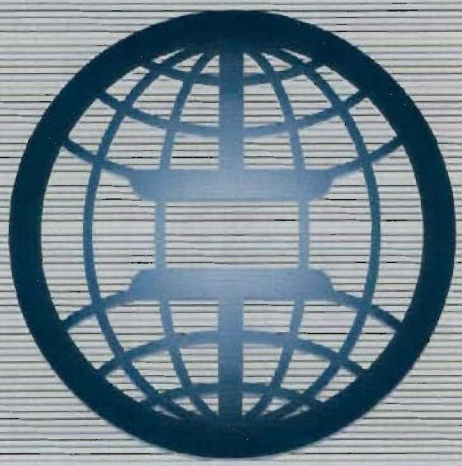

ISDEIV XXI

XXIth International Symposium on Discharges and Electrical Insulation in Vacuum

Yalta, Crimea,
Sept. 27, 2004 – Oct. 1, 2004

Hosted by

TAVRIDA ELECTRIC

Proceedings
VOLUME 1

PROCEEDINGS

ISDEIV

XXIth International Symposium on Discharges and Electrical Insulation in Vacuum

Yalta, Crimea,
Sept. 27, 2004 - Oct. 1, 2004

Hosted by

Sponsored by

TAVRIDA ELECTRIC
IEEE
DEIS
Sandia National Laboratories
ABB
Toshiba
Russian Academy of Science

Secondary Electron Emission of Dielectric Materials under High Temperature Condition

Suharyanto[1,2], S. Michizono[3], Y. Yamano[1], Y. Saito[3], S. Kobayashi[1]
[1]Department of Electrical and Electronic Systems, Saitama University
255 Shimo-Okubo, Sakura-ku, Saitama, 338-8570, Japan
(Tel: +81-48-858-3469, Fax: +81-48-855-7832, email: s.kobayashi@ees.saitama-u.ac.jp)
[2]Department of Electrical Engineering, Gadjah Mada University, Jl. Grafika 2, Yogyakarta, 55281, Indonesia
[3]High Energy Accelerator Research Organization, 1-1 Oho, Tsukuba, Ibaraki 305-0801, Japan

Abstract–Secondary electron emission (SEE) coefficients of alumina, sapphire, SiO_2, and MgO were measured by using a SEM with short-pulsed electron beam under room and high temperatures. An appreciable reduction in the SEE coefficients with increasing temperature was confirmed, except for sapphire. In addition, it was found that at room and high temperature SEE coefficients of alumina increased with purity and grain size.

I. INTRODUCTION

Klystrons, the high power microwave generators, are used for particle acceleration energy sources in a high-energy accelerator. In the klystron, there is an rf window which made of an insulator. Surface flashover along the rf window insulator is a present problem in the klystron applications for high power use [1]-[3]. Therefore, it is necessary to understand the surface flashover phenomena in vacuum and thus improve transmission capability of the high power microwave.

The surface flashover along the insulator in vacuum is initiated by primary electrons emitted from the tripple junction [4]. Then these emitted electrons are accelerated and multiplied due to the high secondary electron emission (SEE) coefficients of the insulator. Multiplication of the secondary electrons (multipactor) induces the excess surface heating, leading to the localized surface melting [2]. Therefore, studies on SEE characteristic under high temperature condition are required to understand the breakdown process in the rf window.

Many theories have been proposed to explain the SEE phenomena [5]-[9]. However, there are still few experimental data of SEE under high temperature condition, especially for technical material such as alumina ceramics. This study aims to observe the SEE coefficients of various kinds of commercial alumina ceramics under room and high temperature conditions. Sapphire (single crystal alumina), SiO_2, and MgO were also investigated.

II. EXPERIMENTAL SETUP

SEE Measurement System

SEE measurements were carried out using a scanning electron microscope (SEM) under room and high temperature conditions. Sample stage of the SEM was modified to enable a sample to be heated up to 750°C [10]. Schematic diagram of the measurement system is shown in Fig. 1. Single short-pulsed electron beam (1 ms duration, 100 pA magnitude) was used as primary current to minimize surface charging on the insulator sample. The primary current was measured using a Faraday cup installed on the heat reflector set above the sample. The primary electron was irradiated to the sample through a hole (about 2 mm in diameter) of the heat reflector. Then the secondary electrons emitted from the sample were captured by the heat reflector, which was coated with a diamond like carbon (DLC) film in order to minimize the SEE from the reflector surface. A positive bias voltage (+40 V) is applied to the reflector to ensure most of the secondary electrons were captured.

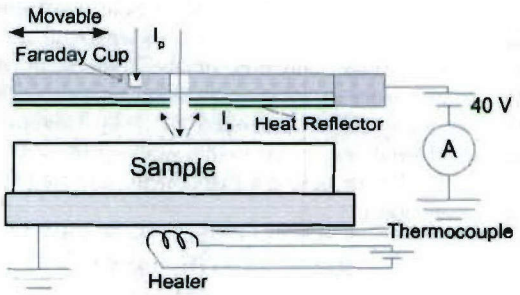

Fig. 1. Schematic diagram of the SEE measurement system.

Examined Samples and Annealing Treatment

Examined samples were HA series (HA-92, HA-960, HA-997) and KP series (KP-990, KP-999) alumina ceramics, sapphire, SiO_2 and MgO. Properties of the samples are listed in Table 1. HA series aluminas are developed for electrical insulator applications in vacuum, such as an rf window in a high energy accelerator. Alumina HA-960 is specially sintered to make the boundary additives crystallized, which contributes to reduction in the dielectric loss tangent to be as small as that of sapphire (single crystal alumina). KP series aluminas have high mechanical strength and smaller grains [11].

0-7803-8461-X/04/$20.00 ©2004 IEEE

TABLE I.
PROPERTIES OF EXAMINED SAMPLES

Material name	Purity (%)	Grain size (μm)
Alumina HA-92	92	4
HA-960*	96	-
HA-997	99.7	18
KP-990	99.5	2-3
KP-999	99.9	-
Sapphire	Single crystal	
SiO_2	Single crystal	
MgO	Single crystal	

*Grain boundaries are crystallized.

It is well known that ceramic materials may have trapped charges in their vacancies. The trapped charges are not desired because they influence the secondary electron emitted from the ceramic. Sato et. al. reported that the annealing treatment in atmosphere at 1500°C for 1 hour is effective to remove the mechanical stress of insulators which affects their properties concerning reduction of the trapped or stored charges in the vacancies of alumina ceramics, especially for relative low purity alumina (about 90%) [11]. Therefore, all of ceramic materials examined in this study were annealed in atmosphere for 1 hour before measurements. Annealing temperatures were 600°C for SiO_2 and 1400°C for other samples.

III. RESULTS AND DISCUSSION

SEE Coefficients of Alumina Ceramics

The SEE coefficients of alumina ceramics were measured at room temperature and 700°C. Fig. 2 and Fig. 3 show the SEE coefficients of HA series aluminas (HA-92, HA-960, HA-997) and KP series aluminas (KP-990, KP-999), respectively.

Although there is scattering of data, the SEE coefficients of the alumina ceramics at high temperature are generally lower than those obtained under room temperature. At present, there are still only few theories of the SEE under high temperature condition. However it is considered that the decrease of SEE coefficient of insulators at high temperature may be caused by the shorter mean free path of the secondary electrons due to the larger phonon and electron scattering in the bulk, affecting the shorter escape depth [5]-[7]. Therefore, under high temperature condition the secondary electrons approaching the surface are less than those at room temperature.

Moreover, it is found that for HA series alumina ceramics, decrease level of SEE coefficients of alumina HA-960 at high temperature are smaller than those of HA-92 and HA-997. This is because the alumina HA-960 is produced by a special method, which makes the grain boundaries of the alumina crystallized [12]. The crystallized boundaries of the alumina HA-960 may affect its decrease level of SEE coefficient due to high temperature.

In addition, decrease of SEE coefficients of HA series aluminas at high temperature are fairly larger than those of KP series aluminas, because the production methods of the HA and KP series aluminas are different. The production methods may determine the properties of the alumina ceramics such as grain size, grain boundaries, etc [11].

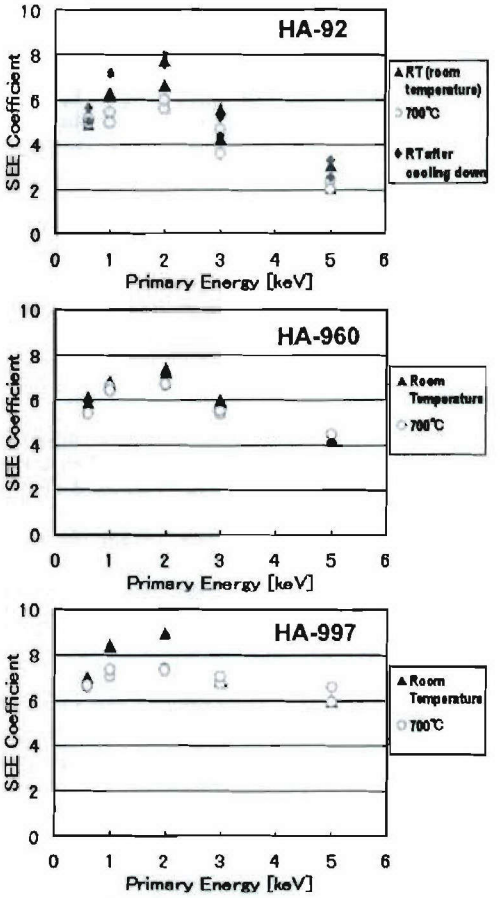

Fig. 2. SEE coefficients of HA series aluminas at room temperature and 700°C.

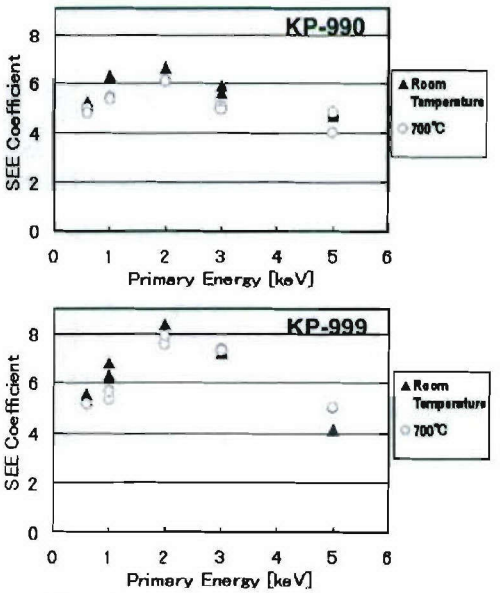

Fig. 3. SEE coefficients of KP series aluminas at room temperature and 700°C.

Relationship between SEE Coefficient and Purity of Alumina

Dependence of the maximum SEE coefficients on the purity of various type aluminas at room temperature and 700°C is shown in Fig. 4. The data were compiled from Fig. 2 and Fig. 3. The maximum values of SEE coefficients of the aluminas are varying from about 6.5 to about 9 at room temperature, and from about 5.5 to about 7.5 at high temperature.

According to the Fig. 4, it is found that the SEE coefficients of the alumina ceramics having lower purity are smaller than those of higher purity at both room and high temperature conditions. It may be caused by the lower SEE coefficients of sintering additives, such as SiO_2, which will be discussed in the next section. Although alumina HA-997 has higher purity and higher values of SEE coefficients, it shows higher breakdown strength [13]. The breakdown phenomena, especially in the thermal process, are therefore strongly related to the oxygen vacancy rather than the SEE coefficients.

Moreover, it is found that increase gradient of SEE coefficients with purity for HA series aluminas at room temperature is slight, whereas that of KP series aluminas is steep as shown by the both lines in Fig. 4. This tendency is also found for those at high temperature. It indicates SEE coefficients of KP series aluminas are more sensitive to be altered with purity. The SEE coefficients of alumina ceramics may not only be influenced by the purity, but also by the grain size of the alumina, because the grain size of the HA and KP series aluminas is different.

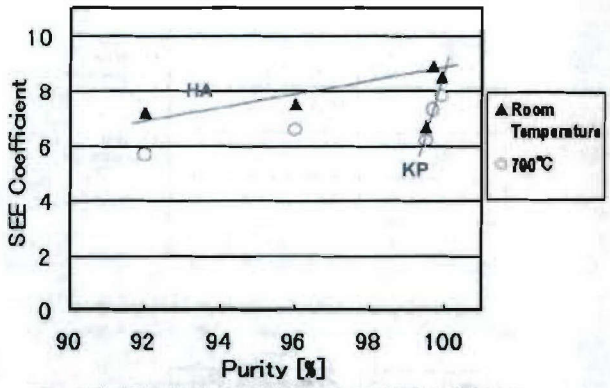

Fig. 4. Relationship between the maximum SEE coefficients and purity of various alumina ceramics.

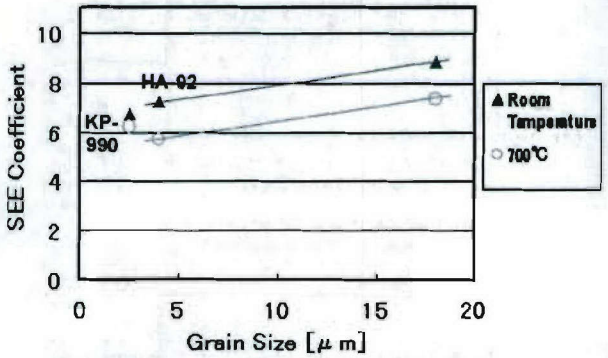

Fig. 5. Relationship between the maximum SEE coefficients and grain size of various type alumina ceramics.

Relationship between SEE Coefficient and the Grain Size of Alumina

The relationship between maximum SEE coefficients and the grain size of alumina ceramics under room and high temperature is shown in Fig. 5. It is found that the SEE coefficients of the alumina ceramics increase with the grain size. For HA series alumina, if a line is drawn from data in the figure of HA-92 at room temperature to that of HA-997, and so for the high temperature data, it results in two exactly parallel lines. It may indicate that the decreases of SEE coefficients of HA-series aluminas at high temperature do not depend on their grain size.

SEE Coefficients of Sapphire (Single Crystal Alumina)

The SEE coefficients of sapphire disk with diameter of 19 mm and thickness of 1 mm were measured at room temperature and 700°C. The measurement result is shown in Fig. 6. It is found that at high temperature the SEE coefficients are higher than those at room temperature. Since the SEE coefficients of this sample after cooling down were almost same as the previous values at room temperature, the increase of SEE coefficients at 700°C was not caused by the surface modification, but by the nature of the insulators.

This tendency is different from measurement results for alumina ceramics. The defect transition from F^+-center to F-center probably enhanced the secondary electron creation because the F-center has a state near to the conduction band, leading the easy electron emission. Although the escape depth of secondary electrons decreased at high temperature due to an increase of the phonon scattering, it is considered that the increase of the secondary electron creation rate at high temperature is dominated in the SEE of the sapphire.

SEE Coefficients of Single Crystal SiO_2 and MgO

SiO_2 and MgO are often used as sintering additives for alumina ceramics [11]. Therefore it is necessary to measure the SEE coefficients of the samples under room and high temperature conditions. Single crystal SiO_2 disk with diameter of 19 mm and thickness of 1 mm was examined in this study. The SEE coefficients of SiO_2 measured at room temperature and 400°C are shown in Fig. 7.

According to the figure, the SEE coefficients of SiO_2 decrease with temperature. The decrease of the SEE coefficients at 400°C was not caused by the surface modification, but by the nature of the insulators because SEE coefficients of this sample after cooling down were almost same as the previous values at room temperature. The decrease of the SEE coefficients of SiO_2 with temperature is interpreted by the smaller escape depth due to phonon scattering at high temperature. Moreover it is found that values of the SEE coefficients of SiO_2 are much smaller than those of alumina ceramics.

Measurements of SEE coefficients of single crystal MgO disk (19 mm in diameter, 1 mm in thickness) were carried out at room temperature and 700°C. Fig. 8 shows the SEE coeffi-

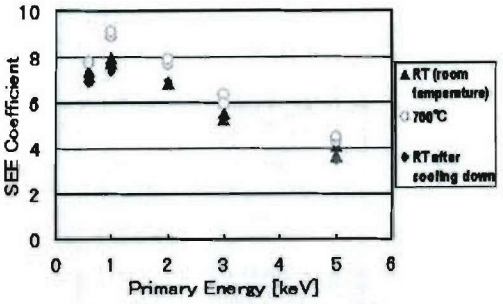

Fig. 6. SEE coefficients of sapphire measured at room temperature, 700°C, and room temperature after cooling down.

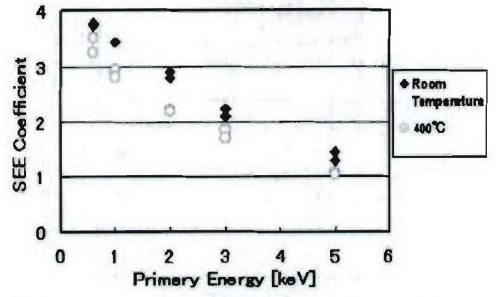

Fig. 7. SEE coefficients of single crystal SiO_2 measured at room temperature and 400°C.

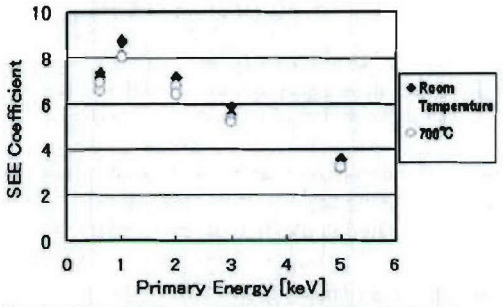

Fig. 8. SEE coefficients of single crystal MgO measured at room temperature and 700°C.

cients of the single crystal MgO at room temperature, 700°C, and room temperature after cooling down.

According to Fig. 8, it is confirmed that at 700°C the SEE coefficients of the MgO are lower than those at room temperature. This result agrees with the earlier work [7]. The decrease of the SEE coefficient is caused by the same reason as those for alumina and SiO_2 samples.

IV. Conclusions

SEE coefficients of several kinds of commercial alumina ceramics for electrical insulation use in vacuum, sapphire, SiO_2, and MgO were investigated under room and high temperatures. The findings of the present experiments are summarized as follows:

1. Although there is scattering of data, decrease of SEE coefficients of the samples with temperature was confirmed, except for sapphire. It is considered that the decrease of SEE coefficients of the insulators at high temperature is caused by the shorter mean free path of the secondary electrons due to the larger phonon and electron scattering in the bulk, resulting the shorter escape depth, and finally decreasing the SEE coefficients.
2. Increase of the SEE coefficients was observed for sapphire. This is probably due to the higher secondary electron creation caused by the defect transition from F^+-center to F-center, since the F-center has a state near to the conduction band, leading the easy electron emission.
3. SEE coefficients of alumina ceramics increase with purities under both room and high temperature conditions. Moreover, it is found that the SEE coefficients of KP series alumina are more sensitive to be altered by purity change than those of HA series alumina. It may be due to difference of production methods of the aluminas, which affect their microstructures.
4. The SEE coefficients of aluminas depend on not only purity, but they also tend to increase with the grain size. In addition, it is also found that decrease of value of SEE coefficient of HA series aluminas due to high temperature did not depend on the grain sizes.

References

[1] Y. Saito, N. Matuda, S. Anami, A. Kinbara, G. Horikoshi and J. Tanaka, "Breakdown of alumina rf windows", *IEEE Transaction on Electrical Insulation*, Vol. 24, pp. 1029-1036, 1989.

[2] Y. Saito, S. Michizono, S. Anami, S. Kobayashi, "Surface Flashover on Alumina RF Windows for High-power Use", *IEEE Transaction on Electrical Insulation*, 28, pp. 566-573, 1989.

[3] S. Yamaguchi, Y. Saito, S. Anami, S. Michizono, "Trajectory Simulation of Multipactoring Electrons in S-Band Pillbox RF Window", *IEEE Transaction on Nuclear Science*, Vol. 39, No. 2, 1992.

[4] R. V. Latham, "High Voltage Vacuum Insulation", Academic Press, London, pp.300-303, 1995.

[5] H. Bruining, "Physic and Application of Secondary Electron Emission", Pergamon Press Ltd., London, 1954.

[6] A.J. Dekker, "Solid State Physics", Maruzen Asian Edition, pp. 440-442, 1968.

[7] J.B. Johnson and K.G. McKay, "Secondary electron emission of crystalline MgO", *Physical Review*, 91, pp. 582-587, 1953.

[8] J. Cazaux, "About the secondary electron emission yield,δ, from e -rradiated insulators", *Mikrochimica Acta*, 132, pp. 173-177, 2000.

[9] G. F. Dionne, "Effects of secondary electron scattering on secondary emission yield curves", *Journal of Applied Physic*, Vol. 44, No. 12, pp.5361-5364, 1987.

[10] Suharyanto, S. Michizono, Y. Yamano, Y. Saito, S. Kobayashi, "Secondary Electron Emission Coefficient Measurements of Semiconductor and Insulator Materials in Vacuum", Proc. of 2003 J-K Joint Symp. on E.D. and H.V.E., pp. 277-280, 2003.

[11] T. Sato, S. Kobayashi, S. Michizono and Y. Saito, "Measurements of secondary electron-emission coefficients and cathodoluminescence spectra for annealed alumina ceramics", *Applied Surface Science*, 144-145, pp. 324-328, 1999.

[12] NTK, "NTK Alumina Characteristics", 2003.

[13] S. Michizono, Y. Saito, S. Yamaguchi, S. Anami, N. Matuda, A. Kinbara, "Dielectric Materials for Use as Output Window in High-power Klystrons", *IEEE Transaction on Electrical Insulation*, 28, pp. 692-699, 1993.

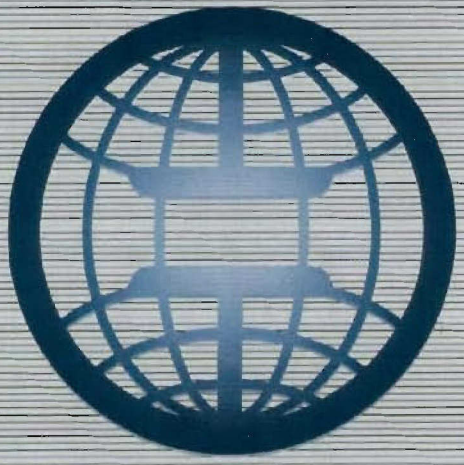

ISDEIV XXI

XXIth International Symposium on Discharges and Electrical Insulation in Vacuum

Yalta, Crimea,
Sept. 27, 2004 – Oct. 1, 2004

Hosted by

TAVRIDA ELECTRIC

Proceedings
VOLUME 1

PROCEEDINGS

ISDEIV

XXIth International Symposium on Discharges and Electrical Insulation in Vacuum

Yalta, Crimea,
Sept. 27, 2004 - Oct. 1, 2004

Hosted by

Sponsored by

TAVRIDA ELECTRIC
IEEE
DEIS
Sandia National Laboratories
ABB
Toshiba
Russian Academy of Science

Secondary electron emission and surface charging from alumina at high temperature

S. Michizono, Y. Saito
KEK -High Energy Accelerator Research Organization, Tsukuba 305-0801, Japan
Suharyanto, Y.Yamano and S.Kobayashi
Faculty of Engineering, Saitama University, Saitama 338-8570, Japan

ABSTRACT

Electrical breakdown is one of the most serious problems for developing compact and/or higher-voltage insulation in a vacuum. High secondary electron emission (SEE) yields result in the multipactor effect (electron multiplication on the dielectric surface). Multipactor induces not only discharging, but also excess surface heating, leading to localized surface melting. Thus, SEE at high temperature is important for understanding the actual breakdown process. The SEE yields of sapphire were measured at high temperature by a single-pulsed beam method with a scanning electron microscope (SEM) so as to avoid surface charging.

In general, the effective SEE decreases by multipactor due to surface charging. Since the electrical conductivity becomes higher at a high temperature, effective SEE can be larger due to less surface charging. In order to estimate the surface charging, multi-pulse beams were injected to sapphire disks at room and high temperature.

I. INTRODUCTION

Dielectric materials, such as alumina ceramics, are widely used as electrical insulators in a vacuum. The electrical breakdown on an insulator surface restricts the minimal size of the insulators. The discharge is well explained by the "secondary electron emission avalanche (SEEA)" model [1]. The SEEA model describes that the primary electrons, emitted from the triple junction (vacuum, metal, insulator), are multiplied due to the high secondary electron emission (SEE) yields on the dielectric surface. When multipactor takes place, localized surface melting appears on the dielectric surface caused by excess electron bombardment [2]. Thus, measurements of the SEE coefficients not only at room temperature, but also at high temperature, are required for understanding the surface-discharge phenomena.

In this study, the SEE yields of single-crystal alumina (sapphire) at 650 degrees C were obtained with a scanning electron microscope (SEM) by a pulsed-beam method [3] as a function of the incident-electron energy. In order to estiate the surface charging, the multi-pulse procedure was also examined.

II. EXPERIMENTAL

The SEE measurement system consists of a scanning electron microscope (SEM), a personal computer (PC) with a digital analog converter (DAC), a current amplifier and an oscilloscope, as shown in Figure 1. A lower pulse current (100 pA, 1 ms) with a single-pulse at a quite low charge density (3 μC/m2)

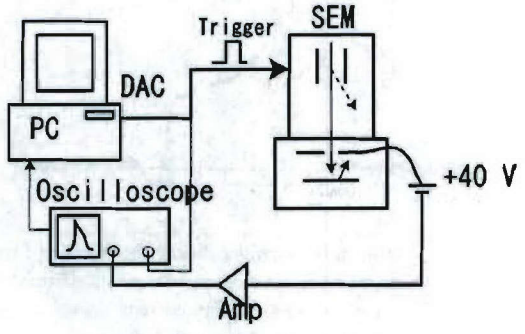

Fig.1. SEE measurement system.

0-7803-8461-X/04/$20.00 ©2004 IEEE

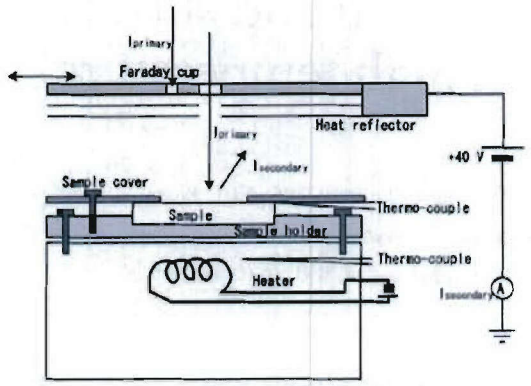

Fig.2. Schematic drawings of the secondary electron emission (SEE) measurements.

compared to the continuous-beam system [4] was applied to a sapphire sample in order to avoid surface charging. The trigger pulse for the primary current is generated by DAC (PCI-3325,Interface Corporation) in the PC. The intelligent DAC board can generate arbitrary pulse sequences.

The primary current is captured at a biased Faraday cup (+40 V) made of graphite, as shown in Figure 2. The primary electrons are injected to the sample through small holes (2 mm in diameter) at the heat-reflectors. The emitted electrons from the sample (secondary electrons) are captured at the biased (+40 V) heat-reflector. The heat-reflector is coated with DLC (diamond-like-carbon) films so as to reduce the SEE yields on the surface. The primary and secondary currents are amplified by current amplifier (Keithley Model 428). The output waveform observed at the oscilloscope (Tektronix TDS 3014B) is stored in the PC simultaneously.

Figure 3 shows the typical waveform observed at the dielectric surface. Even though the total charge is a maximum of 0.1 pC, it induces local charging, leading to a decrease in SEE. Here, the SEE yield on the dielectric surface is defined by the ratio of the secondary-to-primary electrons at the beginning of the pulse.

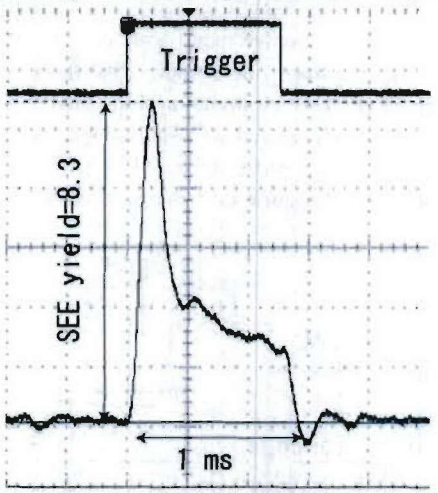

Fig.3. SEE for the sapphire disk. Pulse width of 1 ms, primary electron current of about 100 pA are utilized. The rapid decrease in the secondary currents corresponds to the build-up of the surface charging.

III. RESULTS

III-1 Secondary electron emission from sapphire at high temperature

A sapphire disk (19 mm in diameter and 1 mm thick) was annealed up to 1400 degrees C for one hour in air in order to remove any mechanical defects

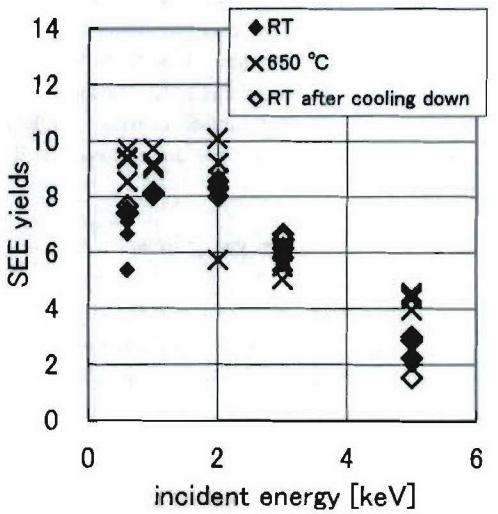

Fig.4. SEE yields of a sapphire disk at room temperature, 650 degrees C and room temperature after cooling down.

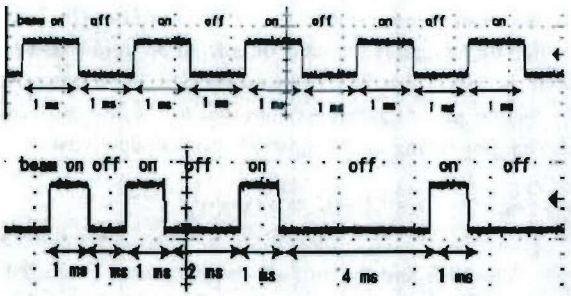

Fig.5. Multi-pulse signal of "mode A" (upper) and "mode B" (lower).

and/or localized surface charging [5]. The SEE yields were measured at room temperature and at 650 degrees C. The results are shown in Figure 4. Although there is rather large scattering at 650 degrees C, the SEE yields appear to become larger at 650 degrees C than those at room temperature. Since the SEE yields after cooling down are almost the same as the previous room-temperature-values, the increase in the SEE yields at 650 degrees C must not be caused by a surface modification, but by the nature of the sapphire sample. This tendency is different from earlier studies for MgO [6], KCl [7] and some of commercial alumina ceramics [8]. These are explained by the shorter mean-free-path of the secondary electrons due to phonon scattering. The defect transformation from the F^+-center to the F-center [9] probably enhances the secondary-electron production because the F-center has a state near to the conduction band [9]. This is especially promoted at single crystal alumina due to the predominant F-center [2]. Although the escape depth of secondary electrons decreases at a high temperature due to an increased scattering with phonons, we assume that the excess surface heating due to multipactor would result in higher SEE yields.

III-2 Multi-pulse method for surface charging observation

As described before, the SEE decreases with time during a pulse, so that the total amounts of the SEE are smaller than the SEE yields. Since the surface electric conductivity becomes higher at a higher temperature, the surface charging would be less at higher temperatures. Thus, the effective SEE would be larger, which enhances SEEA. In order to examine the surface charging, a multi-pulse method was applied. Two modes were utilized for the measurements, as

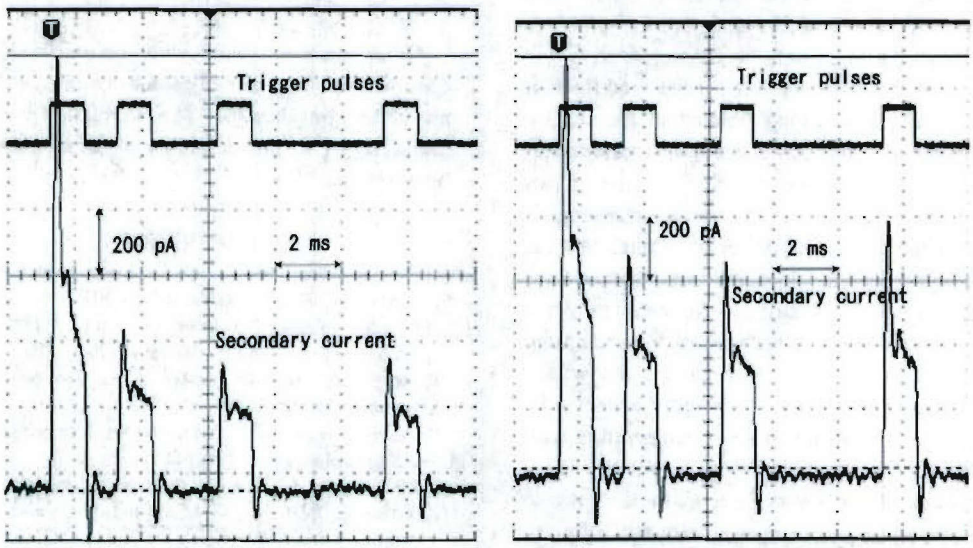

Fig.6. Multi-pulse waveform. (a): "mode A" at room temperature. (b): "mode B" at 650 degrees C. The primary current is 150 pA.

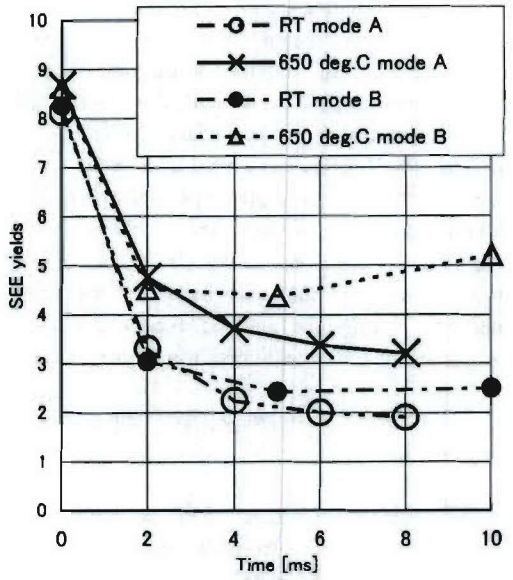

Fig.7. SEE yields obtained by multi-pulse method at room temperature and 650 degrees C.

illustrated in Figure 5.

(1) Mode A: 5 successive pulses (1 ms) with the same intervals (1 ms).

(2) Mode B: 4 successive pulses (1 ms) with increasing intervals (1 ms, 2 ms, 4 ms).

The surface charging might be characterized by (1) the amounts of the charging and (2) the modification time-constant of the charging (related to the electric conductivity). Since the pulse interval is constant at "mode A", a decrease in the SEE at the pulses corresponds to a build-up of the surface charging. If the SEE's are the same at all pulses of "mode A", the surface charging becomes in equilibrium with a 1 ms pulse. The "mode B" is suitable for estimating the modification time-constant because of the increasing interval. The measurements were carried out with a primary electron energy of 1 keV. Figure 6 shows the measured pulse waveforms at room temperature with "mode A" and at 650 degrees C with "mode B". In the case of "mode B" at 650 degrees C, the increase in the SEE at the 4th pulse compared with the 3rd pulse is observed, indicating a typical modification time-constant of about 4 ms.

Figure 7 shows the changes in SEE with two modes at room temperature and 650 degrees C. The horizontal axis is the total time from the initial pulse. It is found that the decrease in SEE with time is smaller at a high temperature due to the less surface charging owing to the higher electric conductivity.

IV. SUMMARY

The SEE and the surface charging were evaluated by SEM with the pulsed-beam method. It is found that the SEE yields of the sapphire disks at 650 degree C are larger than those at room temperature. Although the mean-free path of the secondary electrons decreases due to phonon scattering, the defect transformation from the F^+-center to the F-center probably enhances the secondary-electron production. The multi-pulse method is applied to estimate the surface charging. It is found that the SEE decreases more slowly at a higher temperature due to less surface charging. The recovery of SEE is observed at high temperature in the case of increasing pulse-interval. This corresponds to a shorter modification time-constant, which is consistent with the higher electric conductivity. The smaller surface charging at a high temperature results in a larger effective SEE, leading to an enhancement of the SEEA.

Other measurements with commercial alumina ceramics and/or anti-multipactor coatings, such as TiN, are under consideration. The correlation between the surface charging and durability of the materials should be examined.

REFERENCES

[1] R.V. Latham (Ed), High Voltage Vacuum Insulation, ACADEMIC PRESS, London, 1995, p. 301.

[2] S.Michizono et al., IEEE Trans. Electr. Insul. 28 (1993) 692.

[3] S. Michizono and Y. Saito, Vacuum 60 (2001) 235.

[4] M.P. Seah and S.J. Spencer, J. Electron Sepc. and Rel. Phenomena 109 (2000) 291.

[5]A.Berroug et al., Le Vide, les Couches Minces-Supplement au no.260, Janvier-Fevrier (1992) 427.

[6] J.B.Johnson and K.G.McKay, Phys.Rev. 91 (1953) 582.

[7] J. Cazaux, J. Electron Sepc. and Rel. Phenomena 105 (1999) 155.

[8] Suharyanto et al., this conference.

[9] K. H. Lee and J. H. Crawford Jr., Phys. Rev. B19 (1979) 3217.

Available online at www.sciencedirect.com
SCIENCE DIRECT
ELSEVIER
Applied Surface Science 235 (2004) 227–230
applied surface science
www.elsevier.com/locate/apsusc

Secondary electron emission of sapphire and anti-multipactor coatings at high temperature

Shinichiro Michizono[a,*], Yoshio Saito[a], Suharyanto[b], Yasushi Yamano[b], Shinichi Kobayashi[b]

[a]*High Energy Accelerator Research Organization (KEK), 1-1 Oho, Tsukuba, Ibaraki 305-0801, Japan*
[b]*Faculty of Engineering, Saitama University, Saitama 338-8570, Japan*

Available online 4 July 2004

Abstract

Electrical breakdown (surface discharge) is one of the most serious problems for developing compact and/or higher voltage insulation in a vacuum. Electron multiplication (multipactor) due to high secondary electron emission (SEE) yields from an insulator surface is one of the reasons for the discharge. Multipactor induces not only discharging but also excess surface heating, leading to localized surface melting. Thus, SEE at high temperature is important for understanding the actual breakdown process. The SEE yield of single crystal alumina (sapphire) and anti-multipactor coatings, such as TiN and DLC films having low SEE yields, are measured in a scanning electron microscope (SEM).

Keywords: Secondary electron emission; Sapphire; Anti-multipactor coatings

1. Introduction

Dielectric materials, such as alumina ceramics, are widely used as electrical insulators in vacuum. The electrical breakdown on an insulator surface restricts the minimal size of insulators. The breakdown is often described by the "secondary electron emission avalanche (SEEA)" model [1]. The SEEA model consists of (1) primary electron emission (from the interface of the metal and the insulator, called "triple junction") and (2) secondary electron multiplication (multipactor) on the insulator surface having high secondary electron emission (SEE) yields. When multipactor takes place, localized surface melting appears on the dielectric surface caused by excess electron bombardment [2]. Thus, measurements of the SEE coefficients not only at room temperature, but also at high temperature, are required for understanding the surface-discharge phenomena.

The SEE phenomena could be analytically understood by using such models as the constant-loss model [3,4] and/or the dynamic double layer model [5]. The constant-loss model is as follows:

(1) SEE by primary electron impact.
(2) Escape of secondary electrons toward the surface (the escape depth is related to the mean free path of the electrons).

Since the primary electrons can reach much deeper than the secondary electron escape depth, the double

* Corresponding author. Tel.: +81 29 864 5697; fax: +81 29 864 3182.
E-mail address: shinichiro.michizono@kek.jp (S. Michizono).

0169-4332/$ – see front matter
doi:10.1016/j.apsusc.2004.05.131

layer of the charging (due to the primary electron dose and to the secondary electron emission) is concerned in the dynamic double layer model. In both models, large SEE yields at the insulators are attributed to the large escape depths of the secondary electrons. In order to suppress multipactor, conducting materials having shorter mean free path of electrons, such as TiN, are sometimes coated (so-called "anti-multipactor coatings"). In this study, the SEE of anti-multipactor coatings (TiN and DLC (diamond-like-carbon) films) at 400 °C were measured with a scanning electron microscopye (SEM) by a pulsed-beam method [6] as a function of the incident-electron energy. The SEE yields of single crystal alumina (sapphire) at 650 °C were also obtained by the single-beam method [6] so as to avoid surface charging.

2. Secondary electron emission measurements

The primary current (I_{pr}) was measured with a Faraday cup located at either the floating sample holder or the heat reflector, as shown in Fig. 1. A negatively biased (−40 V) holder and a positively biased (+40 V) heat reflector capture the absorption (I_{ab}) and secondary currents (I_{sec}), respectively. The heat reflector was coated with DLC film in order to minimize the SEE from the reflector itself. The total SEE yields were calculated by:

$$\text{SEE yield} = \frac{I_{sec}}{I_{pr}} = 1 - \frac{I_{ab}}{I_{pr}}$$

Pulsed beams (400 pA, 4 ms, 50 Hz) were applied to TiN, DLC samples. Averaging the signal about 10 times was carried out in order to remove the electric noises emitted from the sample heater. A lower pulse current (100 pA, 1 ms) with a single-pulse at quite low charge density (3 μC/m^2) compared to the continuous beam system [7] was applied to a sapphire sample in order to avoid surface charging. Even under such a condition, surface charging took place, resulting in a decrease in the secondary current during the pulse, as shown in Fig. 2. Although the single-pulse method is applied to obtain the true SEE yield of the insulator without beam-induced-charging, larger scattering of SEE yields is observed due to the difference in local surface condition such as defects.

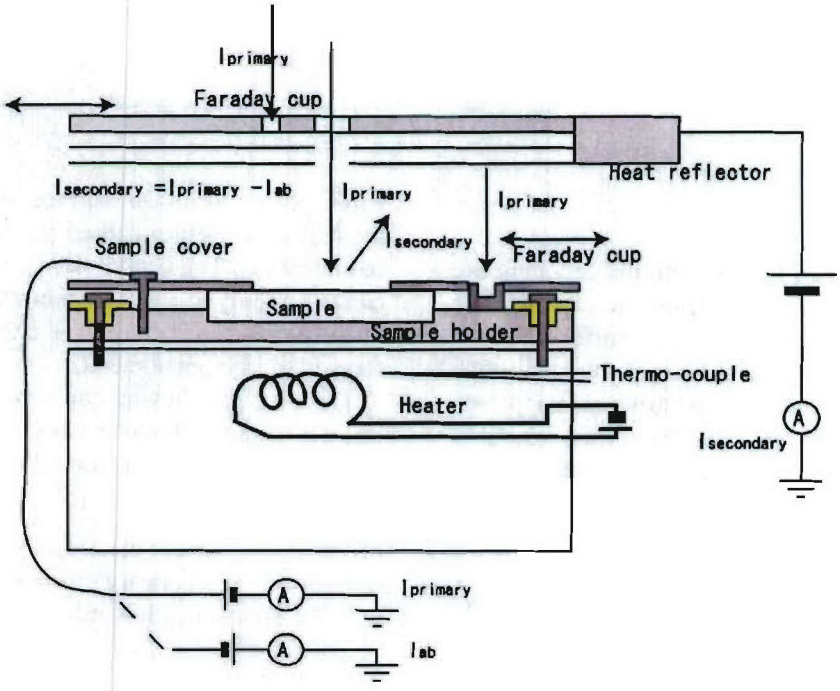

Fig. 1. Schematic drawings of the secondary electron emission measurements.

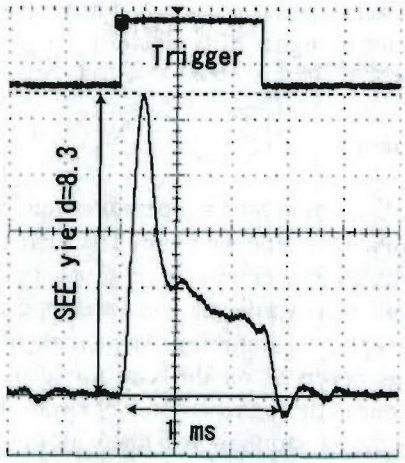

Fig. 2. SEE for the sapphire disk. Pulse width of 1 ms, primary electron current of about 100 pA are utilized. The rapid decrease in the secondary currents corresponds to the build-up of the surface charging.

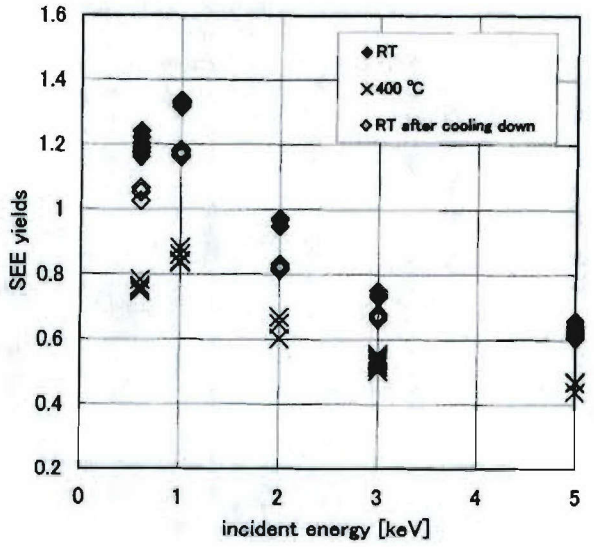

Fig. 3. SEE yields of TiN coatings at room temperature, 400 °C and room temperature after cooling down.

3. Results

3.1. Anti-multipactor coatings

Both TiN and DLC (diamond-like-carbon) coatings are known for their attractive mechanical, electrical and tribological properties [8–10]. Because TiN films have rather low SEE yields, they can also be used for anti-multipactor coatings [2,9]. The SEE yields of the TiN and DLC coatings on stainless steel were measured at both room temperature and 400 °C. Because both coatings had a thickness of more than 1 μm (about 100-times larger than the electron escape depth [4]), the effects on SEE from the substrate were negligible. The SEE yields of TiN coatings were measured at room temperature, 400 °C and room temperature again after cooling down, as shown in Fig. 3. It was found that the SEE yields decreased at 400 °C, which is also interpreted by the smaller escape depth due to phonon scattering at high temperature [11]. The SEE yields after cooling down did not completely recover to the first values obtained at room temperature, because the oxide layer, having higher SEE yields, was thinned after high-temperature annealing in a vacuum [10]. Hence, the values obtained after the cooling step should be considered as the true yields. Measurements were also carried out on DLC coatings at room temperature and 400 °C. The SEE yields become again lower at 400 °C, as shown in Fig. 4, which might be referred to the same reason as that for the TiN samples. After cooling down, the SEE yields were lower than those of the first measurements at room temperature, too.

The SEE yields of amorphous carbon strongly depend on the bonding, dopants and the hydrogen termination [12–15]. It is further reported that heating of hydrogenated DLC results in the removal of the

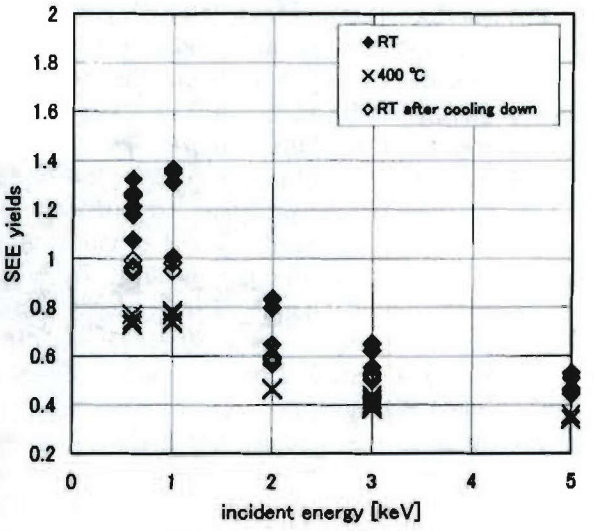

Fig. 4. SEE yields of DLC coatings at room temperature, 400 °C and room temperature after cooling down.

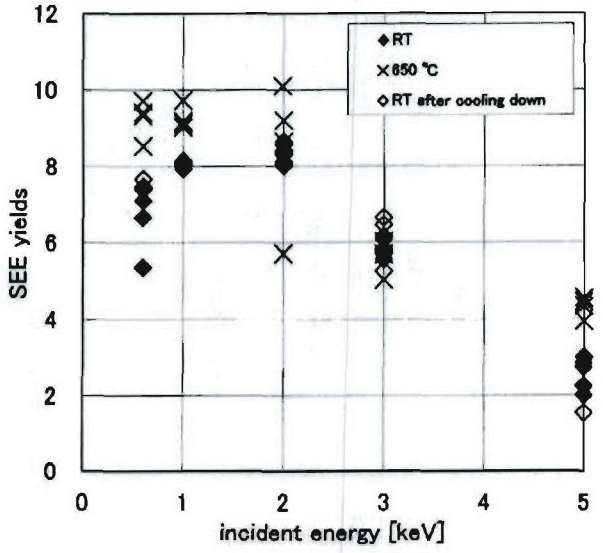

Fig. 5. SEE yields of sapphire disk at room temperature, 650 °C and room temperature after cooling down.

hydrogen, which starts at around 400 °C [8]. This structure change would also explain the lower value after cooling down.

3.2. Sapphire

A sapphire disk (19 mm in diameter and 1 mm thick) was annealed up to 1400 °C for one hour in air in order to remove any mechanical defects and localized surface charging [16]. The SEE yields were measured at room temperature and at 650 °C. The results are shown in Fig. 5. Although there is rather large scattering at 650 °C, the SEE yields appears to become larger at 650 °C than those at room temperature. Since the SEE yields after cooling down are almost the same as the previous room-temperature values, the increase in the SEE yields at 650 °C must not be caused by the surface modification, but by the nature of the sapphire sample. This tendency is different from earlier studies for MgO [17] or KCl [4]. The defect transformation from F^+-center to F-center [18] probably enhances the secondary-electron production because the F-center has a state near the conduction band [18]. Although the escape depth of secondary electrons decreases at high temperature due to an increased scattering with phonons, we assume that the excess surface heating due to multipactor would result in higher SEE yields.

4. Summary

The SEE yields at high temperature were measured for the TiN, DLC and sapphire. The yields become lower at higher temperature, except for sapphire. This can be explained by a decrease in the escape depth due to electron–phonon scattering. An increase of the SEE yields was observed on the sapphire disk. This is probably due to the higher secondary electron creation caused by the transformation of the oxide defects. This tendency is not desirable for vacuum insulation because of the multipactor enhancement due to electron-impact heating. Anti-multipactor coatings, such as TiN, are effective from the viewpoints of a decrease in the SEE yields at high temperature.

Further studies of the SEE measurement at high temperature are necessary, especially for commercial alumina ceramics with TiN coatings. Since the surface charging plays important roles for total SEE from a insulator surface, surface charging should be measured at high temperature in order to examine its influence on SEE yields.

References

[1] R.V. Latham (Ed.), High Voltage Vacuum Insulation, Academic Press, London, 1995, p. 301.
[2] S. Michizono, et al., IEEE Trans. Electr. Insul. 28 (1993) 692.
[3] G.F. Dionne, J. Appl. Phys. 46 (1975) 3347.
[4] J. Cazaux, J. Electron Sepctrosc. 105 (1999) 155.
[5] A. Melchinger, S. Hofmann, J. Appl. Phys. 78 (1995) 6224.
[6] S. Michizono, Y. Saito, Vacuum 60 (2001) 235.
[7] M.P. Seah, S.J. Spencer, J. Electron Sepctrosc. 109 (2000) 291.
[8] A. Grill, Diam. Relat. Mater. 8 (1999) 428.
[9] A.R. Nyaiesh, et al., J. Vac. Sci. Tech. A4 (1986) 2356.
[10] A.R. Nyaiesh, et al., J. Vac. Sci. Tech. A5 (1987) 2977.
[11] J.B. Johnson, K.G. McKay, Phys. Rev. 93 (1954) 668.
[12] A. Shih, et al., J. Appl. Phys. 82 (1997) 1860.
[13] J. Robertson, Semicond. Sci. Technol. 18 (2003) S12.
[14] G.T. Mearini, et al., Appl. Phys. Lett. 65 (1994) 2702.
[15] D. Ruzic, et al., J. Vac. Sci. Technol. 20 (1982) 1313.
[16] A. Berroug et al., Le Vide, les Couches Minces-Supplement au no.260, Janvier-Fevrier (1992) 427.
[17] J.B. Johnson, K.G. McKay, Phys. Rev. 91 (1953) 582.
[18] K.H. Lee, J.H. Crawford Jr., Phys. Rev. B19 (1979) 3217.